

**Towards Pancreatic  $\beta$ -Cell Regeneration:  
Modulating Islet Microenvironment and Identifying Markers of  $\beta$ -Cell Maturation**

By

Diane Caitlin Saunders

Dissertation

Submitted to the Faculty of the  
Graduate School of Vanderbilt University

in partial fulfillment of the requirements

for the degree of

DOCTOR OF PHILOSOPHY

in

Molecular Physiology and Biophysics

May 11, 2018

Nashville, Tennessee

Approved:

David Jacobson, Ph.D., Chair

Antonis Hatzopoulos, Ph.D.

Ambra Pozzi, Ph.D.

Roland Stein, Ph.D.

## ACKNOWLEDGEMENTS

My training and this work has been supported by multiple grants from the National Institute of Diabetes and Digestive and Kidney Disease, the U.S. Department of Veterans Affairs, the Juvenile Diabetes Research Foundation, and the Leona M. and Harry B. Helmsley Charitable Trust. Our group is privileged to work with the Network for Pancreatic Organ Donors with Diabetes and the Integrated Islet Distribution Program for studies of the human pancreas, and we are grateful to Organ Procurement Organizations partnering with the International Institute for Advancement of Medicine and National Disease Research Interchange for making this research possible. We are especially thankful to organ donors and their families. Work in this Dissertation also relied heavily on institutional core facilities: the Vanderbilt Imaging Shared Resource, the Islet Procurement and Analysis Core of the Vanderbilt Diabetes Center, the Flow Cytometry Shared Resource, and the Antibody and Protein Resource.

I am most indebted to my wonderful mentor, Al Powers, for his unwavering support and commitment to my training as a scientist. I most appreciate your enthusiasm, dedication to my professional growth, and generosity with your time. Thank you also for humoring my fussy design choices, giving me the opportunity to take on artistic projects, and reading countless drafts of manuscripts, grants, and abstracts— often at the very last minute. I feel fortunate to have landed in your lab for my graduate career. Marcela Brissova has also been an outstanding mentor over the past four years, devoting countless hours to reviewing my work, providing critical feedback on experiments, and brainstorming next steps at all stages of my projects. Thanks for answering so many of my questions and patiently revising my PowerPoint slides and color-coded spreadsheets. Your belief in my abilities and encouragement through setbacks has meant so much to me.

The work in this Dissertation would not have reached fruition without guidance from members of my dissertation committee: David Jacobson, Antonis Hatzopoulos, Ambra Pozzi, and Roland Stein. I appreciate your patience and encouragement as I developed confidence in presenting and critically thinking, and for the many suggestions and discussions that helped direct my experiments. Thanks also to David for your feedback and reassurance during my quals.

I cannot imagine my predoctoral training without the outstanding group of graduate students and postdoctoral fellows with whom I was fortunate to work: Danielle Dean, Rachana Haliyur, Nathaniel Hart, Neil Phillips, Erick Spears, and Jack Walker. Thanks for your willingness to both challenge and assist me at all stages of my training, and for always complimenting my baking. I am especially grateful to former graduate students Kristie Aamodt and Nora Kayton— from the very first conversations I had with you before rotating in the lab, you have been immensely supportive, reassuring, and generous, and I have learned so much from both of you as scientists and people.

Thanks to the members of the Islet Procurement and Analysis Core, particularly Anastasia Coldren and Heather Durai, for assistance with human islet preps and core equipment, and for their uplifting camaraderie. None of the mouse experiments would have been possible without our extraordinary lab technicians, Radhika Aramandla and Greg Poffenberger: thanks for ensuring that everything in the lab ran smoothly and for elevating our science to such an impressive technical standard. To other members

of the Powers research group— Chunhua Dai, Regina Jenkins, Jill Lindner, and Alena Shostak— thanks for your collaboration and collegiality during my time in the lab. Also special thanks to Alec Hopkirk, a hard-working undergraduate from the University of Alabama who assisted me for two summers.

There are many people who deserve recognition for their tireless commitment to graduate education at Vanderbilt. Thank you to Josh Gamse, David Miller, and Danny Winder, who helped greatly in my transition to graduate school and provided invaluable training during my IGP year. I am also grateful to Carolyn Berry and Michelle Grundy for their guidance, support, and wisdom. Thanks to Alyssa Hasty and Richard O'Brien for maintaining such a supportive, enriching training environment in the Department of Molecular Physiology and Biophysics.

A large portion of this work relied on collaborations with Cristina Nostro at the University of Toronto and Jean Sévigny at Laval University in Quebec. Thanks to both of you for your willingness to share reagents and ideas, and for giving me the chance to contribute to ongoing scientific projects taking place in your respective labs. I was also fortunate to work closely with Shristi Shrestha and Nripesh Prasad at the HudsonAlpha Institute of Biotechnology, to whom I am extremely grateful for the countless phone calls, data analyses, discussions, and explanations of bioinformatics. We are very lucky to consider you part of our group! At Vanderbilt, special thanks is due to Dave Flaherty and Kevin Weller in the Flow Cytometry Core, who provided advice and expertise that enabled us to develop our human islet cell sorting techniques, including answering my frantic texts for scheduling equipment and generously accommodating our experiments. It has truly been a pleasure working with you.

I am grateful to my IGP and MPB classmates for commiserating and sharing successes during all stages of graduate school. Thanks especially to Kim Alexander, Caleigh Azumaya, Diana Contreras, Meredith Frazier, Stephanie Moore-Lotridge, and Kristin Peterson.

Finally, thank you to the members of the Goessling lab, and especially to my mentor Wolfram Goessling, for the invaluable training I received during my time in Boston, and for continuing to encourage and support me during graduate school.

## TABLE OF CONTENTS

	Page
ACKNOWLEDGEMENTS .....	ii
LIST OF TABLES.....	vii
LIST OF FIGURES .....	viii
LIST OF ABBREVIATIONS .....	ix
Chapter	
<b>I. BACKGROUND AND SIGNIFICANCE .....</b>	<b>1</b>
The Pancreas.....	1
Anatomy, physiology, and function .....	1
Pancreatic development and establishing $\beta$ -cell mass .....	1
Differences between human and rodent islets .....	3
Diabetes .....	4
Epidemiology and pathophysiology.....	4
Treatments aimed at $\beta$ -cell replacement.....	5
Proliferation of endogenous $\beta$ -cells.....	6
Mechanisms of $\beta$ -cell proliferation.....	6
Hormone and growth factor activity.....	7
Changes in glucose metabolism .....	8
Small molecules .....	8
Other potential targets.....	8
Pancreatic Islet Microenvironment.....	9
Macrophages .....	9
Macrophages in pancreatic development and homeostasis .....	11
Macrophages in tissue injury and inflammation .....	11
Macrophages in $\beta$ -cell regeneration.....	12
Endothelial cells .....	13
Formation of islet vasculature .....	14
Endothelial cells in pancreatic development and homeostasis .....	15
Endothelial cells in islet inflammation, injury, and aging .....	15
Endothelial cells in tissue regeneration.....	16
Extracellular matrix.....	17
Components of islet extracellular matrix .....	17
Homeostasis and function of extracellular matrix.....	17
Extracellular matrix in $\beta$ -cell development and proliferation.....	18
Extracellular matrix in islet function, inflammation, and injury.....	19
Aims of Dissertation .....	20
<b>II. MATERIALS AND METHODS .....</b>	<b>22</b>
Mouse Models.....	22

DNA extraction and genotyping .....	23
Compound preparation and administration .....	24
Tissue Collection and Fixation .....	24
Islet isolation .....	26
Culture and assessment of pancreatic islet function .....	27
Pancreatic tissue fixation .....	27
Culture and Differentiation of hESCs .....	27
Immunohistochemistry, Imaging, and Analysis .....	28
Flow Cytometry and Fluorescence-Activated Cell Sorting .....	29
Human islet cell sorting .....	30
Flow cytometry and FACS of hESCs .....	30
RNA Isolation, Sequencing, and Analysis .....	31
Islet Transplantation .....	31
<i>In vivo</i> Imaging .....	32
Statistical Analysis .....	32
<b>III. ENDOTHELIAL CELLS IN THE ISLET MICROENVIRONMENT, IN CONCERT WITH MACROPHAGES, MODULATE BETA CELL PROLIFERATION .....</b>	<b>33</b>
Introduction .....	33
Results .....	34
Acute ablation of VEGFR2 in ECs does not affect islet vasculature or $\beta$ -cell proliferation .....	34
Proliferative ECs are required for macrophage polarization and maximal macrophage recruitment .....	34
VEGFR2 knockout in quiescent ECs accelerates EC regression, promoting $\beta$ -cell recovery .....	35
ECs are most abundant in human islets during early postnatal pancreatic development .....	36
Discussion .....	45
<b>IV. MOLECULAR MARKERS OF DEVELOPING HUMAN PANCREAS AND MATURE BETA CELLS FACILITATE UNDERSTANDING OF HUMAN ISLET BIOLOGY AND FUNCTION .....</b>	<b>47</b>
Introduction .....	47
Results .....	48
GP2 marks putative pancreatic progenitors in human neonatal pancreas .....	48
Purified GP2 <sup>+</sup> pancreatic progenitor cells give rise to $\beta$ -like cells <i>in vitro</i> .....	48
NTPDase3 is expressed specifically in adult human $\beta$ -cells, including those in islets from individuals with T1D and T2D .....	49
NTPDase3 is dynamically expressed during human pancreas development .....	49
NTPDase3 antibody effectively and efficiently isolates $\beta$ -cells from live dispersed human islet cells .....	49
Targeting NTPDase3 detects human $\beta$ -cells <i>in vivo</i> .....	50
Discussion .....	62
<b>V. SIGNIFICANCE AND FUTURE DIRECTIONS .....</b>	<b>64</b>
Role of islet endothelial cells in the recruitment and polarization of macrophages .....	65

Direct contribution of islet endothelial cells to $\beta$ -cell proliferation.....	66
Endothelial cells and macrophages in the human islet microenvironment .....	67
Concluding commentary: microenvironment in $\beta$ -cell proliferation .....	68
Molecular characterization of pancreatic progenitors: GP2 .....	69
Molecular characterization of mature $\beta$ -cells: NTPDase3.....	69
REFERENCES .....	72

## LIST OF TABLES

Table	Page
1. Mouse Models.....	22
2. Breeding scheme to generate $\beta$ VEGF-A; VEGFR2 <sup><math>\Delta</math>EC</sup> mice.....	23
3. PCR primers and conditions for genotyping .....	24
4. Demographic information of human donors used for histology.....	25
5. Demographic information of human donors used for cell sorting, RNA-seq, and islet transplantation .....	26
6. Primary antibodies for immunohistochemistry .....	29
7. Secondary antibodies for immunohistochemistry .....	29
8. Antibodies for flow cytometry and sorting .....	30

## LIST OF FIGURES

Figure	Page
1. Anatomy of the pancreas .....	1
2. Glucose-stimulated insulin secretion in $\beta$ -cells .....	2
3. Pancreatic morphogenesis .....	3
4. Islet morphology varies between mice and humans .....	4
5. Main strategies to restore functional $\beta$ -cell mass .....	5
6. PI3K/Akt and ERK/MAPK pathways contribute to human $\beta$ -cell proliferation .....	6
7. Selected inducers, markers, and functions of M1 and M2 macrophages .....	10
8. Proposed mechanisms of communication between $\beta$ -cells and endothelial cells .....	13
9. Schematic illustration of intracellular VEGFR2 signaling .....	14
10. ECM-cell interactions within islets .....	18
11. Islet microenvironment, modulated by VEGF-A signaling, promotes $\beta$ -cell regeneration .....	37
12. Acute ablation of VEGFR2 in ECs .....	38
13. VEGF-A induction and VEGFR2 inactivation in proliferative ECs .....	39
14. Islet changes following VEGFR2 knockout in proliferative ECs .....	40
15. VEGF-A induction and VEGFR2 inactivation in quiescent ECs .....	41
16. Islet changes following VEGFR2 knockout in quiescent ECs .....	42
17. Macrophage and ECM phenotypes after VEGFR2 knockout in quiescent ECs .....	43
18. ECs in developing human islets .....	44
19. Validation of the multipotent pancreatic progenitor marker GP2 in human tissue .....	51
20. Multipotent pancreatic progenitors are present in the developing human pancreas after birth .....	52
21. Purified GP2 <sup>+</sup> pancreatic progenitor cells give rise to ' $\beta$ -like' cells <i>in vitro</i> .....	53
22. NTPDase3 is expressed specifically in adult human $\beta$ -cells .....	54
23. Expression of NTPDase3 in adult pancreatic endocrine and exocrine cells .....	55
24. NTPDase3 antibody effectively and efficiently isolates $\beta$ -cells from live dispersed human islet cells .....	56
25. NTPDase3-based cell sorting method can be applied to islets from various disease states .....	57
26. Transcriptome analysis by RNA-seq reveals genes critical to $\alpha$ -cell function are differentially expressed in T1D $\alpha$ -cells .....	58
27. T2D $\alpha$ - and $\beta$ -cells show reduced expression of islet-enriched transcription factors and elevated expression of inflammatory markers .....	59
28. Detection of IV-injected NTPDase3 antibody in human islet graft on kidney capsule of NSG mice .....	60
29. Targeting NTPDase3 detects human $\beta$ -cells <i>in vivo</i> .....	61



## COMMON ABBREVIATIONS

Arx	aristaless
BM	basement membrane, of extracellular matrix
CD31	cluster of differentiation 31 (endothelial cell marker; also platelet endothelial cell adhesion molecule, PECAM-1)
Cdh5	cadherin 5, also vascular endothelial cadherin
Cdk	cyclin-dependent kinase
Col-IV	collagen type IV
Cre	Cre recombinase
CSF-1	macrophage colony-stimulating factor 1
CTGF	connective tissue growth factor
DM	diabetes mellitus
Dox	doxycycline
DT	diphtheria toxin
E	embryonic day
EC	endothelial cell
ECM	extracellular matrix
ERK	extracellular signal-regulated kinase
FACS	fluorescence-activated cell sorting
FAK	focal adhesion kinase
FGF	fibroblast growth factor
<i>fl</i>	flox, flanked by loxP sites
Fox	forkhead box
G(w)	gestational week
Gcg	glucagon
GCK	glucokinase
GDM	gestational diabetes
GP2	pancreatic secretory granule membrane major glycoprotein 2
GSIS	glucose-stimulated insulin secretion
HA	hyaluronic acid
hESCs	human embryonic stem cells
HFD	high fat diet
HGF	hepatocyte growth factor
hiPSCs	human induced pluripotent stem cells
Hnf	hepatocyte nuclear factor
HO-1	heme oxygenase 1
HS	heparan sulfate
IAPP	islet amyloid polypeptide
Iba1	ionized calcium-binding adaptor molecule 1 (macrophage marker)
ICAM	intracellular adhesion molecule
IL	interleukin
Ins	insulin

Isl1	islet 1, transcription factor
Maf	musculoaponeurotic fibrosarcoma oncogene homolog
MCP1	monocyte chemoattractant protein 1
MODY	maturity-onset diabetes of the young
Mrc1	mannose receptor C-type (M2 macrophage marker)
MSC	mesenchymal stem cell
NeuroD1	neurogenic differentiation 1
Ngn3	Neurogenin 3
Nkx6.1	NK6 homeobox 1
NO	nitric oxide
NOD	non-obese diabetic (mouse model)
NOS	nitric oxide synthase
NTPDase3	nucleoside triphosphate diphosphohydrolase 3
Pax	paired box
PDGF	platelet-derived growth factor
PDL	pancreatic duct ligation
Pdx1	pancreatic and duodenal homeobox 1
PG	proteoglycan
PI3K	phosphoinositide 3-kinase
PP	pancreatic progenitor
Ptf1a	pancreas specific transcription factor 1a
RIP	rat insulin promoter
RNA-seq	RNA-sequencing
scRNA-seq	single cell RNA-sequencing
STZ	streptozotocin
T1D	type 1 diabetes
T2D	type 2 diabetes
TGF $\beta$	transforming growth factor $\beta$
Tmx	tamoxifen
TNF $\alpha$	tumor necrosis factor $\alpha$
VCAM	vascular cell adhesion molecule
VEGF-A	vascular endothelial growth factor A
VEGFR1	vascular endothelial growth factor receptor 1
VEGFR2	vascular endothelial growth factor receptor 2
VEGFR2 <sup>i<math>\Delta</math>EC</sup>	<i>Cdh5-CreER</i> ; <i>VEGFR2</i> <sup>fl/fl</sup> mouse model of tamoxifen-inducible EC-specific VEGFR2 inactivation
$\beta$ VEGF-A	<i>RIP-rtTA</i> ; <i>TetO-VEGF</i> mouse model of doxycycline-inducible $\beta$ -cell-specific overexpression of human VEGF-A <sub>165</sub>
WD	withdrawal, from doxycycline

# CHAPTER I

## BACKGROUND AND SIGNIFICANCE

### The Pancreas

#### *Anatomy, physiology, and function*

The pancreas is a bifunctional organ composed of exocrine and endocrine compartments, each of which has distinct morphology and anatomical functions (**Fig. 1**). The exocrine compartment, which makes up nearly 98% of pancreatic mass, consists of acinar cells that secrete digestive enzymes into a branched network of ducts that drain into the duodenum, where the enzymes are activated<sup>1-3</sup>. Embedded within the exocrine tissue are small clusters of hormone-secreting endocrine cells called Islets of Langerhans, whose main purpose is to regulate glucose levels in the blood. The five endocrine cell types in the islet are  $\alpha$ -,  $\beta$ -,  $\delta$ -,  $\epsilon$ -, and PP cells, which secrete glucagon, insulin, somatostatin, grehlin, and pancreatic polypeptide, respectively. Regulation of blood glucose is coordinated mainly by  $\alpha$ - and  $\beta$ - cells, which are the most abundant endocrine cell types<sup>4,5</sup>.

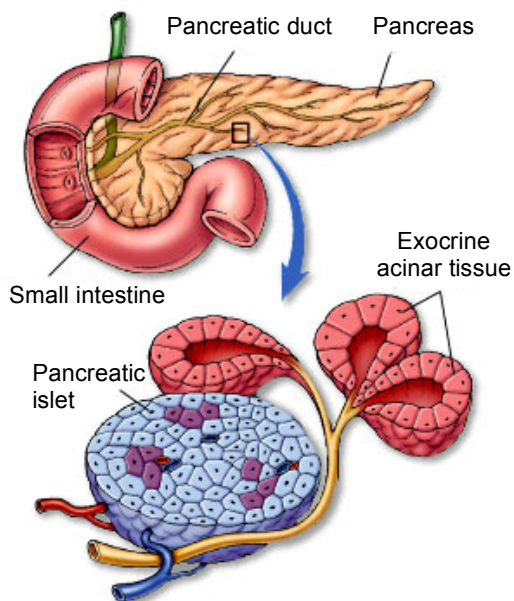


**Figure 1: Anatomy of the pancreas.** The pancreas is a bifunctional organ composed of exocrine tissue, which secretes digestive enzymes into the duodenum, and endocrine tissue, made up of islets that secrete hormones into the bloodstream. Image adapted from Saladin, 2001<sup>3</sup>.

Elevation of the blood glucose stimulates  $\beta$ -cells to secrete insulin, allowing insulin-sensitive tissues such as liver, muscle, and adipose tissue, to take up and store excess glucose as glycogen or fat. Conversely, when blood glucose is low, islet  $\alpha$ -cells secrete glucagon, which stimulates the liver to release glucose by breaking down stored glycogen or producing new glucose through gluconeogenesis. The process of glucose-stimulated insulin secretion (GSIS) is coordinated by a complex cascade of extracellular and intracellular signals<sup>6-8</sup> (**Fig. 2**). At low levels of blood glucose, ATP-sensitive  $K^+$  channels ( $K_{ATP}$  channels) are open, resulting in membrane hyperpolarization and closed  $Ca^{2+}$  channels. When blood glucose levels rise, glucose enters the  $\beta$ -cell through glucose transporters<sup>9</sup>, where its metabolic processing causes a rise in intracellular ATP and subsequent closure of  $K_{ATP}$  channels. This results in membrane depolarization, spurring calcium influx, release of additional calcium from intracellular stores, and exocytosis of insulin vesicles.

#### ***Pancreatic development and establishing $\beta$ -cell mass***

The pancreas develops from dorsal and ventral buds within the foregut endoderm<sup>2,10</sup>. Mouse pancreas development encompasses a “primary transition” from embryonic day (E) 9.5 to E12.5 and a “secondary transition” from E12.5 to birth<sup>11</sup> (**Fig. 3**). The primary transition is marked by bud formation and

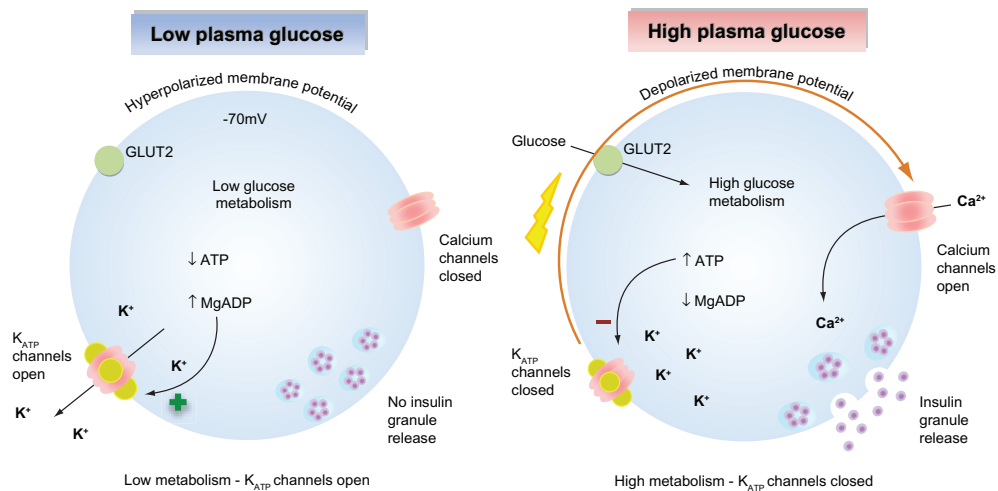


**Figure 2: Glucose-stimulated insulin secretion in  $\beta$ -cells.** Glucose enters the  $\beta$ -cells through the GLUT transporter and undergoes glycolysis, increasing the intracellular ATP/ADP ratio. This results in closure of ATP-sensitive potassium channels, membrane depolarization, and opening of voltage-gated calcium channels. Calcium influx causes exocytosis of insulin granules. Image from Lang & Light, 2010<sup>8</sup>.

pancreatic proliferation. The dorsal pancreatic bud evaginates at E9.5, followed by the ventral bud at E9.75, while epithelial cells form microlumens<sup>12-14</sup>. Epithelial cells at this stage express a number of pancreas-specific transcription factors (Pancreas specific transcription factor 1a, Ptf1a; Pancreatic and duodenal homeobox 1, Pdx1; Sex-determining region Y-box 9, Sox9) and receive growth and differentiation signals from surrounding mesenchymal cells<sup>15,16</sup>. Around E13, microtubules converge into a branched tube and epithelial cells form “tip” and “trunk” domains. In the distal tip lie multipotent Ptf1a<sup>+</sup> progenitors, which will become acinar, duct, and endocrine cells, whereas the trunk harbors bipotent progenitors expressing NK6 homeobox (Nkx6), which give rise to duct and endocrine cells.

The secondary transition includes pancreatic branching, cell differentiation, and pancreatic morphogenesis. During this time the “tip” region loses multipotency, generating only acinar cells, while the “trunk” produces duct and endocrine cells. Again, cell differentiation and morphogenesis are highly dependent on reciprocal signaling between the epithelium, mesenchyme, and blood vessels<sup>17,18</sup>. Unipotent, postmitotic progenitors that express Neurogenin 3 (Ngn3) give birth to each of the different endocrine cell types<sup>19-21</sup>. Islets are formed by delamination of Ngn3<sup>+</sup> epithelial cells that coalesce into clusters. Complex cascades of transcription factors define such differentiation. Key transcription factors for the  $\alpha$ -cell lineage include *Forkhead box A2 (Foxa2)*, *NK2 homeobox 2 (Nkx2.2)*, *Paired box 6 (Pax6)*, and *Aristaless (Arx)*. Differentiation of  $\beta$ -cells requires, among others, transcription factors *Musculoaponeurotic fibrosarcoma oncogene homolog B (MafB)*, *Pdx1*, *Pax4*, *Pax6*, *Islet 1 (Isl1)*, *Nkx2.2*, and *Nkx6.1*.

Importantly, although insulin<sup>+</sup>  $\beta$ -cells are observable in the mouse pancreas from E13.5, they do not attain functional maturity until postnatally. This is achieved by some of the same transcription factors involved in differentiation, such as *MafB*, *Isl1*, *Pdx1*, and *Ngn3*, but also involves *Neurogenic differentiation 1 (NeuroD1)*<sup>19</sup>, *MafA*<sup>22-24</sup>, and *Von Hippel-Lindau (Vhl)*<sup>25,26</sup>. Additionally, there is burst of postnatal  $\beta$ -cell proliferation in the mouse that is necessary for establishing mature  $\beta$ -cell mass. Transcriptional regulation of this process comes from factors including *Foxm1*<sup>27</sup>, *Isl1*<sup>28</sup>, *Survivin*<sup>29</sup>, and *Enhancer of zeste homolog 2 (Ezh2)*<sup>30</sup>.

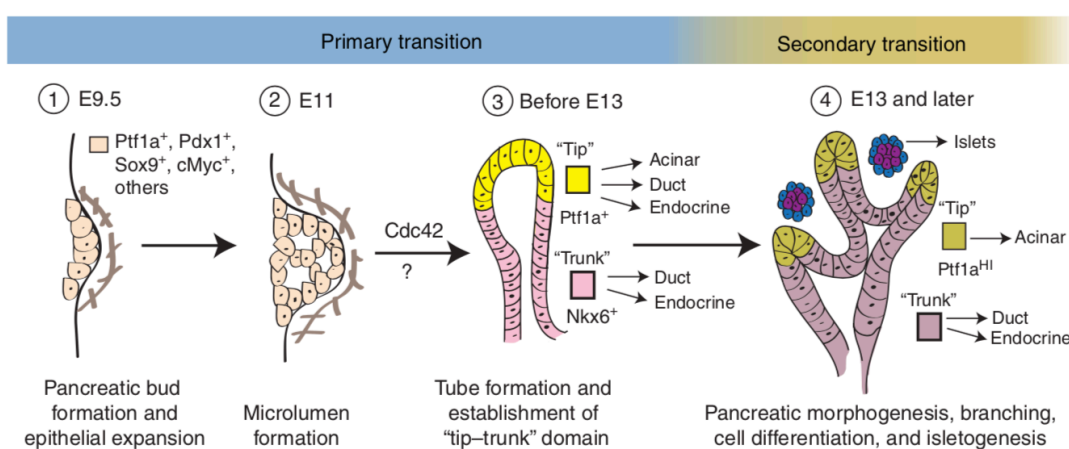


**Figure 3: Pancreatic morphogenesis.** Mouse pancreatic development includes "primary" (E9.5-E12.5) and "secondary" (E13-birth) transitions. Budding initiates at E9.5 (1), followed by epithelial proliferation and microlumen formation (2). Tubulogenesis establishes "trunk" and "tip" domains (3), the latter giving rise to ductal and endocrine cells. The secondary transition (4) encompasses pancreatic branching, cell differentiation, acinar cell expansion, and islet formation. Image from Benitez *et al.*, 2012<sup>11</sup>.

Our knowledge of human pancreas development, unlike that of the mouse, comes largely from cross-sectional analysis of histological specimens and is much more limited. Molecular markers of pancreatic differentiation are largely conserved in mouse and human, as are the general processes of bud formation, epithelial migration, and branching morphogenesis<sup>31-33</sup>. Insulin-expressing cells are first observed at gestational week (G) 7.5w, remaining the most abundant endocrine cell type for the first trimester<sup>31,34</sup>. The composition of  $\alpha$ -,  $\beta$ -, and  $\delta$ -cells is approximately 1:1:1 by the last trimester, with this ratio maintained through birth<sup>34-36</sup>. Endothelial cells are associating with clusters of endocrine cells at G10w, with vascular structures observable at G14w<sup>37</sup>. This thesis describes work that is adding to our knowledge of human pancreas development.

### Differences between human and rodent islets

Although many aspects of pancreatic islet morphology and function are conserved among mammals, there are important differences in cellular composition, gene expression, and function. First, the composition of endocrine cells is much more variable in humans, with  $\beta$ -cells making up 50-70% of human islet mass compared to 75-80% in mouse<sup>4,5</sup>. Additionally, the cell arrangement in mouse islets is such that  $\beta$ -cells compose the core of the islet with  $\alpha$ - and  $\delta$ -cells mainly occurring around the periphery, which is in contrast to the adult human islet, in which  $\alpha$ -,  $\beta$ -, and  $\delta$ -cells are intermingled<sup>4,38</sup> (**Fig. a-b**). As a result, human islets display many more  $\alpha$ -to- $\beta$ -cell contacts than do mouse islets<sup>38</sup> and may rely on different mechanisms to synchronize pulsatile insulin release<sup>4</sup>. The vascular architecture of human islets is also quite striking compared to that of rodents, with human islets exhibiting fewer blood vessels than mouse islets<sup>39</sup> (**Fig. 4c-d**).

While the general process of GSIS is conserved between rodents and humans, a number of distinctions have been noted. Among these are the fact that humans have only one insulin gene (*INS*), while rodents have two (*Ins1*, *Ins2*), and GLUT-1 is the major glucose transporter in human  $\beta$ -cells rather than GLUT-2<sup>9,40,41</sup>. As a result of these and other metabolic nuances, basal insulin secretory rate differs between human and rodent islets<sup>42</sup>. There are also subtle but critical distinctions in gene expression of transcription factors<sup>43,44</sup> and antioxidant enzymes<sup>44,45</sup>, as well as epigenetic signatures that influence proliferative capacity<sup>46,47</sup>.

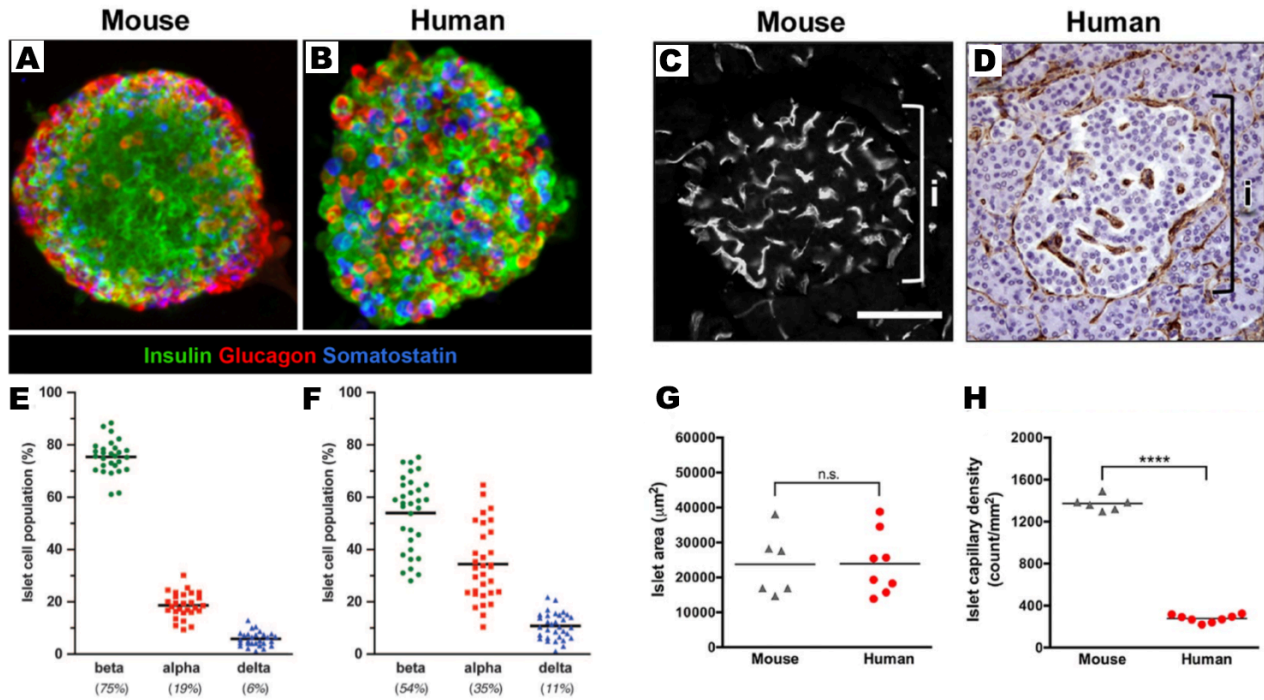


**Figure 4: Islet morphology varies between mice and humans.** (A-B) Mouse and human islets labeled for insulin (green), glucagon (red), and somatostatin (blue). (C-D) Islet vasculature visualized by endothelium-binding lectin-FITC (C, mouse) or endothelial cell marker CD34 (D, human). (E-F) Analysis of endocrine cell composition. (G-H) Islet area and capillary density in mouse and human islets. Horizontal bars in E-H represent the mean of each population. Images adapted from Brissova *et al.*, 2005<sup>5</sup> and 2015<sup>39</sup>.

## Diabetes

### *Epidemiology and pathophysiology*

Diabetes mellitus (DM) is a metabolic disorder characterized by abnormally elevated blood glucose levels, or hyperglycemia. The National Diabetes Statistics Report estimates that 30.2 million U.S. adults—over 12% of the adult population—had diabetes in 2015, with another nearly 40% having elevated fasting glucose levels or elevated post-meal glucose considered to be “prediabetes”<sup>48</sup>. Although we often refer to ‘diabetes’ as a single disorder, it is actually quite heterogeneous. About 5% of all diabetes cases are classified as type 1 DM (T1D)<sup>48</sup>, in which autoimmune destruction of  $\beta$ -cells renders patients unable to maintain blood glucose levels through endogenous insulin production. These cases are often diagnosed during childhood and require lifelong treatment with exogenous insulin. Type 2 DM (T2D) represents the bulk of DM patients, about 90-95%, who develop insulin resistance in peripheral tissues that requires increasing insulin levels to lower blood glucose<sup>48</sup>. Individuals become hyperglycemic when their  $\beta$ -cells are no longer able to meet the increased insulin demand, but depending on the degree of  $\beta$ -cell dysfunction, symptoms may be managed by lifestyle modifications or oral medications before resorting to exogenous insulin. Additionally, some women who fail to adapt to the metabolic stress of pregnancy develop gestational diabetes mellitus (GDM), which may occur in 4-14% of all pregnancies and is an established risk factor for later development of T2D<sup>49,50</sup>. While GDM and T2D undoubtedly share some underlying causes and mechanisms of  $\beta$ -cell dysfunction, there is also evidence for genetic and environmental causes that are unique to GDM<sup>51-53</sup>, and epigenetic changes

induced by maternal hyperglycemia have far-reaching effects on glucose tolerance in offspring<sup>54,55</sup>. Finally, there is a small subset of individuals (less than 2% of all DM cases) whose diabetes arises from a single genetic mutation, usually of *hepatocyte nuclear factor (HNF) 1A*, *HNF4A*, or *glucokinase (GCK)*, which negatively impacts  $\beta$ -cell function<sup>56</sup>. These mutations are autosomal dominant forms of DM that are collectively known as maturity-onset diabetes of the young (MODY). MODY cases are sometimes misdiagnosed as T1D, though many can and should be treated by oral medication rather than exogenous insulin.

### **Treatments aimed at $\beta$ -cell replacement**

Because  $\beta$ -cell loss and/or dysfunction are hallmarks of all types of DM, there is great interest in developing methods to restore  $\beta$ -cell mass and function in affected patients. These efforts, summarized in **Fig. 5**<sup>57</sup>, include providing  $\beta$ -cells from exogenous sources (including transplantation of cadaveric islets<sup>58,59</sup> or  $\beta$ -like cells derived from pluripotent stem cells, hPSCs<sup>60-62</sup>) and endogenous sources (including expansion of existing  $\beta$ -cells<sup>63-65</sup> or  $\beta$ -cell formation through transdifferentiation of other pancreatic cell types<sup>66-69</sup> and differentiation of multipotent precursors<sup>70-72</sup>).

Although exogenous  $\beta$ -cell replacement can be a very effective treatment for diabetes, immune challenges and scarcity of islets available for  $\beta$ -cell transplant make this an impractical long-term therapeutic tool. Differentiation of hPSCs to  $\beta$ -like cells has made significant progress in the past decade, using knowledge from developmental biology to create a protocol for sequential stimulation and inhibition of specific developmental pathways with growth factors and small molecules<sup>72-75</sup>. However, there are challenges with these  $\beta$ -like cells that need to be overcome related to lower insulin secretion compared to human  $\beta$ -cells, and capacity and efficiency with which these cells can be produced.

Endogenous  $\beta$ -cell replacement has been explored extensively in mice, where severe  $\beta$ -cell ablation has led to conversion of  $\beta$ -cells from  $\alpha$ - and  $\delta$ - cells<sup>76-78</sup> and reprogramming of  $\alpha$ -cells has successfully

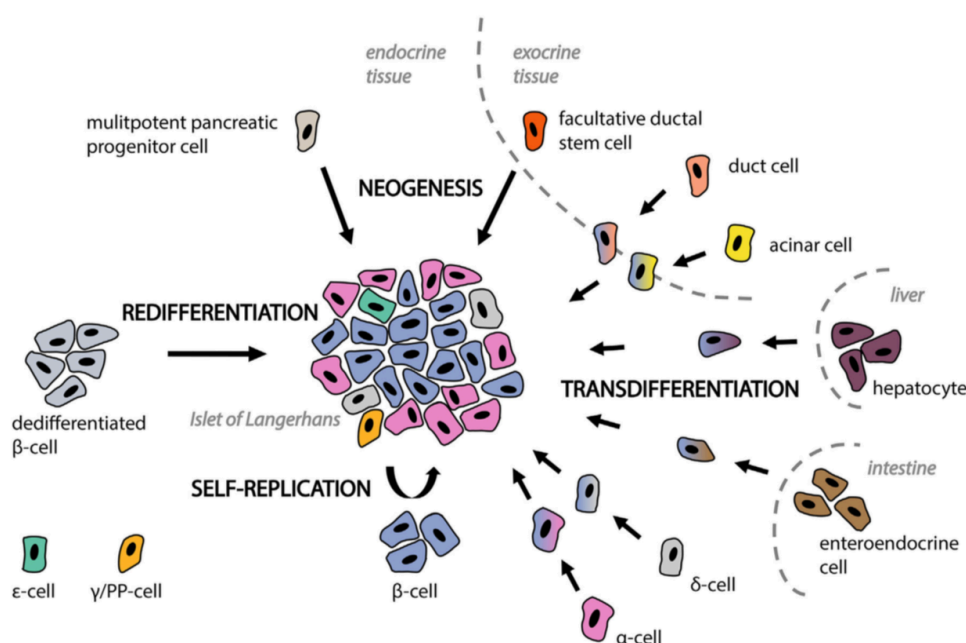


**Figure 5: Main strategies to restore functional  $\beta$ -cell mass.** Potential sources of  $\beta$ -cells include existing  $\beta$ -cells (self-replication), progenitor or de-differentiated cells (neogenesis, redifferentiation), and other islet or extra-islet cell types (transdifferentiation). Image from Tritschler *et al.*, 2017<sup>57</sup>.

restored  $\beta$ -cell mass to reverse diabetes<sup>66,67,79</sup>. Exocrine cells may also be converted into  $\beta$ -like cells with cytokine and growth factor treatment<sup>68,69,80</sup>, and recent work using gut organoids has even showed that gastrointestinal cells are capable of transdifferentiation into insulin-responsive cells<sup>81,82</sup>. Like with  $\beta$ -cell differentiation from hPSCs, there are many challenges to overcome before these transdifferentiation strategies are tested in clinical trials. Because of this, harnessing the ability of  $\beta$ -cells to proliferate *in vivo*, even if at limited capacity, offers an attractive alternative in which an individual's  $\beta$ -cells could intrinsically improve or restore  $\beta$ -cell function.

### **Proliferation of endogenous $\beta$ -cells**

Treatments for stimulation of endogenous  $\beta$ -cell proliferation have taken two approaches: (1) harnessing the mechanisms, growth factors, hormones, and signals used under normal physiology (neonatal, pregnancy, insulin resistance); and (2) identifying small molecules and/or compounds that induce proliferative pathways. Unfortunately, many of the compounds/pathways that have been studied in rodent  $\beta$ -cells do not promote replication in human  $\beta$ -cells<sup>63,64,83</sup>, while other proliferative mechanisms, such as the non-canonical Janus kinase (JAK)/signal transducers and activators of transcription (STAT) signaling, and signaling through serotonin membrane receptors, have not yet been extensively investigated in human  $\beta$ -cells<sup>64,84,85</sup>. The information presented here will focus on human  $\beta$ -cells, as promoting human  $\beta$ -cell proliferation is the ultimate therapeutic goal.

### **Mechanisms of $\beta$ -cell proliferation**

It is likely that balancing the activity of multiple pathways will be necessary to promote proliferation while

maintaining  $\beta$ -cell identity and function. A few of the key pathways and molecules are depicted in **Fig 6**, and discussed below.

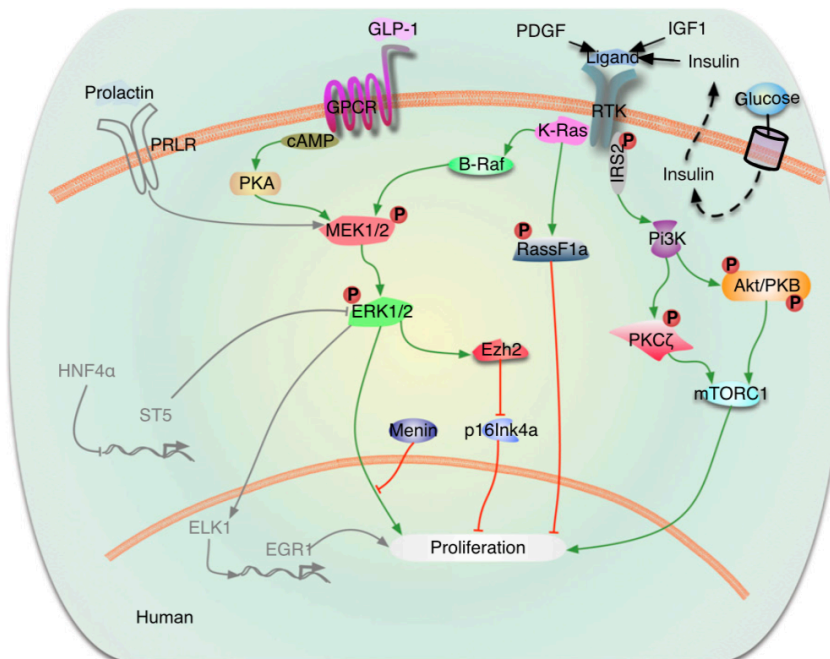


**Figure 6: PI3K/Akt and ERK/MAPK pathways contribute to human  $\beta$ -cell proliferation.** Growth factors (PDGF, IGF-1) bind tyrosine kinase receptors (RTK) to activate PI3K/Akt and ERK1/2 signaling, while other incretin hormones (GLP-1) initiate signaling through GPCRs. Gray lines indicate molecules/pathways that are known to exist in rodents but unknown in human  $\beta$ -cells. Image from Stewart *et al.*, 2015<sup>64</sup>.

The canonical phosphoinositide 3-kinase (PI3K) pathway is one major source of proliferative signals, activating protein kinase C (PKC) and protein kinase B (PKB/Akt)<sup>63,83</sup>. Studies of intact and dispersed human islets overexpressing Akt directly have shown increased  $\beta$ -cell proliferation<sup>86</sup>. PKC $\zeta$ , which is less often studied as part of the PI3K/Mechanistic target of Rapamycin (mTOR) cascade, was recently shown to be necessary for “compensatory”



human  $\beta$ -cell replication induced by glucose<sup>87</sup>. Indirect activation of Akt by Transforming growth factor beta (TGF $\beta$ ) has led to context-dependent effects on  $\beta$ -cell proliferation<sup>88</sup>, which suggests that ligands such as TGF $\beta$  may activate multiple signaling cascades simultaneously. Leibiger and colleagues recently showed that PI3K class II  $\alpha$  (PI3K-C2 $\alpha$ ) knockdown promoted insulin receptor B (IR-B)/extracellular signal-regulated kinase (ERK) signaling, inducing proliferation, while still maintaining alternate PKB/Akt signaling necessary for basal  $\beta$ -cell metabolism<sup>89</sup>.

Modulation of cell cycle machinery is another mechanism of  $\beta$ -cell proliferation that has been of recent focus. In the transition from G1 to S phase, cyclins and cyclin-dependent kinases (CDKs) are sequentially phosphorylated to drive proliferation. The machinery for cell cycle progression is largely conserved between rodent and human  $\beta$ -cells; however, there are a few key differences. Notably, the  $\beta$ -cells of human islets express high levels of CDK6 (absent in rodent  $\beta$ -cells) and low levels of cyclin D2 (critical to rodent  $\beta$ -cell proliferation)<sup>83</sup>. Recent studies have enumerated additional subtlety; for example, although CDKs 4 and 6 and cyclin D3 are readily detectable in both rodent and human  $\beta$ -cells, other cyclins that are abundant in rodent  $\beta$ -cells are not consistently expressed by human  $\beta$ -cells<sup>90,91</sup>. Even manipulation of the most conserved cyclins and CDKs gave mixed results in different systems. For example, Cdk5 activation induced proliferation in rodent  $\beta$ -cells, but has previously been implicated in apoptotic pathways of various human cell types<sup>92</sup>. A key inter-specific difference is the subcellular localization of cell cycle molecules. In human  $\beta$ -cells the majority of cyclins and CDKs are sequestered in the cytoplasm rather than the nucleus, which may contribute to the reluctance of human  $\beta$ -cells to proliferate basally<sup>90,93</sup>. Indeed, there is evidence that cytoplasmic and nuclear trafficking play a regulatory role in human  $\beta$ -cell proliferation<sup>94</sup>. Once in the nucleus, cell cycle molecules can be influenced by additional proteins like menin, which further controls  $\beta$ -cell transcription and replication by modulating methylation activity<sup>95</sup>. Finally, there is considerable variability between experiments using human  $\beta$ -cells – activation of cyclin isoforms induced  $\beta$ -cell proliferation in human islet grafts<sup>90</sup>, but not in the human cell line EndoC-bH1<sup>96</sup>.

### **Hormone and growth factor activity**

Some peptide hormones, including parathyroid hormone-related protein (PTHrP), stimulate  $\beta$ -cell replication *in vitro*<sup>97,98</sup>, and prolactin is a known mitogen of compensatory  $\beta$ -cell proliferation during rodent pregnancy<sup>99,100</sup>. Recently it was shown that prolactin receptor (PRLR)-JAK2-STAT5 signaling is not prominent in human  $\beta$ -cells; interestingly, however, murine Stat5a induced proliferation of human  $\beta$ -cells<sup>84</sup> and there is evidence that prolactin may augment traditional T1D therapies by reducing lymphocytic infiltration<sup>101,102</sup>. Signaling of steroid hormones, such as estrogens, androgens, and progesterone, also modulate proliferation and appear disrupted under diabetic conditions<sup>64,100</sup>. The amino acid derivative serotonin, extensively studied during  $\beta$ -cell adaption during pregnancy<sup>54,103</sup>, also shows potential for inducing *de novo*  $\beta$ -cell proliferative activity<sup>55</sup>. Additionally, hepatocyte growth factor (HGF)<sup>54,104,105</sup> may exert proliferative effects through the PKC pathway<sup>97</sup>. Altered insulin-like growth factor 1 (IGF-1) signaling, via phosphorylation of insulin receptor substrate 2 (IRS-2) and glycogen synthase kinase 3 (GSK3)<sup>106</sup>, promoted  $\beta$ -cell proliferation in both isolated and transplanted human islets incubated with protease inhibitor SerpinB1<sup>107</sup>. Identifying growth factors that induce human  $\beta$ -cell proliferation continues to be a research focus in the field, as many factors used to reverse diabetes in mice have delivered unpromising results when tested in human islets.

## Changes in glucose metabolism

There is robust data indicating that insulin resistance and/or hyperglycemia in rodents stimulates  $\beta$ -cell proliferation<sup>63,65,87</sup>. Porat and colleagues showed that glucose-induced proliferation was regulated by GSK metabolism, with increased glycolytic rate causing the  $\beta$ -cell to upregulate proliferative pathways<sup>65</sup>. Carbohydrate response element binding protein (ChREBP) was essential for this downstream proliferative response<sup>63</sup>, as was PKC $\zeta$ -mediated mTOR/cyclin D2 activity<sup>87</sup>. While stimulation at very high glucose concentration increased  $\beta$ -cell proliferation in isolated human islets, lower levels of glucose were not sufficient to produce this effect<sup>87</sup>. Dai and colleagues recently investigated human  $\beta$ -cell proliferation *in vivo*, performing human islet transplants in immunodeficient mice and then induction of hyperglycemia  $\pm$  insulin resistance; they found that neither chronic nor acute hyperglycemia stimulated  $\beta$ -cell proliferation in human islet grafts, in contrast with grafts of mouse islets<sup>108</sup>. These data again underscore an apparent difference in the proliferative capacity between rodent and human islets.

## Small molecules

Using a candidate molecule approach, several classes of drugs, hormones or growth factors such as peroxisome proliferator-activated receptor gamma (PPAR $\gamma$ ) agonists, glucagon-like peptide 1 receptor (GLP-1R) agonists, dipeptidyl peptidase 4 (DPP-4) inhibitors, glycogen synthase kinase 3 beta (GSK3 $\beta$ ) inhibitors, prolactin, IGF-1, HGF, and PTHRP have been tested for the ability to stimulate  $\beta$ -cell proliferation. While several of these have clear activity in rodent islets, none have proven useful in stimulating human  $\beta$ -cell proliferation. This inability to stimulate human  $\beta$ -cell proliferation has led to intense efforts by several groups to use high-throughput small molecule screening approaches to identify compounds or small molecules that stimulate  $\beta$ -cell proliferation<sup>109-112</sup>. Interestingly, recent, independent discoveries have identified the dual-specificity tyrosine-regulated kinase 1a (DYRK1A) as the likely target of compounds such as harmine and 5-iodotubercidin, both of which stimulate adult human  $\beta$ -cell proliferation<sup>110,111</sup>. Another group was able to stimulate adult human  $\beta$ -cell proliferation using an RNA interference strategy to silence cell cycle-dependent kinase inhibitors CDKN2C/p18 or CDKN1A/p21, suggesting that p18 and p21 may be attractive targets to promote  $\beta$ -cell proliferation<sup>109</sup>. Efforts to identify additional compounds and to optimize identified compounds are underway. One challenge is that no currently identified pathway is  $\beta$ -cell specific; thus an approach to only deliver the active compound to  $\beta$ -cells will be required. A portion of this thesis describes a new  $\beta$ -cell target that may be useful in delivering such compounds.

## Other potential targets

Based on the results of many molecules inducing  $\beta$ -cell proliferation in rodents, several groups have focused on identifying mitogens, receptors, and signaling molecules that have not previously or extensively been studied in  $\beta$ -cells. For example, aminopyrazine compounds, which are robustly mitogenic in human  $\beta$ -cells, likely target GSK3 $\beta$  and DYRK1A<sup>113</sup>. Membrane-bound sodium glucose co-transporter 2 (SGLT2) inhibitor has an insulin-independent effect on  $\beta$ -cells, increasing  $\beta$ -cell mass and proliferation rate when  $\beta$ -cells are destroyed using the toxin streptozotocin (STZ)<sup>114</sup>. Transcription factor PAX4, which is required for  $\beta$ -cell maturation, appears elevated in a subset of mature  $\beta$ -cells that proliferate preferentially during adaptive  $\beta$ -cell expansion<sup>115</sup> and induced proliferation in cultured human islet cells<sup>116</sup>. Engineered peptides mimicking extracellular proteins increased numerous proliferative indexes and  $\beta$ -cell-specific gene expression in rat INS-1 cells; proposed mediators include integrin

receptors and subsequent activation of focal adhesion kinase (FAK) and ERK<sup>117</sup>. Circulating fatty acids such as palmitate and oleate, which are elevated considerably during pregnancy, had synergistic effects in the presence of prolactin-induced  $\beta$ -cell proliferation<sup>118</sup>. In certain contexts, lipids have also preserved  $\beta$ -cell proliferative capacity in non-pregnant rodents<sup>119</sup>.

### **Pancreatic Islet Microenvironment**

Pancreatic islets are highly vascularized mini-organs, and although islets make up only 1-2% of total pancreatic mass, they receive a disproportionately larger fraction of blood flow than the surrounding exocrine tissue<sup>120,121</sup>. In addition, the capillary network within the islet is thicker, denser, and more tortuous<sup>122,123</sup>, ensuring that endocrine cells have adequate access to gas exchange, nutrition, and waste removal. Vascular endothelial cells (ECs) are highly fenestrated, allowing endocrine cells to rapidly sense and secrete hormones directly into the bloodstream. Pericytes, which are associated with ECs and reside in the shared basement membrane (BM), help regulate vascular contraction; their loss compromises vascular perfusion and EC membrane structure<sup>124</sup>. They also secrete molecules that promote EC differentiation and maturation<sup>124,125</sup> and  $\beta$ -cell function<sup>126</sup>. Their depletion in islets results in reduced insulin content and impaired GSIS<sup>127</sup> as well as impaired  $\beta$ -cell proliferation<sup>128</sup>.

The islet is innervated by parasympathetic, sympathetic, and sensory nerves, which help coordinate insulin secretion and response to other environmental cues<sup>129,130</sup>. Autonomic axons directly contact endocrine cells in the mouse pancreas, while in human islets, these nerves are closely associated with capillaries and axons preferentially innervate smooth muscle cells<sup>130-132</sup>. Cell-to-cell communication is also mediated by extracellular matrix (ECM), including a peripheral, discontinuous capsule that separates the islet from surrounding endocrine tissue. In mouse, ECs produce the only intra-islet ECM<sup>133</sup>, whereas in contrast, human islet endocrine cells make an additional basement membrane that is distinct from that of the endothelium<sup>134</sup>. In both species, the islet microenvironment encompasses the interface between many different cell types, including endocrine cells, ECs, macrophages, nerves, and fibroblasts. The respective contributions of macrophages, ECs, and ECM will be discussed in detail below.

### ***Macrophages***

Macrophages are specialized immune cells of myeloid lineage, derived during embryogenesis and maintained through production of adult hematopoietic stem cells in the bone marrow. Upon immune assault or chemotactic cue, monocytes can leave the circulation, undergoing extravasation through blood vessel wall and differentiating into macrophages once they reach the target tissue. They are among the first responders to sites of injury and help to rapidly induce cell signaling cascades that mobilize lymphocytes, neutrophils, and other monocyte lineages. In addition to functioning as phagocytes, they also secrete various cytokines, such as interleukin (IL)-1 $\beta$ , IL-6, IL-12, IL-23, tumor necrosis factor  $\alpha$  (TNF $\alpha$ ), and nitric oxide synthase 2 (NOS2), that provide chemotactic cues facilitating a coordinated immune response<sup>135-138</sup>.

Though macrophages were initially defined as a cell population based on their morphology and

phagocytosis ability during the immune response, more recent discoveries of their tissue restorative effects prompted a new classification that distinguishes them functionally<sup>136,139,140</sup>. Pro-inflammatory “M1” macrophages are classically activated by apoptotic cells, IgG complexes, toll-like receptor (TLR) ligands, and cytokines such as interferon gamma (IFN $\gamma$ ), and play key roles in immune surveillance and inflammatory response<sup>141,142</sup>. They express a canonical set of inflammation-associated signaling genes that includes *Il12b*, *Il1b*, *Tnf*, *Monocyte chemoattractant protein 1 (Mcp1)*, and *Cyclooxygenase 2 (Cox2)*<sup>143-145</sup>. In contrast, alternately activated or “M2” macrophages are considered anti-inflammatory, sensing and responding to heightened immune activity induced by M1 macrophages<sup>146-148</sup>. Maintaining IL-10 and TGF $\beta$  expression to suppress inflammation, M2 macrophages express a common signature of lipoproteins (CD11c; CD206, CD163, CD14) as well as distinct metabolic genes (*Arginase 1*, *Arg1*; *Resistin like beta*, *Retnlb*)<sup>136,149-154</sup>. **Fig. 7** depicts some key characteristics of M1 and M2 phenotypes. Debate is ongoing in the macrophage community as to the usefulness of segregating macrophages into distinct classes of M1 or M2, especially due to our expanding knowledge of macrophage plasticity and the capacity for interconversion between phenotypes<sup>140,155,156</sup>. This has led many to adopt a more fluid concept of classification that exceeds functional gene expression and acknowledges the dynamic nature of macrophage populations<sup>157-159</sup>. Technological advancements have further accelerated the ability to generate detailed genotypic arrays<sup>160</sup>, and the present literature employs phrases such as “M1-like” or “M2-like” to describe context-specific macrophage function<sup>140,161-163</sup>.

In addition to their classification related to phenotype and gene expression profile, macrophages can also be grouped depending on whether they reside in a particular tissue type (self-renewing “resident”

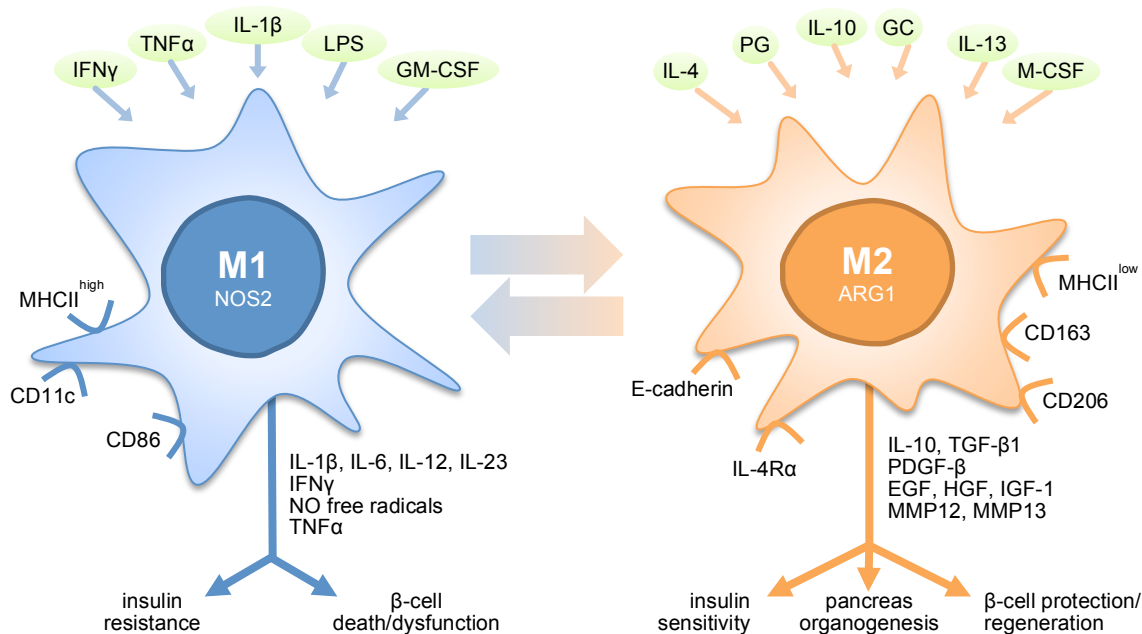


**Figure 7: Selected inducers, markers, and functions of M1 and M2 macrophages.** Effector molecules shown above cells, with secreted factors and effects on pancreas biology shown beneath. Abbreviations: Arg, arginase; CD, cluster of differentiation; EGF, epidermal growth factor; GCs, glucocorticoids; GM-CSF, granulocyte-macrophage colony-stimulating factor; HGF, hepatocyte growth factor; IFN, interferon; IGF, insulin-like growth factor; IL, interleukin; M-CSF, macrophage colony-stimulating factor; MHC, major histocompatibility complex; MMP, matrix metalloproteinase; NO, nitric oxide; NOS, nitric oxide synthase; PDGF, platelet-derived growth factor; PG, prostaglandin; TGF, transforming growth factor; TNF, tumor necrosis factor. Image adapted from Van Gassen *et al.*, 2015<sup>146</sup>.

macrophages) or differentiate from circulating monocytes that home to tissue in response to a stimulus (“recruited” macrophages)<sup>140,146,164,165</sup>. Resident macrophage populations themselves differ considerably in different tissues<sup>166</sup>. Recruited macrophages populations tend to engage in the initial inflammatory immune response<sup>167-169</sup>, whereas resident macrophages become activated during the resolution of inflammatory phase<sup>146,169</sup>. Still, resident and recruited populations are not always easily parsed, and likely have much more functional plasticity than is currently understood<sup>149</sup>.

### **Macrophages in pancreatic development and homeostasis**

Macrophage progenitors can be detected as early as E12.5 in mouse, and mature fetal macrophage expansion is required for successful development of  $\beta$ -cells<sup>170</sup>. This effect is mediated by macrophage colony-stimulating factor 1 (CSF-1), which is produced by endothelial cells<sup>162</sup> and fibroblasts<sup>152</sup> and facilitates macrophage expansion that is necessary for angiogenesis. Accordingly, macrophage-deficient (Csf1<sup>op/op</sup>) mice<sup>171</sup> exhibit impaired pancreatic islet architecture, including greatly reduced  $\beta$ -cell mass that persists through adulthood<sup>172</sup>.

As a whole, islet-associated hematopoietic cells (CD45<sup>+</sup>; representing 6-8% of all islet cells)<sup>173</sup> can be separated using flow cytometry based on a typical macrophage “signature,” with cell surface markers F4/80, CD11b, CD11c, CD64, and major histocompatibility complex class II (MHC-II)<sup>151</sup>. A recent analysis suggested that this resident endocrine macrophage population exhibited a gene expression profile skewed toward M1 (high levels of *Il1b*, *Tnfa*)<sup>151</sup>, which was relatively consistent with previous studies<sup>170,173</sup>, although a few groups have reported a second resident population with differential expression of MHC-II (MHC-II<sup>lo</sup>) that seemed to be more M2-like<sup>146</sup>. Islet-associated macrophages originate from hematopoietic stem cells and are replaced by circulating monocytes at extremely low rates.

Compared to islet macrophages, hematopoietic cells in exocrine tissue were much more heterogeneous in F4/80 and CD11b expression, as well as that of other surface markers<sup>151</sup>. RT-PCR analysis indicated that they predominantly expressed M2 transcripts (*Retnlb*; *Macrophage galactose-type lectin*, *Mgl*)<sup>151</sup>. Interestingly, however, two subpopulations emerged that slightly favored different M2 genes; CD206<sup>+</sup> cells upregulated *Il10*, whereas CD206<sup>-</sup> cells expressed *Chitinase-like protein 3* (*Chil3*)<sup>151</sup>. Moreover, elegant parabiosis experiments demonstrated that macrophages in the CD206<sup>-</sup> subpopulation were actually replaced by circulating cells at higher frequently than either CD206<sup>+</sup> or endocrine-associated macrophages<sup>151</sup>. Together, these findings highlight the extreme diversity of myeloid cells residing in the pancreatic exocrine tissue compartment and suggest functional differences that warrant future investigation.

### **Macrophages in tissue injury and inflammation**

Models of acute inflammation in pancreatic exocrine tissue show that inflammatory M1 macrophages flock to injury sites during the initial peak response<sup>139,147,149,152,174</sup>, with evidence that M2 macrophages gradually accumulate as inflammation subsides<sup>152</sup>. This second wave of macrophage activation has been experimentally linked to specific regulatory cytokines— for example, upregulation of IL-6, IL-8, MCP-1, and CSF-1— that sustain recruitment of M2 macrophages critical for tissue repair<sup>142,152</sup>. If the ability to resolve inflammation is compromised, inflammation persists and robustly impairs the healing

process<sup>149,175</sup>. Thus, macrophages seem to be critical not just for curbing inflammation, but also for facilitating tissue morphogenesis and wound healing<sup>137,176,177</sup>. Such “restorative” macrophage populations have emerged in a variety of tissues, including skeletal muscle<sup>155,178-180</sup>, liver<sup>181,182</sup>, kidney<sup>183</sup>, and neurons<sup>156,184-186</sup>, where they provide signals necessary for recovery following injury.

There is growing evidence that macrophages are involved in both the onset and progression of T2D<sup>135,165,187-189</sup>, with chronic inflammation observed in mouse models of T2D<sup>140,190</sup> and tissues from T2D human pancreatic donors<sup>189,191</sup>. At disease onset in *db/db* mice, resident islet-associated macrophage populations increased about fourfold, with enhanced recruitment of pro-inflammatory CD68<sup>+</sup> F4/80<sup>-</sup> cells<sup>140</sup>. Some reports have proposed that T2D-associated inflammation stems from elevated levels of free fatty acids (FFA), which can activate secretion of stress-related cytokines by islet cells and perpetuate pro-inflammatory infiltration of M1 macrophages<sup>135,190,192,193</sup>. Similarly, deposition of islet amyloid polypeptide (IAPP) in islets from T2D donors correlated with increased numbers of islet-associated macrophages<sup>188,191</sup>; amyloidogenic human IAPP is known to activate macrophage production of both pro-inflammatory (IL-1, IL-6, TNF $\alpha$ ) and anti-inflammatory (IL-10; IL-1 receptor antagonist, IL-1Ra) cytokines when it is expressed in islets of transgenic mice<sup>165</sup>. Finally, activation of endocrine cell TLR-2 and TLR-4, the ligands of which are often elevated in T2D patients<sup>195</sup>, promotes M1 macrophage recruitment that ultimately impairs  $\beta$ -cell insulin production and function<sup>135,189,196</sup>. Most likely, a combination of these pathways collectively create a condition of chronic “injury” that leads to  $\beta$ -cell deterioration. There is some evidence from mouse models that cytokine expression profiles shift in later stages of T2D, suggesting that fibrosis of pancreatic islets may be a result of unresolved inflammation<sup>140</sup>.

In addition to responding to environmental cues of inflammation, macrophages also seem to prevent the onset of inflammatory response. In T1D the immune system specifically targets  $\beta$ -cells, but decreased incidence of disease is correlated with elevated levels of M2 macrophages in the gut and pancreas<sup>150,197</sup>. Recent experiments indicate that these effects can be mediated by secreted peptides with pro-proliferative, anti-inflammatory effects<sup>197</sup>, and further experiments will be necessary to determine whether such peptides can be manipulated to prevent the onset of autoimmune  $\beta$ -cell destruction. Additionally, several groups have identified activity of the heme oxygenase 1 (HO-1) pathway, whose induction confers protection from oxidative damage<sup>198,199</sup> and protects pancreatic islets from T1D-associated inflammation<sup>153,161,174,200</sup>.

### **Macrophages in $\beta$ -cell regeneration**

With demonstrated requirement for macrophages in the regeneration of other tissues, macrophage populations in the pancreatic islet have garnered recent interest. Our group first reported the importance of macrophages in  $\beta$ -cell regeneration using a mouse model in which vascular endothelial growth factor A (VEGF-A)-induced  $\beta$ -cell loss was followed by  $\beta$ -cell regeneration; partial bone marrow ablation demonstrated that recruitment of macrophages to pancreatic islets was necessary for the  $\beta$ -cell proliferative response<sup>201</sup>. Criscimanna and colleagues made a similar observation with  $\beta$ -cell injury induced by diphtheria toxin (DT), where the initial appearance of a large islet-associated M1 population was followed by a shift to more M2-like macrophages<sup>202</sup>. By flow cytometry they documented a progressive loss of M1 marker (TNF $\alpha$ <sup>+</sup> IL-6<sup>+</sup>) expression and gain of M2 (IL-10<sup>+</sup> CD206<sup>+</sup>) phenotype that corresponded to the peak of  $\beta$ -cell regeneration<sup>202</sup>. Ablating either resident macrophages or circulating

monocytes strongly impaired this  $\beta$ -cell regenerative response<sup>202</sup>. Even when an injury inflames exocrine tissue and leaves  $\beta$ -cells intact, as is the case in pancreatic duct ligation (PDL), Xiao and colleagues documented a proliferative  $\beta$ -cell response that was secondary to heavily increased infiltration of M2 macrophages around islets<sup>139</sup>. They proposed that macrophage-secreted TGF $\beta$ 1 and epidermal growth factor (EGF) mediated  $\beta$ -cell proliferation, a finding that reinforces the paradigm of cytokine and growth factor production that has been put forward by others as the means by which macrophages modulate  $\beta$ -cell growth<sup>146,147</sup>.

### Endothelial cells

Like other vascular endothelia, the islet capillary structure is highly specialized. Intra-islet ECs are elongated, only about 100nm wide, and extensively fenestrated, with small fusions of apical and basolateral plasma membranes acting as pores through which nutrients and growth factors can permeate<sup>124,203,204</sup>. ECs also contain caveolae, 60-80nm plasma membrane pits involved in endocytosis<sup>124,204</sup>. These specialized structures enable rapid sensing of nutrients in the blood and allow ECs to secrete hormones accordingly in response<sup>205,206</sup>. Another major function of ECs is the secretion of ECM proteins, which form a distinct basement membrane that is crucial to cell differentiation, function, and survival<sup>203,206,207</sup>.

Intra-islet ECs are attuned to a myriad of circulating signals and stimuli from neighboring cells. In particular, they respond to hypoxic conditions, inflammation (particularly cytokines and chemokines

released by macrophages), and angiogenic factors. In response to these microenvironmental cues, ECs secrete a number of molecules that perform both autocrine and paracrine signaling, including those that induce vasoconstriction (endothelin-1) or vasodilation (nitric oxide, NO), as well as various growth factors (fibroblast growth factor, FGF; connective tissue growth factor, CTGF; HGF), adhesion molecules (intercellular adhesion molecule 1, ICAM1; vascular cell adhesion molecule 1, VCAM1; E-selectin), and chemokines (IL-8, MCP-1).

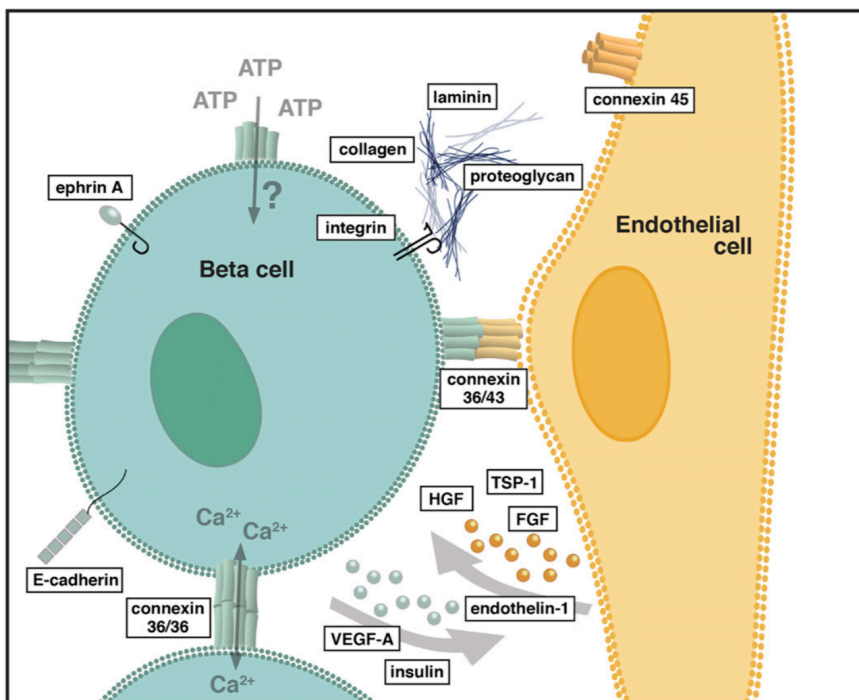


**Figure 8: Proposed mechanisms of communication between  $\beta$ -cells and endothelial cells.** ECs secrete factors (HGF, FGF, TSP-1, endothelin-1) that modulate  $\beta$ -cell survival and function, while  $\beta$ -cells secrete factors (VEGF-A, insulin) that induce changes in EC phenotype. ECs also secrete ECM proteins, which interact with  $\beta$ -cells via integrins. Cell surface molecules (connexins, E-cadherin) mediate cell communication. Image from Peiris *et al.*, 2014<sup>205</sup>.

Growth factors such as CTGF and HGF are particularly important during vascular development<sup>105,208,209</sup>, aiding in

pericyte adhesion and BM formation during angiogenesis<sup>209</sup>, as well as supporting endocrine cell differentiation and proliferation<sup>210</sup>. Thrombospondins, antiangiogenic matricellular glycoproteins, activate TGFβ1 and help maintain islet function<sup>211,212</sup>. Proteins that regulate vascular tone, such as endothelin-1, also have effects on insulin secretion<sup>213,214</sup> and β-cell survival via FOXO1 signaling<sup>215</sup>. Some of the key interactions between ECs and β-cells are depicted in **Fig. 8**.

ECs play an important role in detecting and propagating inflammatory signals. For example, cytokines such as IL-1β and TNFα stimulate ECs to upregulate adhesion molecules, including ICAM1 and VCAM1, to promote adherence of monocytes or other infiltrating immune cells<sup>216,217</sup>. Adhesion molecules also mediate EC-ECM interactions and can affect ECM composition<sup>218,219</sup>. Finally, ECs produce their own cytokines, such as IL-8 and MCP-1, which function as chemotactic cues to sustain immune cell recruitment<sup>124,220,221</sup>.

### Formation of islet vasculature

Development of islet vasculature is primarily controlled via VEGF-A-VEGFR2 signaling, where vascular endothelial growth factor A (VEGF-A) produced by islet endocrine cells activates the tyrosine kinase VEGF receptor 2 (VEGFR2) expressed on intra-islet ECs<sup>222,223</sup>. VEGF-A binding induces receptor dimerization, which promotes autophosphorylation of intracellular tyrosine residues and activation of multiple signaling pathways (summarized in **Fig. 9**) that support vessel permeability and EC migration, proliferation, and survival<sup>206,224-230</sup>.

Expression and activity of VEGF-A is tightly regulated. Transcription factors (Hypoxia-inducible factor 1, HIF-1; Activator protein 1, AP-1; Specificity protein 1, Sp-1) have a direct influence<sup>231</sup>, but VEGF-A transcription can also be indirectly influenced by hypoxia<sup>232</sup>, low pH<sup>233</sup>, and cytokines<sup>231,234</sup>. In addition to

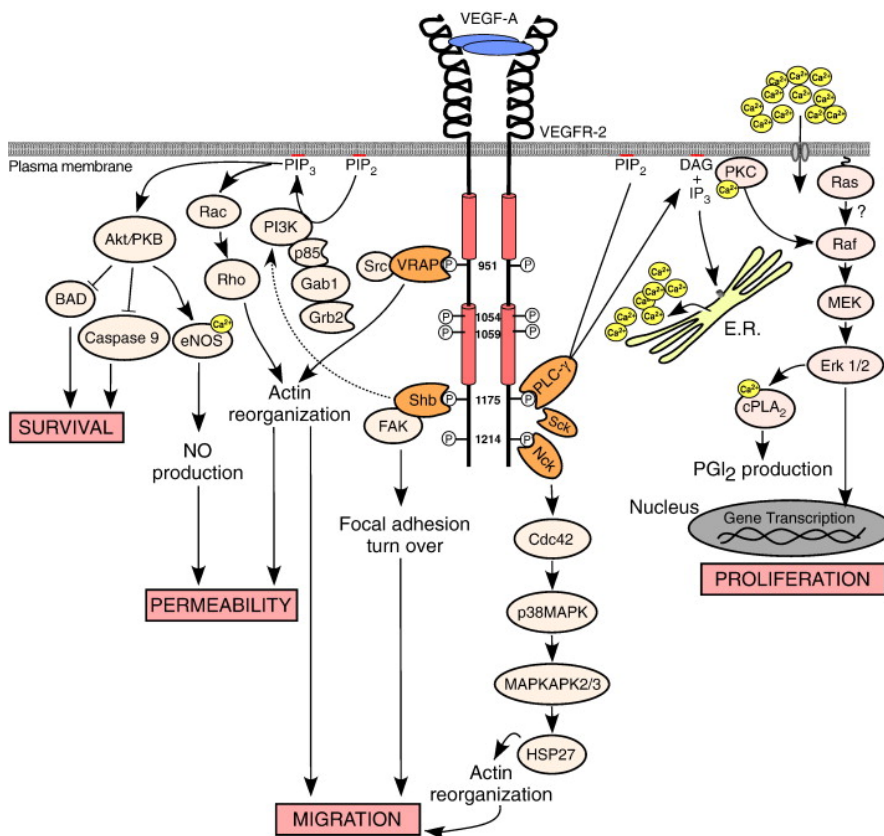


**Figure 9: Schematic illustration of intracellular VEGFR2 signaling.** VEGF-A binds to the receptor, inducing dimerization and autophosphorylation and activating intracellular signaling cascades that promote proliferation, migration, survival and permeability. Abbreviations: BAD, Bcl-2 associated death promoter; cPLA2, cytosolic phospholipase A2; DAG, sn-1,2-diacylglycerol; eNOS, endothelial nitric oxide synthase; Erk 1/2, extracellular regulated kinases 1 and 2; FAK, focal adhesion kinase; Gab1, Grb2-associated binder-1; HSP27, heat-shock protein 27; IP3, inositol (1,4,5)-trisphosphate; PIP3, phosphatidylinositol (4,5)-bisphosphate; PIP2, phosphatidylinositol (3,4,5)-trisphosphate; PKB, protein kinase B; PKC, protein kinase C; PLC-γ, phospholipase C-γ; Sck, Shc-like protein; VEGF, vascular endothelial growth factor; VEGFR-2, VEGF receptor-2; VRAP, VEGFR-associated protein/TsAd T-cell-specific adaptor molecule. Image from Holmes *et al.*, 2007<sup>228</sup>.



changing ligand availability, VEGFR2 co-receptors (neuropillins, heparins) also modulate signaling transduction by affecting the composition and/or stability of the receptor signaling complex<sup>234-236</sup>. Signal strength and duration can be adjusted further by the presence of auxiliary proteins (integrins, ephrins, cadherins), rates of receptor degradation, and dephosphorylation capacity<sup>229,235,237</sup>. Finally, pancreatic ECs also express VEGFR1<sup>238</sup>, which binds VEGF-A and serves as a counter-regulator of angiogenesis by dampening VEGF-A-VEGFR2 signaling<sup>239</sup>.

VEGF-A has been studied extensively in mouse pancreatic development, where it is clear that precise control of VEGF-A production is necessary for establishing a functional vascular network. Global deletion of just a single VEGF-A or VEGFR2 allele severely impairs vascular development and is embryonically lethal between E11-12<sup>240,241</sup>. In the pancreas, loss of VEGF-A limits islet capillary development in a dose-dependent manner, with fewer vessels of reduced size and branching and lower density<sup>222,223</sup>. ECs also display structural abnormalities and fail to establish an intraislet basement membrane<sup>208,223</sup>.

Besides VEGF-A, additional vascular regulation is contributed by the angiopoietin (Ang) family factors (Ang-1, Ang-2, Ang-3/4), which aid survival and structure of vessels via signaling through their tyrosine kinase receptors (Tie-1, Tie-2)<sup>222,233</sup> and mediate EC communication with ECM<sup>242,243</sup>. Angiogenic factor ephrin-A1 is also produced by islet cells, with its receptor (EphB4) expressed in postcapillary venules at the islet periphery<sup>222</sup>.

### **Endothelial cells in pancreatic development and homeostasis**

ECs are the primary source of paracrine signals in the developing pancreas, secreting factors including FGF, CTGF, and bone morphogenic protein (BMP) that specifically regulate progenitor cell differentiation towards exocrine lineage<sup>162,172,210,244,245</sup>. Consequently, intact EC signaling is critical to establishing adequate  $\beta$ -cell mass and when ECs are compromised,  $\beta$ -cell mass is reduced<sup>18,162,246-249</sup>.

VEGF-A inactivation has differential effects on pancreatic and  $\beta$ -cell mass depending on timing. Disruption of VEGF-A during islet development results in greatly reduced  $\beta$ -cell mass and impaired islet function<sup>246,250,251</sup>. In contrast, adult islets with VEGF-A inactivation maintain  $\beta$ -cell mass but show defects in GSIS<sup>222,246,252,253</sup>. Just as islet development is impaired in the absence of VEGF-A, so too is it detrimental to have excess VEGF-A. Conditional overexpression of VEGF-A during embryonic or postnatal periods causes hypervascularization that is detrimental to islet formation and results in  $\beta$ -cell loss<sup>251,254,255</sup>.

### **Endothelial cells in islet inflammation, injury, and aging**

There is some evidence that accumulation of inflammatory signals can cause a gradual deterioration of islet EC function, although it is currently unknown whether the decline in EC health is exacerbated by recruitment of immune cells such as pro-inflammatory macrophages. With aging, ECs tend to become less effective in defending against oxidative stress and may upregulate proteins like VCAM1, which facilitates immune cell recruitment and extravasation, and can lead to vascular inflammation and damage<sup>216</sup>. Interestingly, the ability of ECs to stimulate  $\beta$ -cell proliferation appears to decline with aging.

Almaça and colleagues showed that  $\beta$ -cell proliferation in aged islets was significantly augmented when islets were revascularized by ECs of young recipient mice<sup>256</sup>.

Abnormal EC morphology and dysfunctional EC signaling are linked to both T1D and T2D. In the case of T1D, infiltrating lymphocytes must interact with ECs to reach  $\beta$ -cells, and there is evidence that cytokine-activated ECs mediate  $\beta$ -cell apoptosis. For example, leukocyte homing receptors were upregulated early in insulinitis in the non-obese diabetic (NOD) mouse model; these ECs are unable to promote  $\beta$ -cell regeneration. Treating this T1D environment with bone marrow-derived cells that yield new ECs<sup>257</sup> or administration of VEGFR2 antibody<sup>258</sup> reverses T1D in NOD mice. Pericyte aggregation is accompanied by lymphocyte infiltration in STZ treated mice<sup>259</sup>, and it is likely these cells also interface with ECs under such conditions.

There is evidence of microvascular changes preceding T2D onset; increases in islet vascularization accompany hyperglycemia-induced compensatory  $\beta$ -cell mass expansion<sup>260</sup>. ECs from hyperglycemic, hyperlipidemic T2D patients are thought to be in constant contact with cytotoxic substances that can induce apoptosis via reactive oxygen species (ROS) generation, and, in general, islet capillaries are thickened, dilated, and fragmented<sup>203,260</sup>. Additionally, ECs from *db/db* mice express more markers of inflammation than their wild-type counterparts<sup>261</sup>, as well as exhibiting increased fibrosis and pericyte hypertrophy<sup>262</sup>. Finally, in the context of insulin resistance, Agudo and colleagues showed that increased vascularization and inflammation of islets in high fat diet (HFD)-fed mice was accompanied by increased expression of VEGF-A; sustained overexpression created disorganized, fibrotic vascular networks that produced pro-inflammatory cytokines and recruited macrophages<sup>263</sup>. Dysregulated nitric oxide signaling may also contribute to dilated islet capillaries that are observed in mice with various forms of insulin resistance<sup>264</sup>.

### **Endothelial cells in tissue regeneration**

Cadaveric islet transplant is used as a rare therapeutic treatment for diabetes, but requires severing of islets from their original vascular network. Although chimeric vessels are generated after transplant, implicating both donor and recipient ECs in the revascularization process<sup>265</sup>, islets remain less vascularized with lower oxygen tension (compared to normal islets) even after recovery period<sup>266,267</sup>. As a result, there is interest in (1) creating engineered vascular beds and hydrogels<sup>268-270</sup> and (2) promoting re-vascularization and angiogenesis through treatment with proangiogenic factors, including VEGF-A<sup>269,271-273</sup>, Ang-1<sup>243</sup>, or blockage of antiangiogenic factors such as thrombospondin 1 (TSP-1)<sup>274</sup>. There have also been efforts to culture human ECs and mesenchymal stem cells (MSCs) for co-transplantation<sup>275</sup>. For example, Kaufman-Francis and colleagues developed biodegradable 3D polymeric scaffolds in which they cultured islet cells, human umbilical vein ECs, and fibroblasts; they showed that these cultures gave rise to branched vessel-like structures and that transplantation in to STZ-treated mice resulted in formation of functional vasculature and subsequently improved glucose tolerance<sup>268</sup>. Another group utilized a hydrogel matrix to gradually deliver VEGF-A at the transplantation site, which greatly improved engraftment and revascularization *in vivo*<sup>269</sup>.

The VEGF-A-VEGFR2 pathway mediates production of organ-specific angiocrine factors promoting local tissue self-renewal and regeneration<sup>220,276,277</sup>. In the liver, Ding and colleagues showed that inductive

angiocrine signals from sinusoidal endothelium are required for liver regeneration; hepatocyte proliferation peaks 48 hours after partial hepatectomy<sup>276</sup>. They also showed that endothelial-derived angiocrine signals induce and sustain regenerative lung alveolarization<sup>277</sup>. Finally, another group showed that sinusoidal endothelial cells promote hematopoietic recovery after irradiation, probably by Notch signaling<sup>220</sup>.

Circulating hematopoietic cells are also known to play a role in these processes, and studies suggest that ECs may contribute by regulating macrophage recruitment and/or activating a “restorative” phenotype that aids tissue regeneration<sup>140,159,162,185,186</sup>. Treatment with recombinant forms of human VEGF-A induced monocyte activation and migration<sup>278</sup>, mediated by VEGF receptor 1 (VEGFR1) signaling<sup>279</sup>. ECs have a known role to coordinate inflammatory cell recruitment in response to injury. Stimulated by IL-1 $\beta$  and TNF $\alpha$ , ECs secrete chemokines (IL-6, IL-8, CSF) and adhesion molecules (E-selectin)<sup>229,280</sup>.

### ***Extracellular matrix***

The ECM encompasses two morphologically distinct matrices: the basement membrane is formed mainly by collagen, laminin, and heparan sulfate proteoglycans (HSPGs), while the interstitial matrix includes collagen, elastin, fibronectin, and various polysaccharides<sup>206,281,282</sup>. The ECM plays a role in cell support and anchorage, but also provides tissue-specific microenvironments that influence cell phenotype, affect metabolic function, and regulate cell proliferation<sup>206,207,281-283</sup>.

#### **Components of islet extracellular matrix**

The major components of islet basement membranes are laminins, which are fibrous, heterotrimeric glycoproteins composed of  $\alpha$ -,  $\beta$ -, and  $\gamma$ - polypeptide chains joined by disulfide bonds; and collagen type IV (col-IV), which consists of helical fibrils and is the main structural element of the ECM<sup>206,281,284</sup>. Large glycoproteins called fibronectins form a fibrillar “mesh” that occupies a large portion of the interstitial matrix. Interspersed in this matrix are glycosaminoglycans (GAGs), linear sugar chains that are usually covalently linked to proteins to make proteoglycans. These complexes have binding sites for growth factors, making them important regulators of growth factor bioavailability<sup>206,282</sup>. Heparan sulfate (HS)<sup>285-287</sup> and hyaluronic acid (HA)<sup>283,288</sup> are two GAGs that are frequently associated with ECM in islets. Some major ECM components and their relationship to islet endocrine cells are illustrated in **Fig. 10**.

#### **Homeostasis and function of extracellular matrix**

ECM molecules achieve direct cellular signaling through an array of receptors, the most common of which are integrins. Integrins are heterodimeric, transmembrane glycoprotein receptors composed of  $\alpha$ - and  $\beta$ -subunits, whose varying combinations confer specificity for extracellular ligands. They provide structural adhesion and also initiate signaling cascades mediating gene expression, particularly those that regulate cell differentiation and motility<sup>289-291</sup>. FAKs and other kinases transmit signals downstream of integrins<sup>219,289</sup>.

In addition to direct signaling, ECM molecules also exert cellular effects by modulation of cytokine activity. For example, IL-1 $\beta$  effects are in part mediated by integrin-driven FAK signals<sup>219,289</sup>. In other

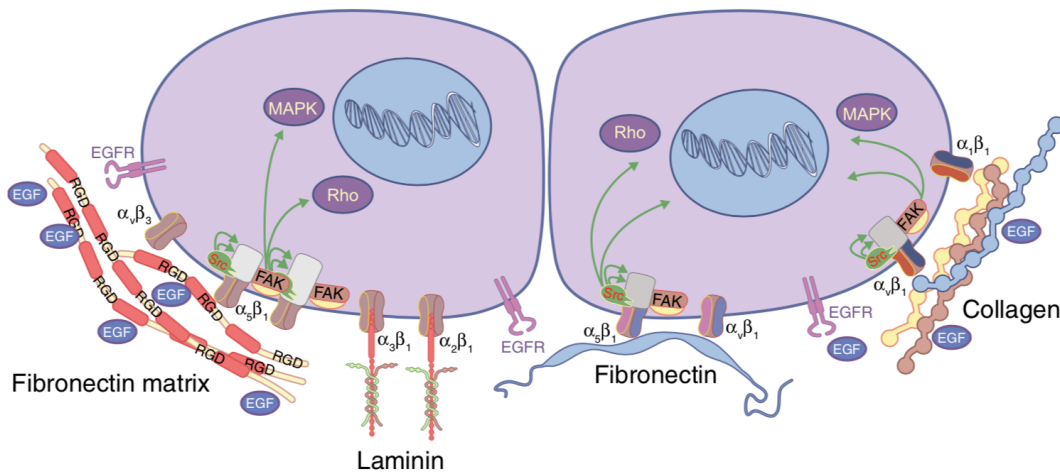


**Figure 10: ECM-cell interactions within islets.** Integrin receptors bind to collagen, fibronectin, and laminin, and Src family kinases and Rho GTPases help transduce signals downstream. In this way, ECM components can influence gene expression, growth, and survival of cells. Image from Llacua *et al.*, 2018<sup>307</sup>.

systems there is evidence that ECM proteins can have cytokine-like properties; ECM-derived fragments mimicked CXC receptor ligands and contributed to neutrophil recruitment in inflamed lungs<sup>292</sup>, and HA fragments were also shown to induce inflammatory genes in alveolar macrophages<sup>218</sup>.

The ECM has been considered a “sink” for storage of growth factors. Charged growth factors and chemokines may interact with HS and HA proteoglycans (which are negatively charged) to impact their concentration and accessibility<sup>282,283</sup>. Many ECM proteins have been shown to interact with growth factors to promote proliferation and differentiation<sup>293</sup>, with some integrin subunits even able to crosstalk with growth factor receptors directly<sup>294</sup>. In addition, proteases secreted by ECs or other cells can facilitate remodeling of ECM components and thereby modulate bioavailability of diffusible proteins deposited in the ECM.

Finally, the ECM is thought to help establish a “polarized microdomain” in the  $\beta$ -cell, as the portion in contact with EC basement membrane is a preferential site for insulin granule fusion<sup>208,295</sup>. In other words, crosstalk between ECM and  $\beta$ -cells help achieve a strong “bias” for exocytosis to occur at the vascular face.

### Extracellular matrix in $\beta$ -cell development and proliferation

Laminins promote  $\beta$ -cell differentiation in fetal mouse pancreas<sup>296,297</sup>, and there is evidence that they help maintain differentiation of cultured human  $\beta$ -cells<sup>298</sup>. Differentiation of stem cells into  $\beta$ -like cells has also been augmented with laminin and fibronectin, which signal through the Akt/ERK pathways<sup>299</sup>. Additionally, netrin (which structurally resembles laminin) was shown to promote differentiation of pancreatic progenitors<sup>291</sup>. Integrins  $\alpha_v\beta_3$  and  $\alpha_v\beta_5$  are critical to adhesion and migration of endocrine progenitors in mouse<sup>300</sup>.

In addition to playing a role in differentiation, integrin-mediated laminin signaling is also critical for  $\beta$ -cell proliferation in mice<sup>208,301</sup>, and laminins 411 and 511 were associated with rare proliferating  $\beta$ -cells of human islets cultured *in vitro*<sup>298</sup>. Inactivation of HA in mouse  $\beta$ -cells also resulted in abnormal islet morphology and reduced  $\beta$ -cell proliferation<sup>285</sup>.

### **Extracellular matrix in islet function, inflammation, and injury**

There has been recent interest in islet ECM components because  $\beta$ -cells or islets anchored to ECM proteins *in vitro* exhibit enhanced survival and insulin secretion<sup>290,302-305</sup>. One group using polyethylene glycol hydrogel capsules showed that supplementation with col-IV and laminin increased insulin secretion approximately six-fold compared to encapsulation alone<sup>303</sup>. Even the inclusion of fibrin, which is not a regular component of the ECM, promotes  $\beta$ -cell function, proliferation, and survival<sup>306</sup>. The addition of heparin (a component of HSPGs) also promoted  $\beta$ -cell survival in cultured mouse islets<sup>286</sup>. Although these results are promising, titrating the concentration of ECM proteins appears to be crucial to achieving a positive effect<sup>307</sup>. The  $\beta_1$  integrin subunit seems to be the primary regulator of insulin secretion<sup>308,309</sup>,  $\beta$ -cell survival<sup>305,306,309</sup>, and  $\beta$ -cell proliferation<sup>301</sup>.

There is a great deal of ECM remodeling during islet inflammation; to reach  $\beta$ -cells, immune cells must exit the microvasculature by adhering to and traversing the endothelium and basement membrane<sup>283</sup>. These migrating immune cells, along with any dying cells, secrete factors that alter expression of ECM components and enzymatic modulators. The subsequent release can be a chemotactic cue for additional cells and/or can polarize cells already present<sup>283,288</sup>. Not surprisingly, abnormal ECM characteristics have been linked to both T1D and T2D. Increased fibronectin was observed in young postnatal pancreas of NOD mice, along with more macrophages and altered islet morphology<sup>310</sup>. NOD mice also have increased expression of heparanase, which degrades HSPGs normally found in the islet<sup>286</sup>. Hyaluronan, a GAG that is produced during inflammation and contributes to T-cell retention and phenotype, accumulates in increased amounts in human T1D islets, underscoring the impact of ECM dynamics on disease pathogenesis<sup>288,311</sup>.

The matrix is also disrupted in rodent models and human T2D, with fibrosis caused by collagen deposition and influx of pericytes and inflammatory cells<sup>312</sup>. Removal of HSPGs with heparinase decreased amyloid deposition and cell death in INS-1 cells treated with IAPP<sup>287</sup>, suggesting a role for HSPGs in islet amyloidogenesis, which is observed in some cases of human T2D. Although further investigation is needed in the pancreas, there is evidence of hyperglycemia-induced ECM regulation: the basement membrane of kidney capillaries undergoes dramatic transformation under high glucose conditions, showing increased fibronectin deposition and col-IV accumulation<sup>313</sup>. Importantly, it is the trafficking of these proteins that seems to be aberrantly regulated and not merely the expression.

ECM dynamics change in the context of acute injury, and have been manipulated therapeutically in the setting of islet transplantation, which is an artificial “injury” that severs native vasculature and can adversely affect cell viability and immune response. Recently the use of encapsulation technologies, which aim to modulate immune interactions, as well as other bioengineering devices, have been supplemented with ECs and ECM components<sup>270,307,314,315</sup>. For example, the addition of laminin and col-IV enhanced viability and insulin secretion of transplanted mouse islets<sup>270</sup>, and supplementation with ECM and growth factors was also shown to improve transplant outcome through inhibition of apoptosis and by promoting revascularization<sup>314</sup>. Fibrin has also been utilized successfully as a “temporary” scaffold to enhance vascularization and islet engraftment<sup>315</sup>.

## Aims of Dissertation

Regeneration of endogenous  $\beta$ -cells represents a promising therapy to treat diabetes, but there are still considerable gaps in our understanding of  $\beta$ -cell regeneration. Among these are not only the molecular mechanisms that are unique to human  $\beta$ -cell proliferation, but also the contribution of non- $\beta$ -cells and the islet microenvironment to the regenerative process and the specific characteristics that render some cells more capable of proliferation.

The goal of this dissertation is twofold: (1) to further understand how the microenvironment, specifically vascular ECs, affects  $\beta$ -cell proliferation; and (2) to advance the methodologies for studying the human  $\beta$ -cell transcriptome during development and disease. Together, these projects provide a framework for future efforts aimed at promoting  $\beta$ -cell regeneration and increasing functional  $\beta$ -cell mass. To accomplish these aims, we utilized and improved existing technologies and developed new experimental approaches as described in **Chapter II**.

In **Chapter III**, to test the hypothesis that interactions between macrophages and ECs promote  $\beta$ -cell proliferation, we built on our existing mouse model of VEGF-A overexpression where a rapid  $\beta$ -cell loss upon VEGF-A induction and EC expansion is followed by gradual  $\beta$ -cell proliferation and regeneration during the period of VEGF-A normalization<sup>201</sup> and EC quiescence. Our previous work had shown that macrophages were recruited to the islet upon VEGF-A induction and that this recruitment was required for  $\beta$ -cell regeneration. To determine the role of proliferative and quiescent ECs in the paradigm, we introduced an additional mouse model in which the key receptor mediating VEGF-A signaling, VEGFR2, was conditionally inactivated in ECs. The resulting experiments demonstrated that EC signaling was necessary for maximal macrophage recruitment and phenotype activation, which is consistent with reports of EC-macrophage crosstalk in other regenerative models<sup>140,159,162,185,186</sup>. We also showed that ablation of VEGFR2 in quiescent ECs, during the early regenerative stage, induced rapid vessel regression that promoted  $\beta$ -cell proliferation. This suggests that molecules such as ECM-bound growth factors released from ECM during EC regression could be involved in stimulating  $\beta$ -cell proliferation.

To extend our findings from this *in vivo* mouse model to the human islet microenvironment, we next investigated the vascular changes in human islets during postnatal pancreas development. Our group and others have shown that human  $\beta$ -cell proliferation rates peak postnatally and drop precipitously within the first decade of life<sup>35,316-318</sup>; therefore, the vascular organization during this time period, because of known interactions between the vasculature and islet cells in rodents, is of particular interest in humans. Our analysis revealed that intra-islet EC area was greatest during the peak of  $\beta$ -cell proliferation, suggesting that either vascular arrangement or EC-derived signals may impact postnatal  $\beta$ -cell growth.

To advance our understanding of human islet development and  $\beta$ -cell function, better tools are needed for identifying progenitor populations that can be more effectively differentiated into  $\beta$ -cells, as well as markers of mature  $\beta$ -cells that could be utilized for purification and targeting. In **Chapter IV**, we addressed this challenge by identifying molecular markers of developing and mature human  $\beta$ -cells, first describing a population of multipotent pancreatic progenitor cells in the neonatal human pancreas

expressing secretory granule membrane major glycoprotein 2 (GP2), and then assessing a newly described cell surface marker of adult human  $\beta$ -cells, nucleoside triphosphate diphosphohydrolase 3 (NTPDase3). In collaboration with Dr. Cristina Nostro at University of Toronto, we found that GP2 marks multipotent pancreas progenitors, and Dr. Nostro's group further showed that the selection of GP2-expressing progenitor cells enhances efficiency of  $\beta$ -cell differentiation from hESCs<sup>319</sup>. With regard to NTPDase3, we demonstrated that it has a unique temporal expression pattern during pancreas development. In addition, we showed that this marker has a utility for  $\beta$ -cell purification for RNA-seq analysis and for *in vivo*  $\beta$ -cell imaging. Identification and characterization of these two markers will further not only our knowledge of islet and  $\beta$ -cell development, but will also allow us to assess  $\beta$ -cell gene expression and mass during the disease process and inform the development of future therapies for DM. We demonstrated the application of our islet cell sorting strategy by isolating  $\alpha$ -cells from human donors with T1D and reporting for the first time transcriptional dysregulation in human T1D  $\alpha$ -cells that likely contributes to impaired glucagon secretion<sup>320</sup>.

The studies in this Dissertation suggest new ways in which the islet microenvironment might be manipulated to promote  $\beta$ -cell regeneration, and build upon existing tools to isolate and analyze features of developing and mature human  $\beta$ -cell populations. The significance of these findings, as well as proposed future directions, is discussed in **Chapter V**.

## CHAPTER II

### MATERIALS AND METHODS

Some methods in this chapter have been published in Brissova, Haliyur, Saunders, Shrestha *et al.*, 2018<sup>320</sup> and Cogger, Sinha, Sarangi, McGaugh, Saunders *et al.*, 2017<sup>319</sup>.

#### Mouse Models

All animal studies described in this Dissertation were approved by the Institutional Animal Care and Use Committee at Vanderbilt University Medical Center, and animals were kept in facilities monitored by the Vanderbilt University Division of Animal Care on a 12 hour light/12 hour dark schedule with unrestricted access to standard chow and water. Mouse models and abbreviations used to describe them are summarized in **Table 1**.

Table 1. Mouse models		
Abbreviation	MGI Nomenclature or Strain Name	References
Cd5-CreER	Tg(Cdh5-cre/ERT2)#Ykub	Okabe <i>et al.</i> , 2014 <sup>321</sup>
NOD- <i>scid</i> - <i>IL2r<math>\gamma</math></i> <sup>null</sup>	NOD.Cg- <i>Prkdc</i> <sup>scid</sup> / <i>Il2rg</i> <sup>tm1Wjl</sup> /SzJ	Shultz <i>et al.</i> , 2005 <sup>322</sup>
RIP-rtTA	Tg( <i>Ins2</i> -rtTA)2Efr	Milo-Landesman <i>et al.</i> , 2001 <sup>323</sup>
TetO-VEGF	unlisted	Efrat <i>et al.</i> , 1995 <sup>324</sup> Ohno-Matsui <i>et al.</i> , 2002 <sup>325</sup>
VEGFR2 <sup>fl/fl</sup>	Kdr <sup>tm2Sato</sup>	Hooper <i>et al.</i> , 2009 <sup>326</sup>

The original bitransgenic mice with doxycycline (Dox)-inducible  $\beta$ -cell-specific overexpression of human VEGF-A<sub>165</sub> (abbreviated  $\beta$ VEGF-A) were generated by crossing RIP-rtTA male mice and TetO-VEGF female mice, both on a C57BL/6 background<sup>222,323-325</sup>. These mice were generously provided by Dr. Shimon Efrat of Tel Aviv University and Dr. Peter Campochiaro of Johns Hopkins University, respectively. In this  $\beta$ VEGF-A model the rat *Ins2* promoter drives expression of the tetracycline-responsive rtTA transactivator specifically in pancreatic  $\beta$ -cells. Upon exposure to Dox, the rtTA transactivator binds the tetracycline operator (*TetO*), driving expression of human VEGF-A<sub>165</sub> in  $\beta$ -cells. Details of Dox preparation and administration are included below.

The mice with Tamoxifen (Tmx)-inducible EC-specific knockout of VEGFR2 (abbreviated VEGFR2<sup>i $\Delta$ EC</sup>) were generated by crossing Cd5-CreER male mice and VEGFR2<sup>fl/fl</sup> female mice (see **Table 2**, Scheme A1-A2). Heterozygous VEGFR2<sup>fl/wt</sup> mice on a C57BL/6 background from Jackson Laboratories (stock #018977) were bred to create a homozygous VEGFR2<sup>fl/fl</sup> line. Frozen sperm from the Cd5-CreER line was generously provided by Dr. Yoshiaki Kubota of Keio University. In vitro fertilization (IVF) was performed by the Vanderbilt Transgenic Mouse/ES Cell Shared Resource using female C57BL/6 mice (stock #000664). In the VEGFR2<sup>i $\Delta$ EC</sup> model *loxP* sites are inserted flanking VEGFR2 exon 3, and the *Cdh5* (*VE-cadherin*) promoter drives expression of a Tamoxifen (Tmx)-inducible Cre recombinase in vascular ECs. Upon exposure to Tmx, Cre recombinase translocates to the nucleus, excising VEGFR2



alleles through Cre-*loxP* recombination and subsequently preventing VEGFR2 expression in ECs. Details of Tm preparation and administration are included below.

To generate an inducible model of EC-specific knockdown of VEGFR2 in  $\beta$ VEGF-A mice, Cd5-CreER and VEGFR2<sup>fl/fl</sup> mice were crossed with RIP-rtTA and TetO-VEGF transgenic mice as described in **Table 2**. The final cross produced both  $\beta$ VEGF-A; VEGFR2<sup>iΔEC</sup> mice as well as Cre-negative sibling controls ( $\beta$ VEGF-A; VEGFR2<sup>fl/fl</sup>).

<b>Table 2. Breeding scheme to generate <math>\beta</math>VEGF-A; VEGFR2<sup>iΔEC</sup> mice</b>				
<b>SCHEME A</b>				
	Male breeder	Female breeder	Desired Offspring	Freq
1	Cd5-CreER <sup>tg/+</sup>	VEGFR2 <sup>fl/fl</sup>	Cd5-CreER <sup>tg/+</sup> ; VEGFR2 <sup>fl/+</sup>	50%
2	Cd5-CreER <sup>tg/+</sup> ; VEGFR2 <sup>fl/+</sup>	VEGFR2 <sup>fl/fl</sup>	Cd5-CreER <sup>tg/+</sup> ; VEGFR2 <sup>fl/fl</sup>	25%
3	Cd5-CreER <sup>tg/+</sup> ; VEGFR2 <sup>fl/fl</sup>	RIP-rtTA <sup>tg/tg</sup>	Cd5-CreER <sup>tg/+</sup> ; VEGFR2 <sup>fl/+</sup> ; RIP-rtTA <sup>tg/+</sup>	50%
4	Cd5-CreER <sup>tg/+</sup> ; VEGFR2 <sup>fl/+</sup> ; RIP-rtTA <sup>tg/+</sup>	VEGFR2 <sup>fl/fl</sup>	Cd5-CreER <sup>tg/+</sup> ; VEGFR2 <sup>fl/fl</sup> ; RIP-rtTA <sup>tg/+</sup>	12.5%
<b>SCHEME B</b>				
	Male breeder	Female breeder	Desired offspring	Freq
1	VEGFR2 <sup>fl/fl</sup>	TetO-VEGFA <sup>tg/tg</sup>	TetO-VEGFA <sup>tg/+</sup> ; VEGFR2 <sup>fl/+</sup>	100%
2	TetO-VEGFA <sup>tg/+</sup> ; VEGFR2 <sup>fl/+</sup>	TetO-VEGFA <sup>tg/tg</sup>	TetO-VEGFA <sup>tg/tg</sup> ; VEGFR2 <sup>fl/+</sup>	50%
3	TetO-VEGFA <sup>tg/+</sup> ; VEGFR2 <sup>fl/+</sup>	TetO-VEGFA <sup>tg/tg</sup> ; VEGFR2 <sup>fl/+</sup>	TetO-VEGFA <sup>tg/tg</sup> ; VEGFR2 <sup>fl/fl</sup>	25%
<b>FINAL CROSS</b>				
	Male breeder	Female breeder	Desired offspring	Freq
	Cd5-CreER <sup>tg/+</sup> ; VEGFR2 <sup>fl/fl</sup> ; RIP-rtTA <sup>tg/+</sup>	TetO-VEGFA <sup>tg/tg</sup> ; VEGFR2 <sup>fl/fl</sup>	TetO-VEGFA <sup>tg/+</sup> ; Cd5-CreER <sup>tg/+</sup> ; VEGFR2 <sup>fl/fl</sup> ; RIP-rtTA <sup>tg/+</sup>	25%

For the *in vivo* studies of human islets described in **Chapter IV**, human islets were transplanted into immunodeficient NOD-*scid*-*IL2 $\gamma$* <sup>null</sup> mice<sup>322</sup> obtained in collaboration with Dr. Leonard Shultz from Jackson Laboratories (stock #005557). These mice lack mature T cells, B cells, and natural killer cells, and exhibit deficient cytokine signaling, making them ideal recipients for xenotransplantation.

### **DNA extraction and genotyping**

Mouse models used in our breeding schemes were maintained by genotyping using the primers and PCR conditions listed in **Table 3**. DNA was extracted and PCR reactions were performed with tail snips from mice using the Red Extract N-Amp Tissue PCR kit (XNAT, Sigma), except in VEGFR2<sup>fl/fl</sup> mice, where the Kapa Hot Start PCR kit (KK5621; Kapa Biosystems) was used instead. Both DNA extraction and preparation of PCR reaction mixtures were performed according to the manufacturer's instructions. Primers (Sigma Genosys) were reconstituted in RNase/DNase-free water to 100  $\mu$ M and further diluted 1:20, stored at -20°C for use in PCR reactions. Thermal cycler conditions listed in **Table 3** were used to amplify DNA before resolving on agarose gels with 100 ng/mL ethidium bromide in 1X Tris/Borate/EDTA (TBE) buffer as indicated.

**Table 3. PCR primers and conditions for genotyping**

Mouse Model	Genotyping Primers	PCR Conditions	Expected Products
Cd5-CreER	5'- GCG GTC TGG CAG TAA AAA CTA TC -3' (forward) 3'- GTG AAA CAG CAT TGC TGT CAC TT -3' (reverse)	93°C 3' ----- 93°C 20" 60°C 20" 30 cycles 72°C 45" ----- 72°C 5' 4°C hold	100 bp for Cre (3.0% agarose)
RIP-rtTA	5' - GTG AAG TGG GTC CGC GTA CAG - 3' (forward) 5' - GTA CTC GTC AAT TCC AAG GGC ATC - 3' (reverse)	92°C 2' ----- 94°C 30" 57°C 30" 30 cycles 72°C 30" ----- 72°C 10' 4°C hold	400 bp for transgene (1.5% agarose)
TetO-VEGF	5' - TCG AGT AGG CGT GTA CGG - 3' (forward) 5' - GCA GCA GCC CCC GCA TCG - 3' (reverse)	95°C 4' ----- 95°C 1' 57°C 30" 29 cycles 72°C 1' ----- 72°C 10' 4°C hold	420 bp for transgene (1.5% agarose)
VEGFR2 <sup>fl/fl</sup>	5' - CCA CAG AAC AAC TCA GGG CTA - 3' (forward) 5' - GGG AGC AAA GTC TCT GGA AA - 3' (reverse)	94°C 2' ----- 94°C 20" 65°C 15" 10 cycles 68°C 10" ----- 94°C 15" 60°C 15" 28 cycles 72°C 10" ----- 72°C 1' 4°C hold	179 bp for wild-type; 230 bp for VEGFR2 <sup>loxP</sup> (3.0% agarose)

### **Compound preparation and administration**

VEGF-A transgene expression was activated in  $\beta$ VEGF-A mice by Dox administration (5 mg/mL) in light-protected drinking water containing 1% Splenda<sup>®</sup> for a period of 3-5 days. VEGFR2 knockdown was induced in VEGFR2<sup>iAEC</sup> mice by intraperitoneal injection of 4 mg Tmx (20 mg/mL; 200  $\mu$ L). Tmx (20 mg/mL) was prepared fresh in filter-sterilized corn oil the day before each injection and allowed to dissolve overnight on a nutator at room temperature, protected from light. Vetbond tissue adhesive (3M) was used to seal injection sites to prevent oil leakage.

### **Tissue Collection and Fixation**

Mouse pancreata, as well as kidneys and eyes bearing islet grafts, were collected from anesthetized mice prior to cervical dislocation. Organs were washed in ice-cold 10 mM phosphate buffered saline (PBS) and fat and other excess tissue was removed before pancreata were weighed and fixed as described below.

Pancreata and islets from normal, T1D, and T2D donors were obtained through partnerships with the Alberta Diabetes Institute (ABI), International Institute for Advancement of Medicine (IIAM), Integrated Islet Distribution Program (IIDP), National Disease Research Interchange (NDRI), and Network for

Pancreatic Organ Donors with Diabetes (nPOD). Donor demographic information is summarized in **Table 4** (histological analysis) and **Table 5** (gene expression and *in vivo* experiments) below. The Vanderbilt University Institutional Review Board does not classify de-identified human pancreatic specimens as human subject research. Human pancreata were received within 18 hours from cold clamp and maintained in cold preservation solution on ice until processing. Prior to islet isolation, pancreas was cleaned from connective tissue and fat, measured, and weighed, and then multiple cross-sectional slices with 2-3 mm thickness were obtained from the head, body and distal tail. Pancreatic slices were further divided into four quadrants and then processed for cryosections (described below).

<b>Table 4. Demographic information of human donors used for histology</b>							
<b>Donors</b>	<b>Age</b>	<b>Ethnicity/Race</b>	<b>Disease Duration</b>	<b>Gender</b>	<b>BMI</b>	<b>Cause of Death</b>	<b>Tissue Source</b>
<b>Neonatal</b>	G18 weeks	N/A	--	N/A	N/A	N/A	N/A
	G37 weeks	Caucasian	--	M	N/A	Anoxia	IIAM
	G37 weeks	Caucasian	--	M	N/A	Anencephaly	IIAM
	G40 weeks	N/A	--	F	N/A	Anencephaly	IIAM
	G40 weeks	Caucasian	--	M	N/A	N/A	IIAM
	G41 weeks	Caucasian	--	F	12.6	Anencephaly	IIAM
	G41 weeks	Caucasian	--	F	14.2	Anencephaly	nPOD
	4 days	Caucasian	--	M	13.1	Anoxia	IIAM
	2 months	Caucasian	--	F	14.7	Head Trauma	NDRI
	2 months	Hispanic/Latino	--	F	19.9	Anoxia	IIAM
	2 months	African American	--	F	13.4	Head Trauma	IIAM
<b>Infant</b>	3 months	Hispanic/Latino	--	M	16.1	Head Trauma	NDRI
	3 months	Caucasian	--	M	16.8	Anoxia	NDRI
	3 months	Hispanic/Latino	--	M	17.0	Anoxia	NDRI
	7 months	Hispanic/Latino	--	M	17.3	Head Trauma	IIAM
	10 months	Caucasian	--	F	15.4	Anoxia	NDRI
	10 months	Hispanic/Latino	--	F	23.1	Head Trauma	IIAM
	10 months	African American	--	M	19.6	Anoxia	IIAM
	11 months	Hispanic/Latino	--	M	18.4	Head Trauma	NDRI
	20 months	Caucasian	--	F	23.4	Anoxia	IIAM
21 months	Caucasian	--	M	18.8	Anoxia	IIAM	
<b>Child</b>	3 years	Caucasian	--	M	19.3	Anoxia	IIAM
	4 years	Caucasian	--	F	19.0	Head Trauma	IIAM
	5 years	Caucasian	--	M	16.2	Anoxia	IIAM
	5 years	African American	--	F	15.9	Anoxia	NDRI
	7 years	Caucasian	--	M	26.7	Anoxia	NDRI
	10 years	Caucasian	--	M	19.3	Head Trauma	NDRI
	11 years	African American	--	M	18.3	Anoxia	IIAM
<b>Adult (Control)</b>	18 years	Caucasian	--	M	31.4	Head Trauma	IIAM
	35 years	Caucasian	--	M	26.8	Head Trauma	IIAM
<b>Adult (T1D, T2D)</b>	20 years	Caucasian	7 years (T1D)	M	25.5	Anoxia	NDRI
	47 years	Caucasian	3 years (T2D)	M	31.3	Stroke	IIAM
	49 years	Caucasian	3 years (T2D)	F	33.8	Stroke	IIAM

*BMI – body mass index; IIAM – International Institute for the Advancement of Medicine; N/A – not available; NDRI – National Disease Research Interchange; nPOD – Network for Pancreatic Organ Donors with Diabetes; T1D – type 1 diabetes; T2D – type 2 diabetes*

**Table 5. Demographic information of human islet donors used for cell sorting, RNA-seq, and islet transplantation**

Donors	Age	Ethnicity/Race	Disease Duration	Gender	BMI	Cause of Death	Islet Source
<b>Normal Controls (FACS Purity)</b>	19 years	Caucasian	--	M	27.2	Head Trauma	IIDP
	50 years	African American	--	M	30.2	Stroke	IIDP
<b>Normal Controls (RNA-seq)</b>	26 years	Hispanic/Latino	--	F	35.9	Anoxia	IIDP
	35 years	Caucasian	--	F	23.6	Anoxia	IIDP
	49 years	Caucasian	--	F	31.6	Stroke	IIDP
	50 years	African American	--	M	30.2	Stroke	IIDP
	55 years	Caucasian	--	M	27.8	Stroke	IIDP
<b>T1D Samples (RNA-seq)</b>	14 years	Caucasian	2 years	F	24.3	Anoxia	nPOD
	27 years	Caucasian	17 years	M	18.4	Anoxia	NDRI
	30 years	Caucasian	20 years	M	29.8	Anoxia	NDRI
<b>T2D Samples (RNA-seq)</b>	40 years	Pacific Islander	unknown	F	43.1	Stroke	IIAM
	56 years	Caucasian	3 years	M	31.1	Head Trauma	IIAM
	59 years	Caucasian	10 years	F	27.5	Stroke	IIAM
	64 years	Caucasian	5 years	M	33.2	Head Trauma	IIAM
<b>Additional FACS Samples</b>	12 years	African American	--	F	23.3	Head Trauma	IIAM
	33 years	Caucasian	17 years (MODY)	M	25.6	Head Trauma	IIAM
<b>Normal Controls (Islet Transplants)</b>	10 years	Hispanic/Latino	--	F	25.4	Head Trauma	nPOD
	43 years	Caucasian	--	M	35.0	Stroke	IIDP
	55 years	Caucasian	--	M	30.1	Head Trauma	IIDP
	61 years	N/A	--	M	N/A	N/A	ADI

ADI – Alberta Diabetes Institute; BMI – body mass index; IIAM – International Institute for the Advancement of Medicine; IIDP – Integrated Islet Distribution Program; MODY – Monogenic diabetes of the young; N/A – not available; NDRI – National Disease Research Interchange; nPOD – Network for Pancreatic Organ Donors with Diabetes; T1D – type 1 diabetes; T2D – type 2 diabetes

### **Islet isolation**

Islet isolation was performed by our collaborator Dr. Rita Bottino at the Allegheny-Singer Research Institute in Pittsburgh, PA. Human pancreata were processed for islet isolation using an approach previously described<sup>327</sup>. Briefly, 18G or 22G catheters were inserted into the main pancreatic duct and ducts were clamped to prevent leakage of collagenase solution during infusion. Collagenase solution consisting of collagenase NB1, (1600 U/isolation, Crescent Chemical), neutral protease NB1 (200U/isolation, Crescent Chemical), and DNase I (12000U/isolation, Worthington Biochemical Corporation) was pre-warmed to 28°C and delivered intraductally using a Rajotte's perfusion system and then maintained at 37°C for approximately 20 minutes. The inflated tissue was then transferred to a Ricordi's chamber apparatus for combined mechanical and enzymatic digestion, which was maintained at 36°C for 5-15 minutes prior to warm and cold collection. The digest was incubated in cold RPMI media (Mediatech) supplemented with heat inactivated 10% Fetal Calf Serum (Life Technologies) for 1 hour on ice. If post-digestion tissue pellet was larger than 2 mL and islets were distinguishable from exocrine tissue by dithizone staining (Sigma), a purification step consisting of density gradient (Biocoll, Cedarlane) centrifugation on a COBE 2991 Cell Processor (Gambro-Terumo) was used to separate islets from exocrine tissue. Islets were re-suspended in CMRL 1066 medium (Mediatech) supplemented with 10%

heat-inactivated Fetal Calf Serum (Life Technologies), 100 units/mL Penicillin/0.1mg/mL Streptomycin (Life Technologies), 2 mmol/L L-glutamine (Life Technologies). On average, islet-enriched fraction contained 90,000 islet equivalents (IEQs). Islets were cultured for 12-24 hours and then shipped from Pittsburgh to Vanderbilt University and/or University of Massachusetts for further analysis following shipping protocols developed by the Integrated Islet Distribution Program (IIDP). Subsequent assays with isolated islets were set up within 48 hours of islet arrival.

### ***Culture and assessment of pancreatic islet function***

Upon arrival at Vanderbilt University, human islets were cultured in CMRL1066 media (5.5 mM glucose, 10% FBS, 1% Pen/Strep, 2 mM L-glutamine) in 5% CO<sub>2</sub> at 37°C for 0-48 hours prior to reported studies. Normal function of islets from adult controls (**Table 5**) was confirmed by the Vanderbilt Islet Procurement and Isolation Core, using a dynamic cell perfusion system and radioimmunoassay as described previously<sup>328</sup>.

### ***Pancreatic tissue fixation***

Mouse and human tissue specimens processed for cryosections were fixed in 0.1 M PBS containing 4% paraformaldehyde (Electron Microscopy Sciences) for 2-3 hours on ice with mild agitation, washed in four changes of 0.1 M PBS over 2 hours, and equilibrated in 30% sucrose/0.01 M PBS overnight. After blotting to remove excess sucrose, tissues were mounted in Tissue Tek cryomolds filled with Tissue-Plus Optimal Cutting Temperature (OCT) compound (VWR Scientific Products). Tissue molds were placed on dry ice until the OCT was set, then stored at -80°C. Tissues were sectioned from 5-10 µm thick on a Leica CM1950 cryostat (Leica) and these cryosections were attached to Superfrost Plus Gold slides (ThermoFischer Scientific).

### ***Culture and Differentiation of hESCs***

*Differentiation of hESCs was performed by Dr. Katy Cogger at the University of Toronto.* Briefly, differentiation of H1 hESCs (WiCell) was initiated when the cultures reached 70-80% confluence. Monolayer cultures were treated with RPMI (Gibco) containing 100 ng/ml hActivin A (R&D Systems) and 2 µM CHIR990210 (Tocris) for one day (d0-d1). They were then cultured for 2 days in RPMI media containing 100 ng/ml hActivin A and 5 ng/ml hbFGF (R&D Systems) (d1-d3) to complete stage 1 of differentiation. During stage 2, cells were cultured in RPMI with 1% vol/vol B27 supplement (without vitamin A) (Life Technologies), 50 ng/ml hFGF10 (R&D Systems), 0.75 µM dorsomorphin (Sigma), and 3 ng/ml mWnt3a (R&D Systems) (d3-d6). On day 6, cultures were transferred to stage 3 media, consisting of DMEM (Gibco) with 1% vol/vol B27 supplement, 50 µg/ml ascorbic acid (Sigma), 50 ng/ml hNOGGIN (R&D Systems), 50 ng/ml hFGF10, 0.25 µM SANT-1 (Tocris), and 2 µM all-trans RA (Sigma), and cultured for 2-3 days. During stage 4, the media was changed to DMEM containing 1% vol/vol B27 supplement, 50 µg/ml ascorbic acid and 50 ng/ml hNOGGIN, and supplemented with 10 mM nicotinamide (Sigma) to direct cells toward the PP lineage (d8-d13). H1 cells for FACS sorting received media supplemented with 100 ng/ml hEGF and 3.3 mM nicotinamide at stage 4 to obtain a GP2-low expressing population.

For stage 5 and 6, single cells obtained after FAC-sorting were cultured in suspension at  $2 \times 10^6$  cells/ml in low-adherent tissue culture plates in MCDB131 media (Gibco) containing 1  $\mu$ M T3 (Sigma), 1.5 g/L NaHCO<sub>3</sub> (Gibco), 1% vol/vol L-glutamine (GE Healthcare), 1% vol/vol B27 supplement (Gibco), 15 mM D-(+)-glucose (Sigma), 10  $\mu$ g/ml heparin (Sigma), 0.25  $\mu$ M SANT-1 (Tocris), 10  $\mu$ M RepSox (Tocris), 100 nM LDN193189 (Cayman), 10  $\mu$ M ZnSO<sub>4</sub> (Sigma), 0.05  $\mu$ M all-trans RA (Sigma), and 10  $\mu$ M Y27632 (Tocris) (d13-d16, stage 5). After 72 h, the media was changed to MCDB131 containing 1  $\mu$ M T3, 1.5 g/L NaHCO<sub>3</sub>, 1% vol/vol L-glutamine, 1% vol/vol B27 supplement, 15 mM D-(+)-Glucose, 10  $\mu$ g/ml Heparin, 10  $\mu$ M RepSox, 100 nM LDN193189, 10  $\mu$ M ZnSO<sub>4</sub>, and 100 nM DBZ (Tocris) (d16-d23, stage 6), media was replenished at day 19. Aggregates were collected at day 23 and dissociated with trypsin for flow cytometry analysis. Stage 5 and stage 6 media components are based on the previously described protocols<sup>73,74</sup>.

### Immunohistochemistry, Imaging, and Analysis

Immunohistochemical analysis of pancreas was performed on serial 5-7  $\mu$ m cryosections as described previously<sup>201</sup> using primary and secondary antibodies listed in **Tables 6-7**. Briefly, cryosections were air dried and then either post-fixed with 1% paraformaldehyde in 10mM PBS for 10 minutes before permeabilization, or immediately permeabilized in 0.2% Triton-X in 10nM PBS. After permeabilization sections were washed three times in 10nM PBS for 3-5 minutes each, then blocked in 5% normal donkey serum in 10mM PBS for 60-90 in a humidified chamber at room temperature. Sections were incubated overnight with primary antibodies diluted in antibody buffer (0.1% Triton-X, 1% BSA in 10nM PBS) in a humidified chamber at 4°C, then washed three times with in 10mM for 10 minutes each. Sections were then incubated with secondary antibodies prepared in antibody buffer for 90 minutes in a humidified chamber protected from light, at room temperature. Sections were treated with DAPI (5 mg/mL stock diluted 1:50,000 in 10mM PBS) for 10 minutes, and then washed three times in 10mM PBS for 15 minutes each. Slides were mounted using SlowFade Gold antifade reagent (Invitrogen Molecular Probes) and sealed with fingernail polish prior to imaging.

Digital images were acquired with a Leica DMI6000B fluorescence microscope equipped with a Leica DFC360FX digital camera (Leica), a laser scanning confocal microscope (Zeiss LSM510 META or LSM880, Carl Zeiss), and a ScanScope FL (Aperio). Image analysis was performed using MetaMorph 7.7 software (Molecular Devices), ImageScope software (Aperio), or HALO software (Indica Labs).

For analysis of islet composition, images of entire pancreatic sections were captured at 20x magnification using a ScanScope FL system and islets were annotated based on insulin staining, and HALO algorithms were used to calculate area of  $\beta$ -cells, ECs, and macrophages. For  $\beta$ -cell proliferation, cells were deemed positive for Ki67 only when at least 75% of the nucleus was surrounded by insulin<sup>+</sup> cytoplasm. A minimum of 1,500  $\beta$ -cells was assayed per sample.

**Table 6: Primary antibodies for immunohistochemistry**

Antigen	Species	Source	Catalog #	Dilution
Amylase	Rabbit	Sigma	A8273	1:1000
C-peptide	Mouse	DSHB	GN-ID4	1:2000
Caveolin-1	Rabbit	Abcam	ab2910	1:2000
CD206 (Mrc1)	Rat	BioLegend	141701	1:500
CD31 (human)	Mouse	BD Pharmingen	550389	1:100
CD31 (mouse)	Rat	BD Pharmingen	553370	1:100
CD39L3 (NTPDase3)	Mouse	gift of J. Sévigny	N/A	1:50
Col-IV	Rabbit	Abcam	ab6586	1:1000
Glucagon	Rabbit	Cell Signaling	2760s	1:100
GP2	Mouse	MBL International Corp.	D277-3	1:250
GP2 (HPx1)	Mouse	gift of C. Dorrell	N/A	1:100
Iba1	Rabbit	Wako	019-19741	1:500
Insulin	Guinea pig	Dako	A0564	1:500
Ki67	Rabbit	Abcam	ab15580	1:5000
Nkx6.1	Rabbit	BCBC/P. Serup	N/A	1:2000
Pancreatic polypeptide	Rabbit	Bachem	T-4088	1:1000
Ptf1a	Goat	gift of C. Wright	N/A	1:500
Somatostatin	Goat	Santa Cruz	sc7819	1:500
VEGF-A	Goat	R&D Systems	AF564	1:200
VEGFR2	Goat	R&D Systems	AF644	1:2000

DSHB – Developmental Studies Hybridoma Bank (University of Iowa)

**Table 7: Secondary antibodies for immunohistochemistry**

Host Species	Primary Ab Species	Fluorophore	Source	Catalog #	Dilution
Donkey	Goat	Cy2	Jackson Immunoresearch	705-225-147	1:500
		Cy3	Jackson Immunoresearch	705-165-147	1:500
		Cy5	Jackson Immunoresearch	705-175-147	1:200
Donkey	Guinea pig	Cy2	Jackson Immunoresearch	706-225-148	1:500
		Alexa488	Jackson Immunoresearch	706-545-148	1:500
		Cy3	Jackson Immunoresearch	706-165-148	1:500
Donkey	Mouse	Cy5	Jackson Immunoresearch	706-175-148	1:200
		Cy2	Jackson Immunoresearch	715-225-150	1:500
		Alexa488	Jackson Immunoresearch	715-545-150	1:500
Donkey	Rabbit	Cy3	Jackson Immunoresearch	715-165-150	1:500
		Cy5	Jackson Immunoresearch	715-175-150	1:200
		Cy2	Jackson Immunoresearch	711-225-152	1:500
Donkey	Rabbit	Alexa488	Jackson Immunoresearch	711-545-152	1:500
		Cy3	Jackson Immunoresearch	711-165-152	1:500
		Cy5	Jackson Immunoresearch	711-175-152	1:200
Donkey	Rat	Cy2	Jackson Immunoresearch	712-225-153	1:500
		Alexa488	Jackson Immunoresearch	712-545-153	1:500
		Cy3	Jackson Immunoresearch	712-165-153	1:500
		Cy5	Jackson Immunoresearch	712-175-153	1:200

### Flow Cytometry and Fluorescence-Activated Cell Sorting (FACS)

The flow analysis and sorting experiments described in Chapter IV were performed in collaboration with the Vanderbilt Flow Cytometry Core (human islet cells) and in collaboration with Dr. Katy Cogger at the

University of Toronto (hESCs). The antibodies used are listed in **Table 8**.

<b>Table 8. Antibodies for flow cytometry and sorting</b>						
Primary	<b>Antigen</b>		<b>Species</b>	<b>Source</b>	<b>Catalog #</b>	<b>Dilution</b>
	CD39L3 (NTPDase3)		Mouse (IgG)	gift of J. Sévigny	N/A	1:50
	C-peptide		Rat	DSHB	GN-ID4	1:1000
	GP2		Mouse	MBL International Corp.	D277-3	1:10,000
	HIC0-4F9 [Biotin] (HPi1)		Mouse (IgG)	Novus	NBP1-18872B	1:100
	HIC3-2D12 (HPa3)		Mouse (IgM)	gift of C. Dorrell	N/A	1:100
Secondary	Nkx6.1		Mouse	DSHB	F55A10	1:2000
	<b>Fluorophore</b>	<b>Host</b>	<b>Primary Ab</b>	<b>Source</b>	<b>Catalog #</b>	<b>Dilution</b>
	AF647	Donkey	Mouse	Life Technologies	A31571	1:400
	APC	Goat	Mouse (IgG)	BD Pharmingen	550826	1:500
	BV421–Strep	--	--	BD Pharmingen	563259	1:500
	PE	Goat	Mouse (IgM)	BD Pharmingen	550589	1:1000
	PE	Goat	Rat	BD Pharmingen	550767	1:400

DSHB – Developmental Studies Hybridoma Bank (University of Iowa); Strep – streptavidin

### **Human islet cell sorting**

Human islets from seven normal donors (ages 12-55 years, BMI 23-36), three T1D donors (ages 14-30 years, BMI 18-30), one MODY donor (age 33, BMI 26), and four T2D donors (ages 40-64 years, BMI 28-43) were dispersed using a modified protocol as described previously<sup>329</sup>. Briefly, 0.025% trypsin was used to disperse cells and reaction was quenched with modified RPMI medium (10% FBS, 1% Penn/Strep, 5 mM glucose). Cells were washed in the same medium and counted on a hemocytometer, then transferred to FACS buffer (2 mM EDTA, 2% FBS, 1X PBS). Indirect antibody labeling was completed via two sequential incubation periods at 4°C, with one wash in FACS buffer following each incubation. Primary (HPi1, HPa3, NTPDase3) and secondary antibodies, listed in **Table 8**, have been characterized previously and used to isolate high-quality RNA from  $\alpha$ - and  $\beta$ -cells<sup>47,330</sup>. Appropriate single color compensation controls were run alongside samples. Prior to sorting, propidium iodide (0.05 ug/100,000 cells; BD Biosciences) was added to samples for non-viable cell exclusion. Flow analysis was performed using an LSRFortessa cell analyzer (BD Biosciences), and a FACSAria III cell sorter (BD Biosciences) was used for FACS. Analysis of flow cytometry data was completed using FlowJo 10.1.5 (Tree Star). Gating strategy is shown in **Fig. 25**. Where indicated, a subset of collected cells was washed twice in PBS and collected onto a Plus Gold slide (Fisher Scientific) using a Cytospin 4 cytocentrifuge (ThermoFisher), then fixed in 4% PFA for 10 minutes prior to immunocytochemical analysis.

### **Flow cytometry and FACS of hESCs**

Sorting of hESCs was performed by Dr. Katy Cogger at the University of Toronto. Cells were dissociated from the monolayer using either TrypLE Express (Gibco) or StemPro Accutase (Gibco) and incubated at 37°C to generate a single-cell suspension. Live cells were incubated for 20 min at 4°C with primary antibody (GP2) in 1X PBS/10% fetal bovine serum (FBS; Wisent Inc.) (FACS buffer). After washing



twice with FACS buffer, samples labeled with unconjugated primary antibody were incubated for an additional 20 min at 4°C with secondary antibody in FACS buffer. Cells were re-suspended in 1X PBS/0.1% FBS and sorted using the BD AriaIII-RITT or AriaIII Fusion cell sorters.

For intracellular staining, cells were fixed in 1.6% PFA for 24 h at 4°C. Samples were then washed twice in FACS buffer, and incubated overnight at 4°C with primary antibodies (C-peptide, Nkx6.1) in 1X PBS containing 5 mg/ml saponin (Sigma). After two washes in FACS buffer, the cells were then incubated with secondary antibodies in saponin for 30-45 min at room temperature. Mouse and rat IgGs were used as controls. Flow cytometry was carried out using the BD LSR Fortessa flow cytometer, and data were analyzed using FlowJo software.

### RNA Isolation, Sequencing, and Analysis

*RNA sequencing and analysis was performed at the HudsonAlpha Institute for Biotechnology in Huntsville, AL, with the help of Shristi Shrestha and Dr. Nripesh Prasad.* Sorted  $\alpha$ - and  $\beta$ -cells (5,000-123,000) were stored in 200  $\mu$ L lysis/binding solution (Ambion) at -80°C prior to RNA isolation using the RNAqueous micro-scale phenol-free total RNA isolation kit (Ambion). Trace DNA was removed with TURBO DNA-free (Ambion), RNA integrity was evaluated (Agilent 2100 Bioanalyzer;  $7.90 \pm 0.23$  RIN,  $n=21$ ), and high-integrity total RNA was amplified (Ovation system; NuGen Technologies) per standard protocol as described previously<sup>201</sup>. Amplified cDNA was sheared to target 200bp fragment size and libraries were prepared using NEBNext DNA Library Prep (New England BioLabs). 50bp Paired End (PE) sequencing was performed on an Illumina HiSeq 2500 using traditional Illumina methods<sup>331</sup> to generate approximately 50 million reads per sample. Raw reads were mapped to the reference human genome hg19 using TopHat v2.1<sup>332</sup>. Aligned reads were then imported onto the Avasis NGS analysis platform (Strand life Sciences) and filtered based on read quality followed by read statistics to remove duplicates. Transcript abundance was quantified using the TMM (Trimmed Mean of M-values) algorithm<sup>333,334</sup> as the normalization method. Genes with normalized expression values less than 25 were removed prior to differential expression analysis between control and T1D groups. Fold change (cutoff  $\geq \pm 1.5$ ) was calculated based on p-value estimated by z-score calculations (cutoff 0.05) as determined by Benjamini Hochberg false discovery rate (FDR) correction of 0.05<sup>335</sup>. Differentially expressed genes were further analyzed through Ingenuity Pathway Analysis (IPA, Qiagen) and Gene Ontology (GO) analysis using DAVID v6.8<sup>336</sup>.

### Islet Transplantation

Human islets from four normal donors (ages 10-61 years, BMI 25-35) were obtained through IIDP, ADI, and nPOD (**Table 5**) and transplanted into immunodeficient 10-12 week old NOD-*scid-IL2ry*<sup>null</sup> (NSG) male mice. For each donor, 3-5 mice were transplanted with 100-200 islet equivalents under the contralateral kidney capsule or into the anterior chamber of the eye (ACE) as described previously<sup>337-339</sup>. Briefly, islets were loaded into P10 tubing, mice were anesthetized and their kidneys exposed by dissecting through flank skin and muscle layers. The capsule was separated from the kidney

parenchyma using a 23-gauge butterfly needle and the P10 tubing containing donor islets was inserted into the channel created by the needle. Muscle and skin layers were closed and mice were observed daily for 2 weeks after surgery. Islets were allowed to engraft for 1 month prior to imaging.

### ***In vivo* Imaging**

Mice were anesthetized using a standard dose of isoflurane and injected with 100  $\mu$ L of saline containing 30  $\mu$ g of DyLight550-conjugated NTPDase3 antibody (Vanderbilt Antibody and Protein Resource) or isotype control (Novus) into the left retro-orbital space. After recovery for 24 hours, mice were again anesthetized and placed on the microscope stage with right eye facing up and oriented to reveal islet graft (visible under white light). Images showing the iris bearing grafted islets were obtained using an Olympus SZX12 fluorescent stereomicroscope equipped with a DP80 camera (Olympus) and *CellSens* image acquisition and analysis software (Olympus). Following imaging, mice were sacrificed and grafts were removed and fixed according to the standard protocol for pancreas fixation described above.

### **Statistical Analysis**

Prism software (GraphPad) was used to perform statistical analysis comparing two groups using unpaired t tests and one-way analysis of variance with Tukey's multiple comparison test to compare three or more groups. Unless otherwise noted, data are expressed as mean  $\pm$  standard error of mean. Statistical analysis of RNA-sequencing data is described above (see RNA Isolation, Sequencing, and Analysis).

## CHAPTER III

### ENDOTHELIAL CELLS IN THE ISLET MICROENVIRONMENT, IN CONCERT WITH MACROPHAGES, MODULATE BETA CELL PROLIFERATION

#### Introduction

Vascular endothelial growth factor A (VEGF-A) is the master regulator of islet vascular development<sup>208,222,223,228</sup>. VEGF-A inactivation in pancreatic and islet progenitors leads to dramatic reduction in islet vasculature which is accompanied by reduced  $\beta$ -cell mass and impaired insulin secretion<sup>246,250,251</sup>. However, when VEGF-A is inactivated in the adult islets, they lose approximately 40% of their vasculature, but maintain normal  $\beta$ -cell mass and nearly normal function<sup>222,246,252,253</sup>. These results suggest that islet vasculature and VEGF-A signaling are required for early postnatal  $\beta$ -cell growth but play lesser role in the maintenance of adult  $\beta$ -cell mass and function.

Since VEGF-A reduction during development had a deleterious effect on  $\beta$ -cell mass, our group asked whether an increase in VEGF-A might enhance  $\beta$ -cell proliferation during development. Using the inducible RIP-rtTA; TetO-VEGF-A ( $\beta$ VEGF-A) mouse model, we showed that  $\beta$ -cell-specific overexpression of VEGF-A increased EC proliferation but decreased the number of Ngn3<sup>+</sup> progenitors, leading to altered islet morphology as well as reduced  $\beta$ -cell proliferation<sup>251</sup>. These findings have been corroborated by subsequent reports of enhanced VEGF-A signaling during pancreatic development causing hypervascularization and disrupted islet architecture<sup>254,255</sup>. We next used the same  $\beta$ VEGF-A model to overexpress VEGF-A in adult  $\beta$ -cells, which initially caused rapid EC expansion and marked  $\beta$ -cell death<sup>201</sup>. The most striking observation came after VEGF-A normalization: there was a transient but robust burst of  $\beta$ -cell proliferation leading to restoration of  $\beta$ -cell mass, islet structure, and function after a period of 6 weeks<sup>201</sup> (**Fig. 11a**). EC expansion was accompanied by recruitment of circulating monocytes, and experiments with islets transplanted under the kidney capsule of  $\beta$ VEGF-A mice revealed that regeneration was independent of the site and circulating factors, but was instead derived from the local islet microenvironment<sup>201</sup>. Ablation of macrophage recruitment significantly reduced  $\beta$ -cell proliferation, indicating that macrophages were required for  $\beta$ -cell regeneration<sup>201</sup>.

RNA-seq analysis of ECs, macrophages, and  $\beta$ -cells isolated from  $\beta$ VEGF-A mice indicated that intra-islet ECs increase expression of several growth factors (*Ctgf*, *Igf1*, *Pdgfa*; **Fig. 11b**) that have been previously shown to stimulate  $\beta$ -cell proliferation<sup>160,249,340-343</sup>. Furthermore, they express cell adhesion molecules (*Madcam1*, *Vcam1*) and cytokines (*Il10*) that are capable of recruiting and/or polarizing macrophages to an M2-like or “restorative” phenotype<sup>344-346</sup>. This led us to hypothesize that intra-islet ECs provide crucial microenvironmental cues that promote  $\beta$ -cell regeneration (**Fig. 11c**).

We know much less about the role that islet microenvironment plays in human pancreatic development; limited studies suggest that, like mice, human islets become vascularized early during fetal development<sup>37,316</sup>, but adult human islets have significantly fewer capillaries than the adult mouse<sup>39</sup>. However, it is unknown if human islets are formed with fewer blood vessels at birth or whether islet vasculature declines with aging. Mounting evidence suggests that  $\beta$ -cell mass is largely established

during the early postnatal period and  $\beta$ -cell proliferation declines sharply after birth<sup>35,347,348</sup>. Proliferation rates of the three main endocrine cell types ( $\alpha$ -,  $\beta$ -,  $\delta$ -cells) exhibit distinct trends, with a precipitous drop in  $\delta$ -cell proliferation and  $\delta$ -cell number shortly after birth and gradual increase in  $\beta$ -cell population<sup>349</sup>. Notably,  $\beta$ -cell proliferation also declines postnatally but is still much higher in juvenile period (<10 years of age) compared to adult islets<sup>35</sup>. Our group has also observed that early postnatal development in human islets is marked by dramatic changes in islet cell composition, arrangement, and interaction with vascular and neuronal components. We have shown that endocrine cells undergo dynamic rearrangements in developing islets, with initial mantle-core architecture reminiscent of a rodent islet followed by gradual intermingling of proliferating  $\alpha$ -,  $\beta$ -, and  $\delta$ -cells<sup>349</sup>. Together, these observations suggest the hypothesis that ECs in the developing human islet, like those in our  $\beta$ VEGF-A mouse model, provide local signals to facilitate  $\beta$ -cell proliferation.

In this chapter we have tested our hypothesis that intra-islet ECs, alone or in concert with macrophages, provide permissive signals to promote  $\beta$ -cell proliferation. First, to determine the contribution of intra-islet ECs to macrophage recruitment, macrophage phenotype activation, and  $\beta$ -cell proliferation in the  $\beta$ VEGF-A mouse model, we have targeted VEGFR2, the primary receptor for VEGF-A signaling that is expressed by islet ECs<sup>222,223</sup>. Several groups have demonstrated the importance of VEGF-A-VEGFR2 signaling in tissue regeneration, including in the liver, lung, and hematopoietic systems<sup>220,276,277</sup>. We therefore predicted that knocking down VEGFR2 in proliferative and quiescent ECs would disrupt macrophage recruitment and polarization and impair  $\beta$ -cell proliferation. To extend our hypothesis to human  $\beta$ -cells, we also performed a cross-sectional analysis of angioarchitecture during human pancreas development and aligned the data we collected with existing data on  $\beta$ -cell proliferation.

## Results

### ***Acute ablation of VEGFR2 in ECs does not affect islet vasculature or $\beta$ -cell proliferation***

To define the role of VEGFR2 signaling in adult islet capillary maintenance, we generated a Tamoxifen (Tmx)-inducible mouse model of  $Cad5$ -CreER<sup>T2</sup>; VEGFR2<sup>fl/fl</sup> (VEGFR2<sup>iAEC</sup>). Pancreata were removed 1-2 weeks after initial Tmx or vehicle treatment (8d and 15d time points, respectively; **Fig. 12a**). VEGFR2 was virtually undetectable in ECs from Tmx-treated mice at both time points, indicating efficient knockdown. Importantly, however, vascular structures (visualized by either CD31 or caveolin-1 labeling) remained intact (**Fig. 12b**). There was no significant difference in islet vessel area or density at 8d (**Fig. 12c**), suggesting that acute loss of VEGFR2 signaling does not play a significant role in adult islet vascular homeostasis. There was also no difference in basal  $\beta$ -cell proliferation rates between Tmx- and vehicle-treated mice (0.79 and 0.65% respectively,  $p < 0.05$ ; **Fig. 12d**), indicating that under basal conditions VEGFR2 signaling lost acutely in intra-islet ECs does not affect  $\beta$ -cell proliferation.

### ***Proliferative ECs are required for macrophage polarization and maximal macrophage recruitment***

To investigate the role of proliferative ECs in macrophage recruitment and polarization, we combined the  $\beta$ VEGF-A system (RIP-rtTA; TetO-VEGFA) with our inducible VEGFR2 knockout (VEGFR2<sup>iAEC</sup>), as shown in **Table 2**. This allowed us to modulate VEGF-A-VEGFR2 signaling in an inducible manner by

administering Dox to overexpress VEGF-A in  $\beta$ -cells and Tmx to inactivate VEGFR2 in ECs. Due to possible effects of Tmx administration on compensatory  $\beta$ -cell proliferation<sup>350</sup>, we elected to treat all mice with Tmx and designated Cre-negative ( $\beta$ VEGF-A; VEGFR2<sup>fl/fl</sup>) mice as controls to represent intact VEGFR2. We performed all experiments in both male and female mice; however, due to the inefficient induction of VEGF-A in females (the *TetO* transgene is X-linked, and  $\beta$ VEGF-A; VEGFR2<sup>iAEC</sup> mice only have one copy, so it may be randomly inactivated in some cells), all of the data presented in this chapter is from male mice only.

Administration of Tmx was utilized to knock down VEGFR2 in ECs, followed by Dox treatment for 3 days to induce VEGF-A (**Fig. 13a**). We confirmed effective VEGF-A induction in both  $\beta$ VEGF-A; VEGFR2<sup>fl/fl</sup> and  $\beta$ VEGF-A; VEGFR2<sup>iAEC</sup> genotypes (**Fig. 13b**), as well as efficient knockdown of VEGFR2 in the latter (**Fig. 13c**). We then analyzed various aspects of islet phenotype using mice receiving no treatment (No Dox) as a baseline. After 3 days Dox, vasculature expanded in  $\beta$ VEGF-A; VEGFR2<sup>fl/fl</sup> mice (from 27.9 $\pm$ 2.2 to 48.5 $\pm$ 2.4% of total islet area;  $p < 0.05$ ) but not in  $\beta$ VEGF-A; VEGFR2<sup>iAEC</sup> mice (29.1 $\pm$ 3.6 to 23.9 $\pm$ 3.2%;  $p > 0.05$ ; **Fig. 14a,c**). There was a slight accompanying decrease in  $\beta$ -cell area of control  $\beta$ VEGF-A; VEGFR2<sup>fl/fl</sup> islets due to EC expansion (53.2 $\pm$ 6.6 to 41.2 $\pm$ 2.4% of total islet area), while  $\beta$ -cell area in  $\beta$ VEGF-A; VEGFR2<sup>iAEC</sup> islets did not change (**Fig. 14a,d**).

Macrophage recruitment was observed in both genotypes, though recruitment was higher when VEGFR2 signaling was intact than in  $\beta$ VEGF-A; VEGFR2<sup>iAEC</sup> mice (10.3 $\pm$ 0.7 vs. 7.8 $\pm$ 0.6% of total islet area, respectively;  $p < 0.05$ ; **Fig. 14e**). These data suggest that some macrophages infiltrated islets in response to VEGF-A alone, even with no damage to  $\beta$ -cells, but also indicate that intact VEGF-A-VEGFR2 signaling promotes maximal macrophage recruitment. We next examined macrophage polarization by labeling for the “M2-like” marker MRC1 (CD206) (**Fig. 14b**), which is normally expressed by resident macrophages of the exocrine pancreas but not by intra-islet macrophages<sup>151,351</sup>. However, after VEGF-A induction some infiltrating macrophages in control  $\beta$ VEGF-A; VEGFR2<sup>fl/fl</sup> islets were MRC1<sup>+</sup>, while infiltrating macrophages in  $\beta$ VEGF-A; VEGFR2<sup>iAEC</sup> islets remained MRC1<sup>-</sup> (**Fig. 14f**). This observation suggests that VEGFR2 signaling in proliferative endothelial cells and/or  $\beta$ -cell loss is necessary for macrophage polarization to an M2-like phenotype.

### ***VEGFR2 knockout in quiescent ECs accelerates EC regression, promoting $\beta$ -cell recovery***

To investigate the role of quiescent ECs in  $\beta$ -cell proliferation, we treated  $\beta$ VEGF-A; VEGFR2<sup>fl/fl</sup> and  $\beta$ VEGF-A; VEGFR2<sup>iAEC</sup> mice for 3 days with Dox to induce VEGF-A and allowed 7 days of Dox withdrawal (WD) for VEGF-A to normalize and ECs to return to quiescence (**Fig. 15a**). We sacrificed some animals at this 7d WD time point, then gave the remaining mice one dose of Tmx to knock down VEGFR2. We harvested pancreata 48 hours later (9d WD, 2d post-Tmx) to assess islet phenotype.

As expected, VEGF-A expression declined during Dox WD (**Fig. 15b**), and VEGFR2 was efficiently knocked down in  $\beta$ VEGF-A; VEGFR2<sup>iAEC</sup> mice 48 hours after Tmx treatment (**Fig. 15c**). VEGF-A-induced EC expansion occurred in both  $\beta$ VEGF-A; VEGFR2<sup>fl/fl</sup> (from 27.9 $\pm$ 2.2 to 66.5 $\pm$ 2.3% of total islet area;  $p < 0.05$ ) and  $\beta$ VEGF-A; VEGFR2<sup>iAEC</sup> (29.1 $\pm$ 3.6 to 61.2 $\pm$ 3.2%;  $p < 0.05$ ) mice, with no difference in EC area between the two groups at 7dWD ( $p > 0.05$ ; **Fig. 16a-b**). Within 48 hours of Tmx administration

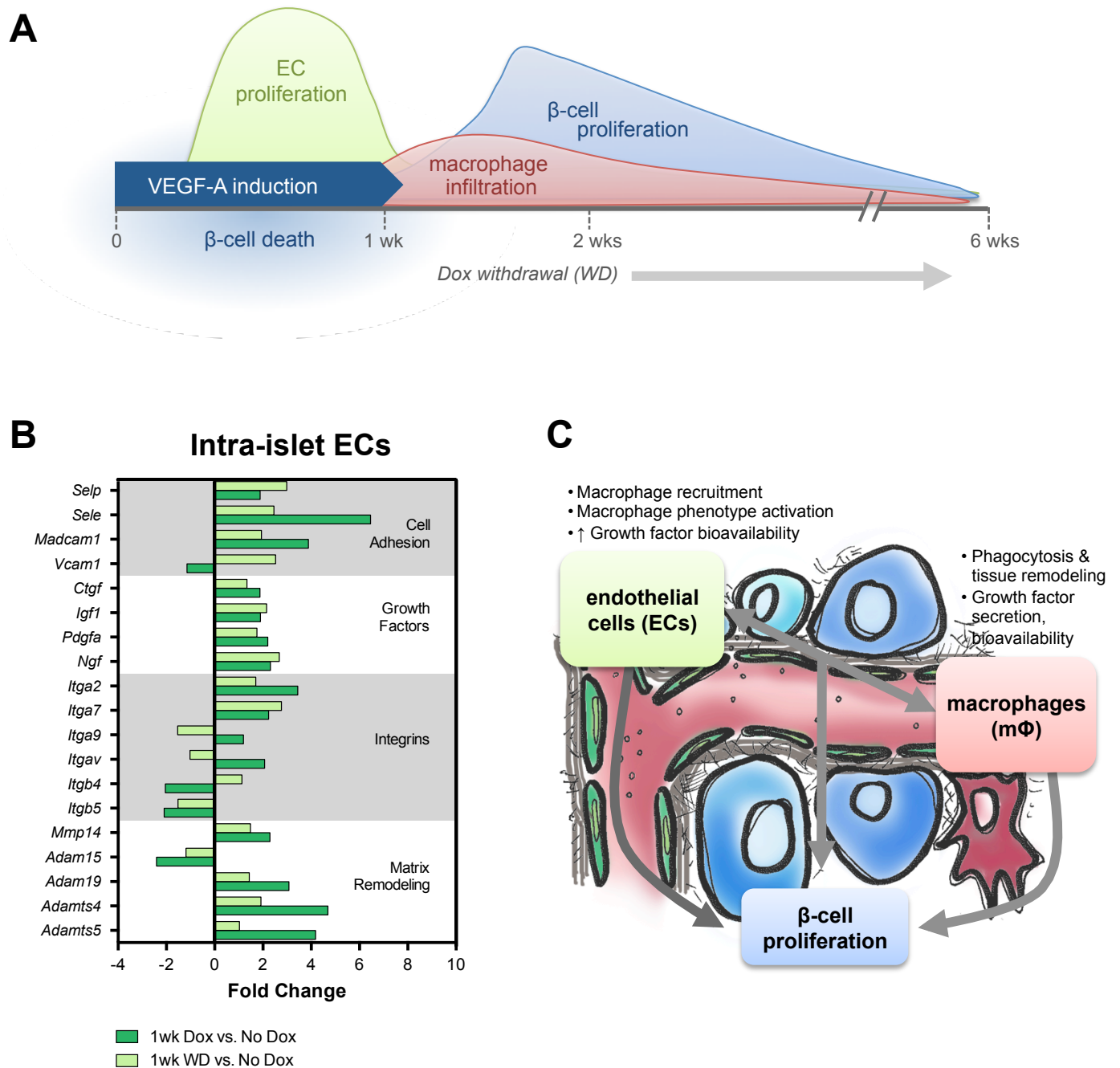
(9d WD), there was significant regression of vasculature in  $\beta$ VEGF-A; VEGFR2<sup>iΔEC</sup> islets (61.2±3.2 to 41.6±1.5% of total islet area; p<0.05), while EC area in  $\beta$ VEGF-A; VEGFR2<sup>fl/fl</sup> islets remained elevated (66.5±2.3 vs. 57.23±4.3%; p>0.05; **Fig. 16b**). Unexpectedly,  $\beta$ VEGF-A; VEGFR2<sup>iΔEC</sup> islets had significantly greater  $\beta$ -cell area as compared to  $\beta$ VEGF-A; VEGFR2<sup>fl/fl</sup> after Tmx (30.4±1.6 vs. 21.4±3.3% of total islet area, respectively; p<0.05; **Fig. 16c**), and  $\beta$ -cell proliferation was slightly higher in  $\beta$ VEGF-A; VEGFR2<sup>iΔEC</sup> compared to  $\beta$ VEGF-A; VEGFR2<sup>fl/fl</sup> (5.0±0.7 vs. 3.2±0.7 percent, respectively; p=0.09; **Fig. 16e**). Together, these data point to VEGFR2 inactivation in quiescent ECs having a surprisingly stimulatory effect on  $\beta$ -cell recovery.

Since EC-secreted factors normally promote  $\beta$ -cell proliferation, we wondered why loss of quiescent EC signaling would have the opposite impact. Noticing the reduction in intra-islet EC area that accompanied VEGFR2 inactivation, we explored the possibility that EC-associated ECM, which includes structural protein components as well as binding sites for growth factors and other signaling molecules, was altered. Visualization of col-IV, a major component of the islet ECM<sup>206,281</sup>, revealed that by two days after VEGFR2 knockdown, when ECs had started to regress, there were pockets (vascular “casts”) of ECM that were not associated with intact ECs (**Fig. 17b**). We hypothesize that vessel regression may have promoted release of growth factors from degraded ECM, thereby promoting  $\beta$ -cell proliferation (**Fig. 17c**).

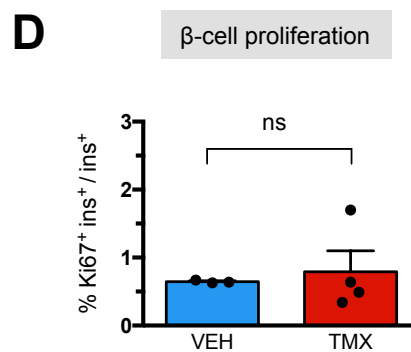
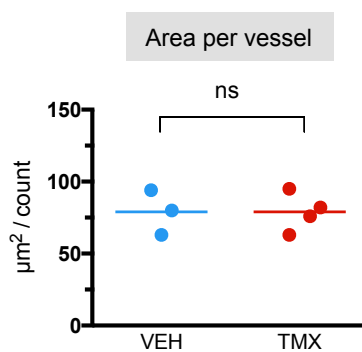
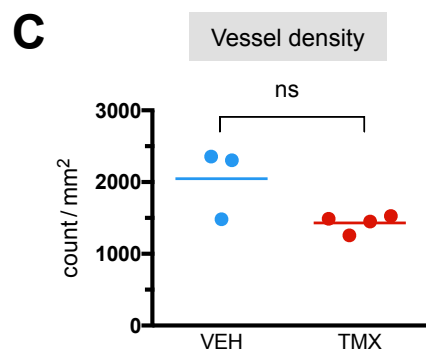
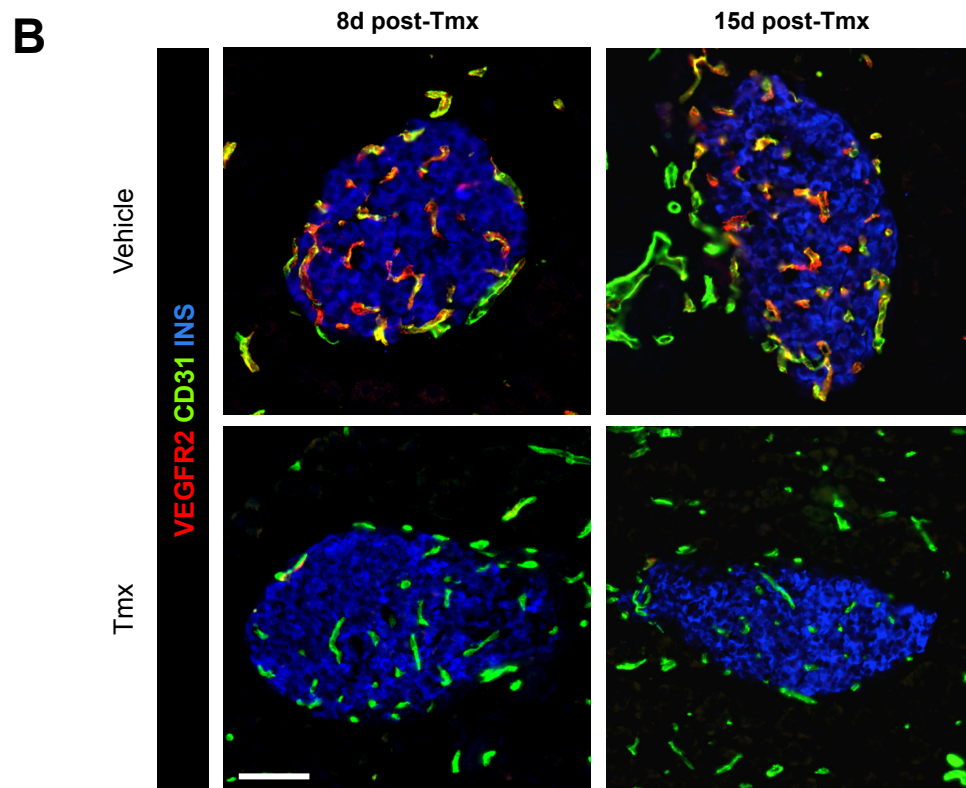
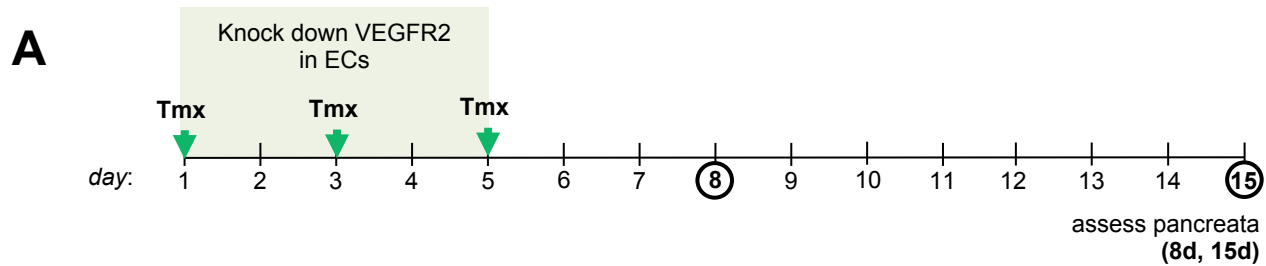
Recruited macrophages persisted in islets even after VEGFR2 knockdown (**Fig. 16d**), suggesting that their retention is not dependent on VEGFR2 signaling in quiescent ECs. MRC1<sup>+</sup> macrophages were present in islets from  $\beta$ VEGF-A; VEGFR2<sup>fl/fl</sup> and  $\beta$ VEGF-A; VEGFR2<sup>iΔEC</sup> mice both before (7d WD) and after (9d WD) Tmx treatment (**Fig. 17a**), indicating that compromised VEGF-A-VEGFR2 signaling at this stage of  $\beta$ -cell recovery does not affect macrophage polarization.

### ***ECs are most abundant in human islets during early postnatal pancreatic development***

To investigate the dynamics of intra-islet vasculature during human pancreatic development, we performed a cross-sectional immunohistochemical analysis on pancreatic tissue sections from 26 human donors ranging from the early postnatal period (born at G37 weeks) to 11 years of age. A complete list of donors and additional characteristics are provided in **Table 4**, with representative images shown in **Fig. 18a**. We quantified EC area, expressed as a percentage of total islet area, in neonates ( $\leq$ 2 months; n=9), infants (>2 month – 2 years; n=11), and children (>2 years – 10 years; n=6). Neonatal islets had the greatest EC component at 9.8% (range 3.5-15.2), but infant islets were very similar (9.2%; range 4.0-18.4). EC area in children was slightly lower (7.6%; range 2.0-10.3), though not significantly different from that of neonates or infants (one-way ANOVA, p>0.05). Despite heterogeneity among donors of the same ages, intra-islet EC area trended highest during early postnatal life ( $\leq$ 2 years) and slightly declined thereafter (**Fig. 18b-c**). Furthermore, this peak correlated to the height of  $\beta$ -cell proliferation observed in the juvenile human pancreas (**Fig. 18b**).

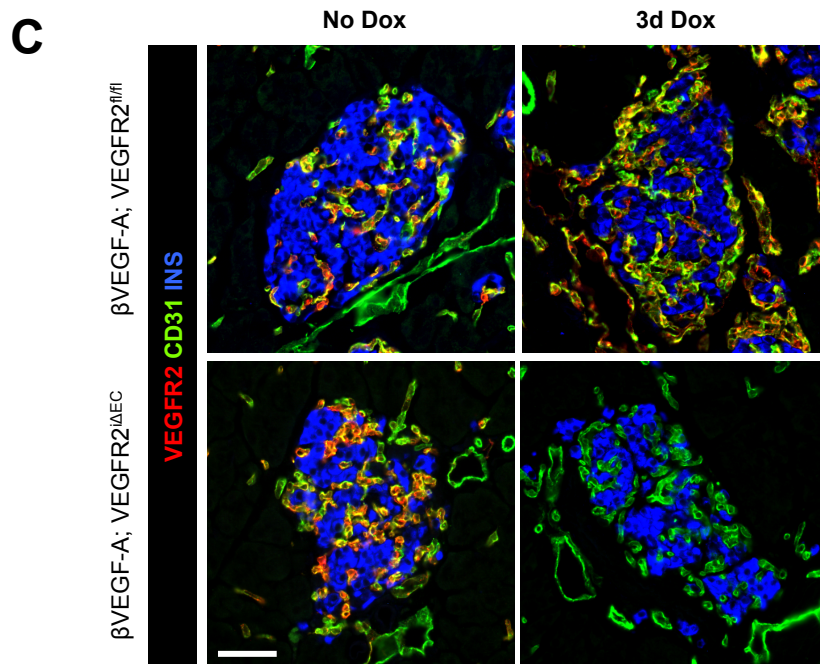
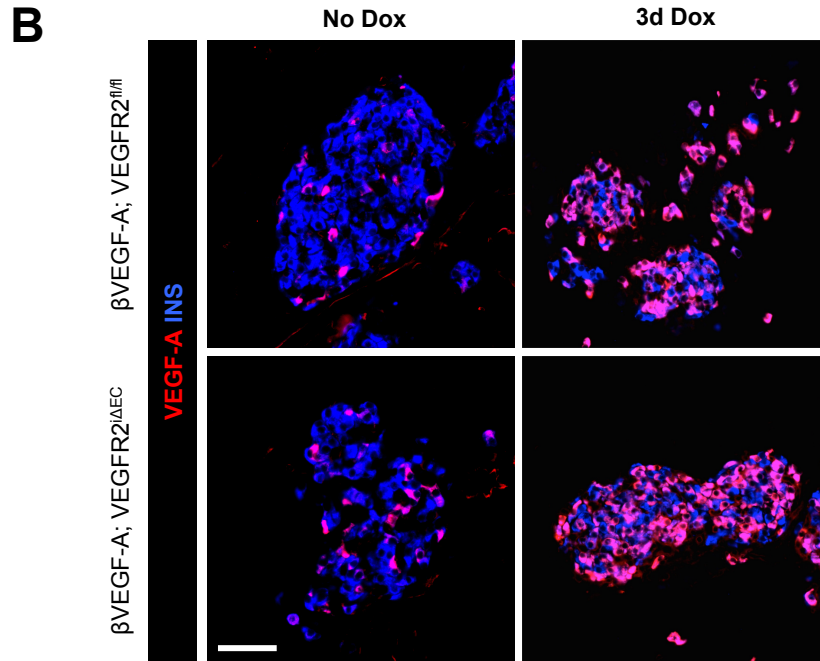
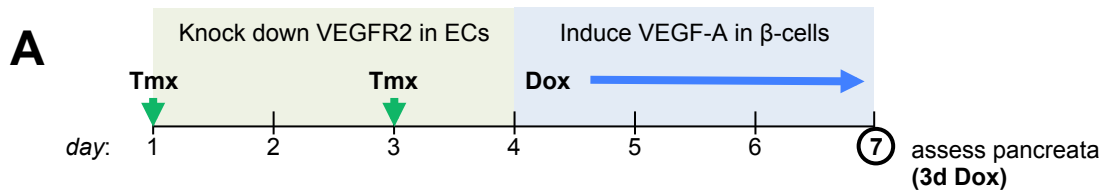


**Figure 11: Islet microenvironment, modulated by VEGF-A signaling, promotes β-cell regeneration.**  
**(A)** Schematic showing dynamics of β-cells (blue), ECs (green), and macrophages (red) in βVEGF-A mice during the induction and subsequent normalization of VEGF-A. **(B)** Transcriptome analysis of ECs isolated from βVEGF-A islets. Changes in selected genes are shown after VEGF-A induction (1wk Dox vs. No Dox, dark green) and then during VEGF-A withdrawal (1wk WD vs. No Dox, light green). **(C)** Model depicting the interaction between ECs and macrophages to promote β-cell proliferation. Images are adapted from Brissova *et al.*, 2014<sup>201</sup>, and graph is generated from sequencing data made available with the same publication.

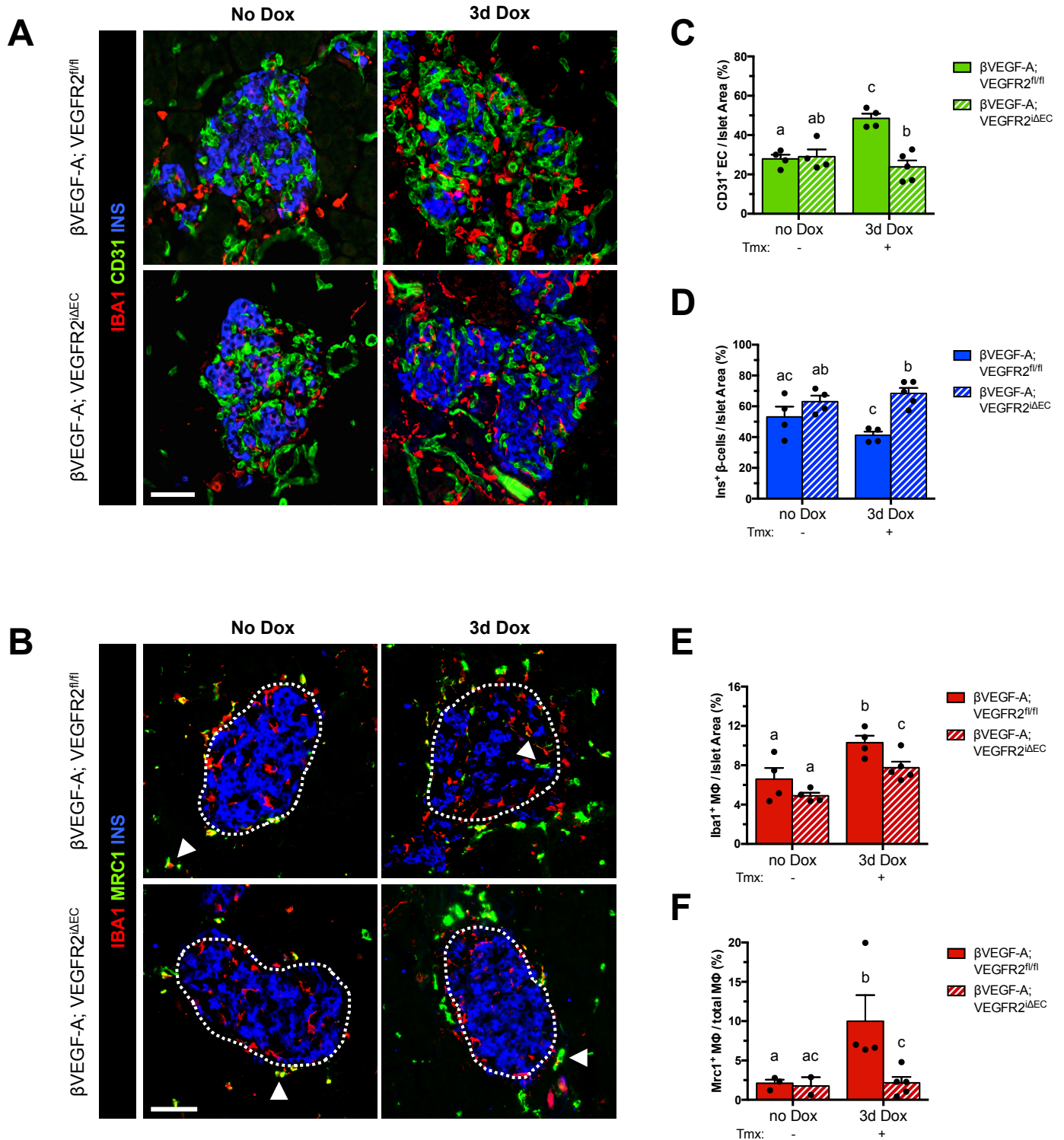


**Figure 12: Acute ablation of VEGFR2 in ECs.** (A) Schematic of Tmx administration. (B) Architecture of islet vasculature (CD31<sup>+</sup> ECs) and β-cells (INS<sup>+</sup>) in vehicle-treated and Tmx-treated Cdh5-CreER<sup>T2</sup>; VEGFR2<sup>fl/fl</sup> (VEGFR2<sup>iΔEC</sup>) mice. VEGFR2 expression shown in red; scale bar is 50 µm. (C) Quantification of islet vasculature (islet area per animal = 13,817 ± 1502 mm<sup>2</sup>) at 8d post-Tmx (t-test, p < 0.05; n = 3-4 per group). (D) Basal β-cell proliferation rates (1,892 ± 259 β-cells) at 8d post-Tmx (t-test, p < 0.05; n = 3-4 per group).

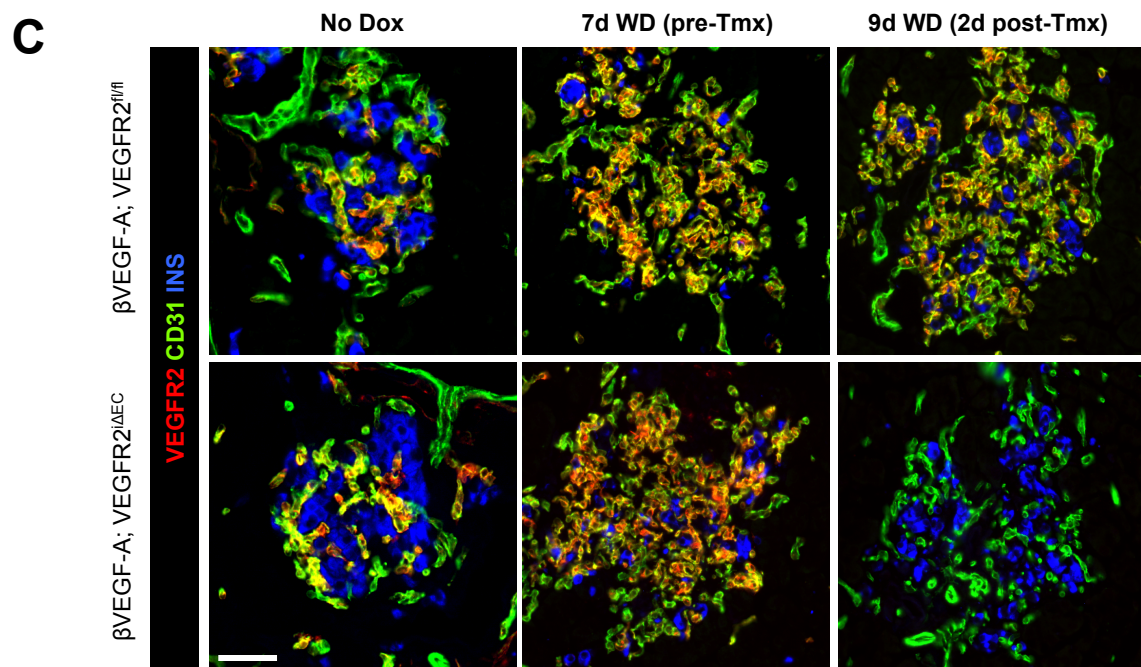
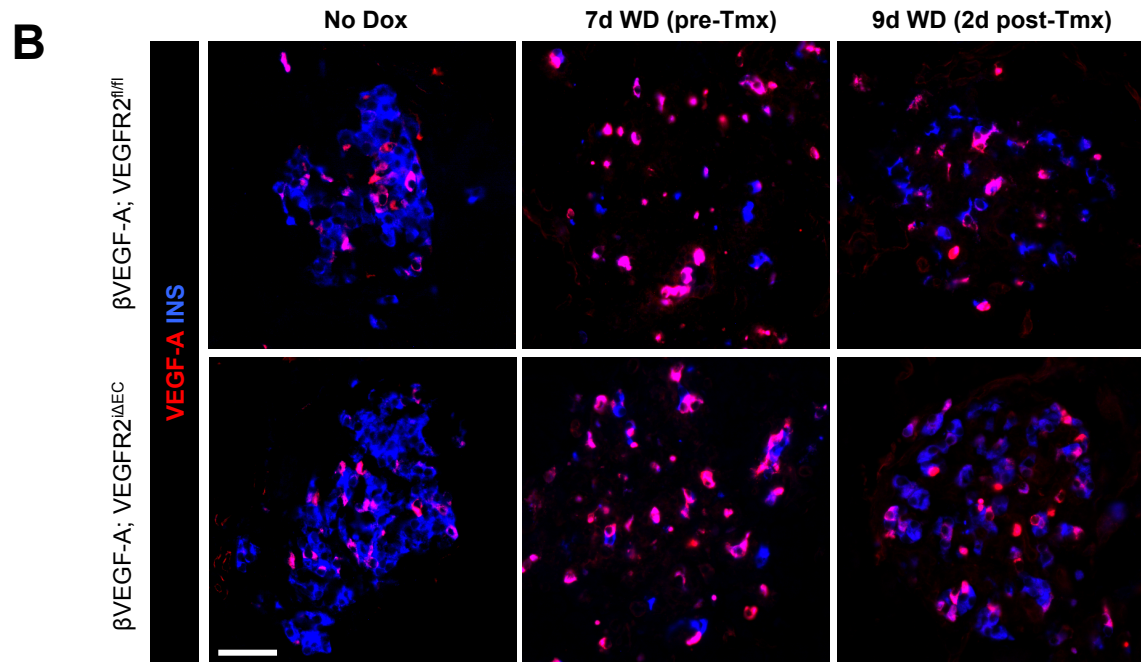
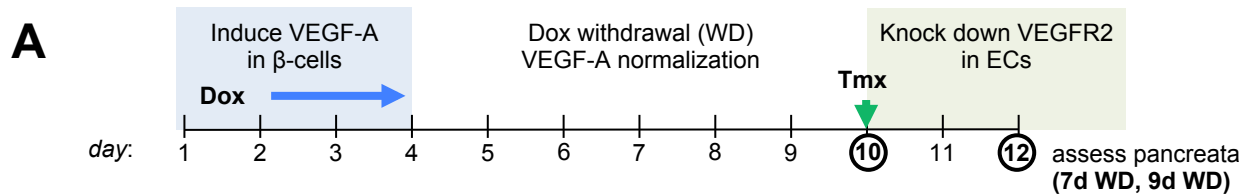




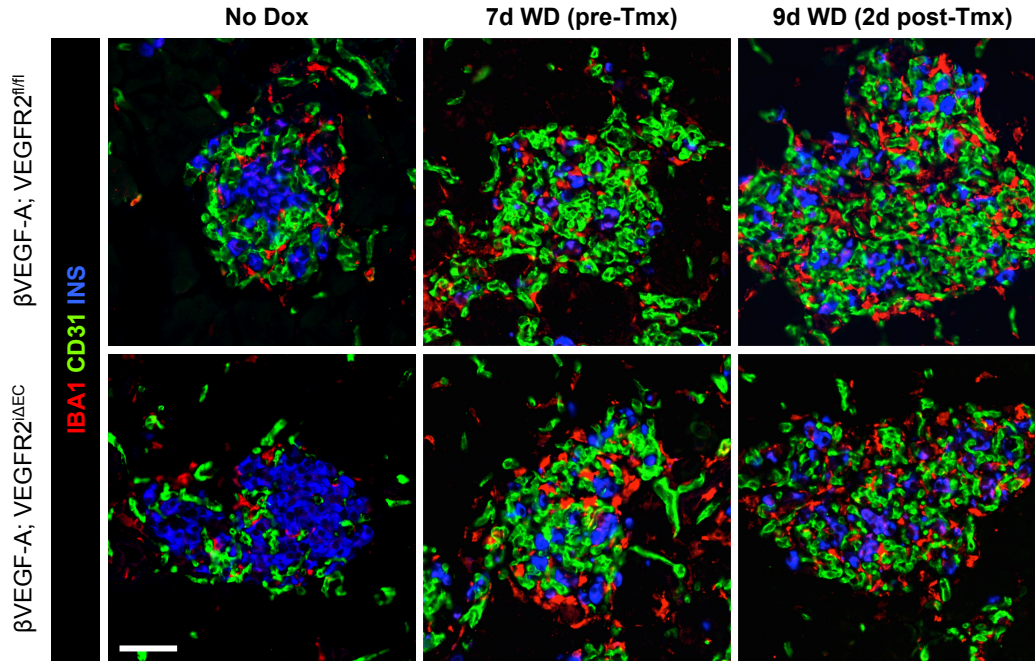
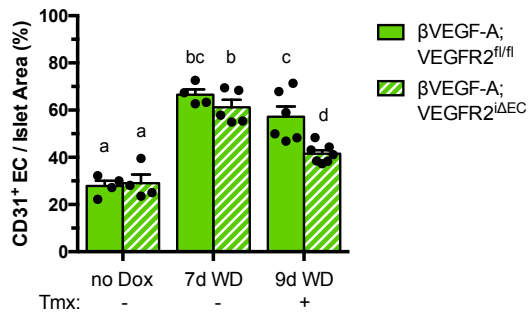
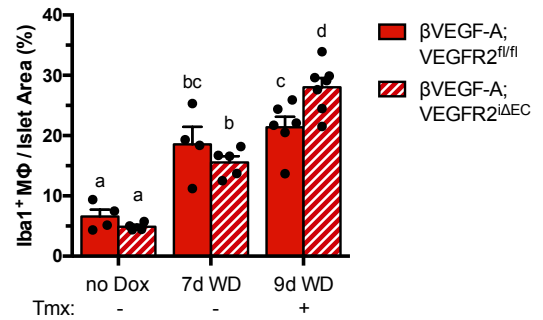
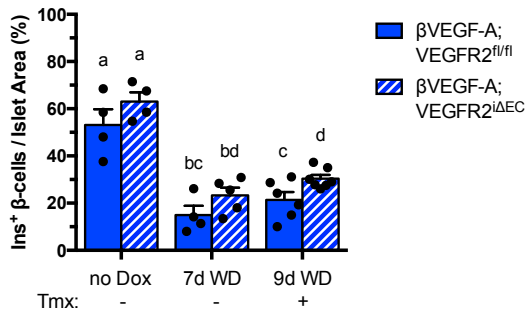
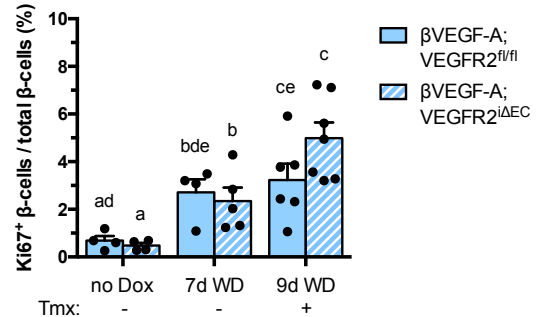
**Figure 13: VEGF-A induction and VEGFR2 inactivation in proliferative ECs.** (A) Schematic of Dox and Tmx administration. (B) VEGF-A expression (red) in  $\beta$ -cells (INS<sup>+</sup>) of  $\beta$ VEGF-A; VEGFR2<sup>fl/fl</sup> and  $\beta$ VEGF-A; VEGFR2<sup>ΔEC</sup> mice at baseline (no Dox) and 3d Dox. (C) VEGFR2 expression (red) in ECs (CD31<sup>+</sup>) at baseline and 3d Dox. Scale bars in B and C are 50  $\mu$ m.



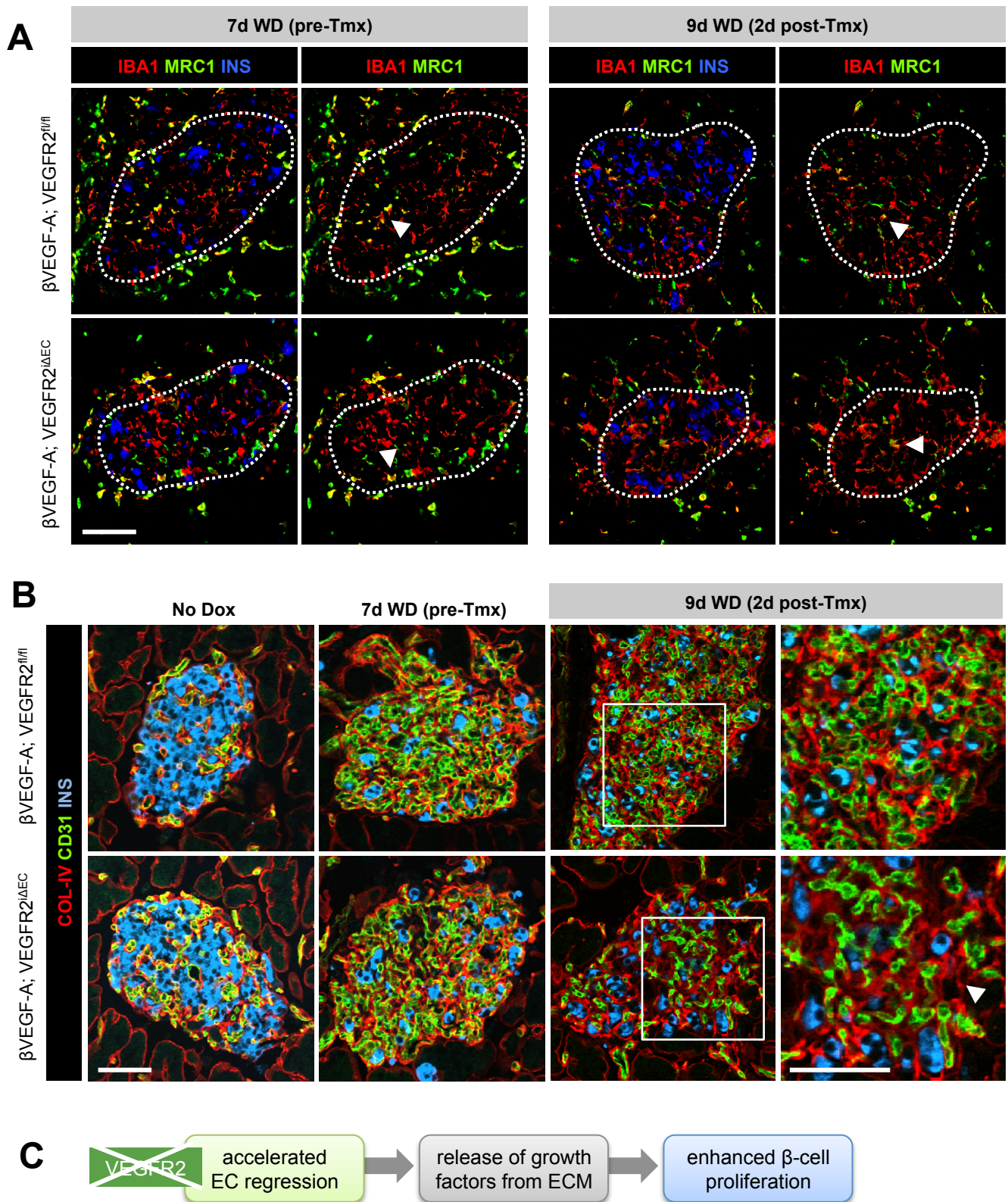
**Figure 14: Islet changes following VEGFR2 knockout in proliferative ECs.** (A) Islet architecture of macrophages (IBA1<sup>+</sup>), ECs (CD31<sup>+</sup>), and  $\beta$ -cells (INS<sup>+</sup>) from  $\beta$ VEGF-A; VEGFR2<sup>fl/fl</sup> and  $\beta$ VEGF-A; VEGFR2 $\Delta$ EC mice at baseline (no Dox) and 3d Dox. Graphs in (C) – (E) show quantification (mean  $\pm$  SEM) of islet composition (674  $\pm$  78  $\mu$ m<sup>2</sup> per animal) by immunohistochemistry. Letters above bars refer to statistical comparison of means; means with different letters are significantly different (t-test comparing genotypes within time point or comparing time point within genotype,  $p < 0.05$ ;  $n = 4-5$  per group per genotype). (B) Islet macrophages with an “M2-like” phenotype (MRC1<sup>+</sup>) at no Dox and 3d Dox. Arrowheads point to examples of these macrophages. Graph in (F) depicts percentage of M2-like intra-islet macrophages (MRC1<sup>+</sup> Iba1<sup>+</sup>). Scale bars are 50  $\mu$ m.



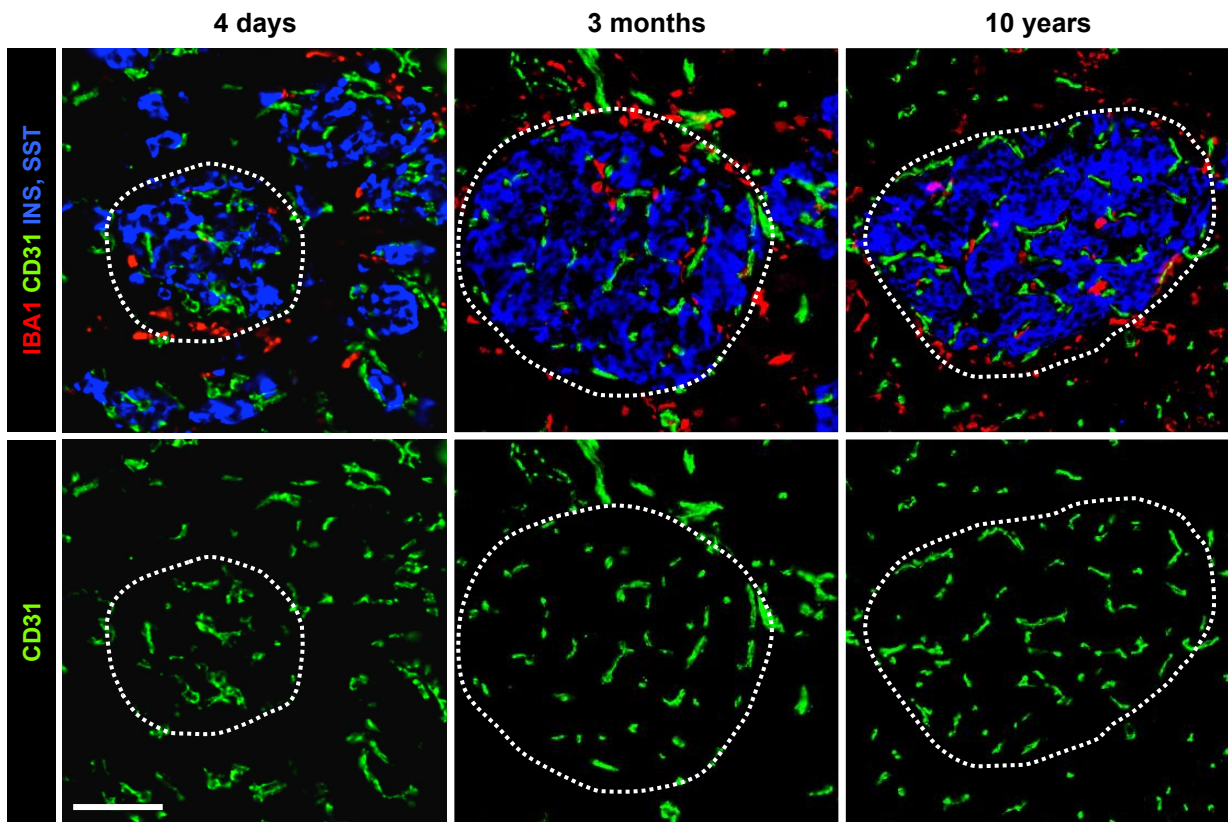
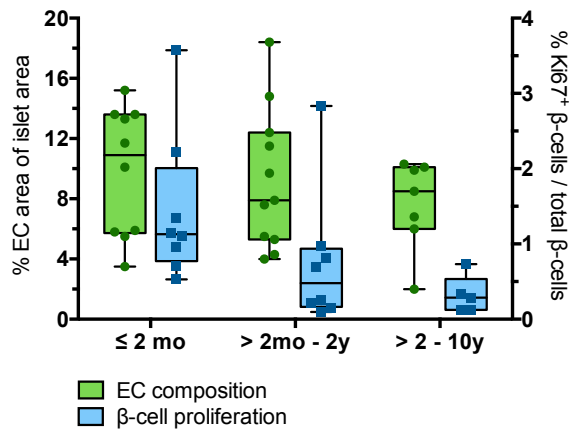
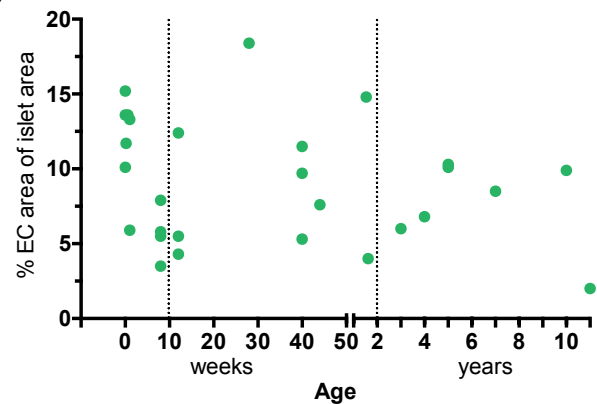
**Figure 15: VEGF-A induction and VEGFR2 inactivation in quiescent ECs.** (A) Schematic of Dox and Tmx administration. (B) VEGF-A expression (red) in  $\beta$ -cells (INS<sup>+</sup>) of  $\beta$ VEGF-A; VEGFR2<sup>fl/fl</sup> and  $\beta$ VEGF-A; VEGFR2<sup>ΔEC</sup> mice at no Dox, 7d WD (pre-Tmx), and 9d WD (2d post-Tmx). (C) VEGFR2 expression (red) in ECs (CD31<sup>+</sup>) at no Dox, 7d WD, and 9d WD. Scale bars in B and C are 50  $\mu$ m.

**A****B****D****C****E**

**Figure 16: Islet changes following VEGFR2 knockout in quiescent ECs. (A)** Islet architecture of macrophages (IBA1<sup>+</sup>), ECs (CD31<sup>+</sup>), and  $\beta$ -cells (INS<sup>+</sup>) from  $\beta$ VEGF-A; VEGFR2<sup>fl/fl</sup> and  $\beta$ VEGF-A; VEGFR2 <sup>$\Delta$ EC</sup> mice at no Dox, 7d WD (pre-Tmx), and 9d WD (2d post-Tmx). Scale bar is 50  $\mu$ m. **(B)-(D)** Quantification (mean  $\pm$  SEM) of islet composition (957  $\pm$  118  $\mu$ m<sup>2</sup> per animal) and **(E)**  $\beta$ -cell proliferation rates (2,427  $\pm$  158  $\beta$ -cells) by immunohistochemistry. Letters above bars refer to statistical comparison of means; means with different letters are significantly different (t-test comparing genotypes within time point or one-way ANOVA/Tukey's post-hoc comparing time points within genotype,  $p < 0.05$ ;  $n = 4-7$  per group per genotype).



**Figure 17: Macrophage and ECM phenotypes after VEGFR2 knockout in quiescent ECs. (A)** Islet macrophages (Iba1<sup>+</sup>) with an “M2-like” phenotype (MRC1<sup>+</sup>) from βVEGF-A; VEGFR2<sup>fl/fl</sup> and βVEGF-A; VEGFR2<sup>ΔEC</sup> mice at 7d WD (pre-Tmx) and 9d WD (2d post-Tmx). Approximate islet area is outlined; right column in each group shows only macrophages (β-cell channel removed). Arrowheads point to examples of M2-like macrophages. **(B)** Architecture of ECM, visualized by COL-IV, prior to and after VEGFR2 knockout. Images in far right column are magnifications of boxed areas in previous column. Arrowhead points to ECM casts where ECs have regressed. **(C)** Proposed model for enhanced β-cell proliferation based on ECM observations. Scale bars in **A** and **B** are 50 μm.

**A****B****C**

**Figure 18: ECs in developing human islets.** (A) Representative images showing ECs (CD31<sup>+</sup>), macrophages (IBA1<sup>+</sup>),  $\beta$ -cells (INS<sup>+</sup>), and  $\delta$ -cells (SST<sup>+</sup>) in developing juvenile human islets. Scale bar is 50  $\mu$ m. (B) Box and whisker plot of intra-islet EC area (green; left axis) and  $\beta$ -cell proliferation rates (blue; right axis) in pancreatic tissue sections from neonates ( $\leq 2$ mo), infants ( $> 2$ mo-2y), and children ( $> 2$ y-10y). Symbols show individual donors; more detailed donor information is available in Table 4. Proliferation data was kindly provided by Nathaniel Hart<sup>349</sup>. (C) Intra-islet EC area stratified by individual donor age. Dotted lines at 2 months and 2 years denote age brackets in B.

## Discussion

Previous studies in our lab have shown that  $\beta$ -cell induction of VEGF-A results in marked intra-islet EC proliferation and  $\beta$ -cell loss<sup>201</sup>. Upon normalization of VEGF-A expression, intra-islet ECs return to quiescence and  $\beta$ -cells undergo recovery through proliferation of pre-existing  $\beta$ -cells<sup>201</sup>. To further investigate this process, we generated an inducible VEGFR2 knockout mouse (VEGFR2 <sup>$\Delta$ EC</sup>) that allowed us to block VEGF-A-VEGFR2 signaling in ECs, and used this model to study the role of proliferative and quiescent ECs, respectively, in  $\beta$ -cell loss, macrophage recruitment, and  $\beta$ -cell recovery.

Surprisingly, we observed some macrophage recruitment even in the absence of intact VEGFR2 signaling (**Fig. 14e**), suggesting that proliferative ECs were not required for the influx of circulating monocytes and their subsequent differentiation into macrophages. Since no changes in  $\beta$ -cell area were detected in  $\beta$ VEGF-A; VEGFR2 <sup>$\Delta$ EC</sup> islets (**Fig. 14d**), it is unlikely that cell death (which is a known stimulator of macrophage recruitment in acute injury<sup>185,186,352</sup>) was responsible. More likely, macrophage recruitment was stimulated by VEGF-A through VEGFR1, which is expressed by circulating monocytes<sup>229,234</sup>. Treating mice with an anti-VEGFR1 antibody or inactivating this receptor may help to determine whether the recruitment was mediated by this receptor. It is also possible that the increase in intra-islet macrophages we observed in  $\beta$ VEGF-A; VEGFR2 <sup>$\Delta$ EC</sup> islets was the result of resident macrophage proliferation, which should be addressed in future studies.

Infiltrating macrophage polarization to an “M2-like” phenotype was blocked with VEGFR2 knockdown, suggesting that signals derived from proliferative EC may be necessary for macrophage polarization (**Fig. 14f**). This is in line with previous reports that the microenvironment can direct macrophage phenotype and specifically polarize macrophages in the context of tissue injury<sup>140,142,159</sup>. Additionally, there is evidence that the M2 marker we used, MRC1 (CD206), plays a role in  $\beta$ -cell regeneration. Van Gassen and colleagues isolated pancreatic macrophages after PDL, and found that CD206<sup>+</sup> macrophages had increased expression of *Tgfb1* and *Egf*<sup>145</sup>. TGF $\beta$ 1 has been shown to directly upregulate SMAD7 in  $\beta$ -cells, which promotes  $\beta$ -cell proliferation by increasing Cyclin D1 and D2<sup>139</sup>. In a model of DT-mediated  $\beta$ -cell ablation, Criscimanna and colleagues showed that infiltrating macrophages initially have an M1-like phenotype (high IL-6, TNF $\alpha$ ) but are polarized to M2 (high IL-10, CD206), a phenotype “switch” that is required for  $\beta$ -cell regeneration<sup>202</sup>. Together, these data highlight a possible role for MRC1 as a mediator of restorative macrophage signaling. Though there is less known about the particular mechanisms by which ECs polarize macrophages, Cao and colleagues did recently show that mesenchymal stem cell-secreted stromal cell-derived factor 1 (SDF-1, also known as CXCL12) was required for M2 macrophage recruitment and  $\beta$ -cell proliferation after STZ-mediated injury<sup>353</sup>. This particular factor may not play a role in our model, but the elevated expression and secretion of chemokines and growth factors by ECs could be involved in our model system.

When we inactivated VEGFR2 in quiescent ECs, after macrophage recruitment had already occurred, we did not observe a decline of intra-islet macrophages (**Fig. 16d**). From this we can conclude that disruption of VEGFR2 signaling, at least for a short period of time, is not necessary for macrophage retention. We also did not detect changes in macrophage polarization in this scenario (**Fig. 17a**), suggesting that EC-derived signals or  $\beta$ -cell loss are more important for induction of an M2-like

phenotype rather than maintenance of this phenotype. Moreover, although macrophage phenotype conversion can be extremely rapid, it is possible that prolonged VEGFR2 inactivation (instead of only for 48 hours) would eventually result in fewer M2-polarized macrophages.

Based on prior work dealing with ECs and the role of VEGFR2 signaling in tissue regeneration, we anticipated that the loss of VEGFR2 signaling in quiescent ECs during the period of  $\beta$ -cell regeneration would inhibit  $\beta$ -cell division. However, we actually observed the opposite; VEGFR2 knockout significantly accelerated EC regression (**Fig. 16b**) and appeared to have a slight stimulatory effect on  $\beta$ -cell proliferation (**Fig. 16e**). While this result is in contrast with the effects of VEGFR2 inactivation on cell proliferation observed during liver and lung regeneration following surgical tissue removal<sup>276,277</sup>, it is conceivable in the context of our experimental paradigm where islet hypervascularization was driving  $\beta$ -cell loss. Although ECs were quiescent by 7d WD, we continued to observe residual VEGF-A by staining in the islet ECM during this period (data not show) which was likely sufficient to sustain extensive and elaborate capillary network in control  $\beta$ VEGF-A; VEGFR2<sup>fl/fl</sup> islets. In contrast, the disruption of VEGF-A-VEGFR2 signaling axis upon VEGFR2 inactivation led to a rapid capillary regression in hypervascularized  $\beta$ VEGF-A; VEGFR2 <sup>$\Delta$ EC</sup> islets and this EC regression was accompanied by increased  $\beta$ -cell proliferation.

To further explore the relationship between EC regression and increased  $\beta$ -cell proliferation, we focused on the important function of ECs in modulating the ECM. Two days after VEGFR2 knockdown, when ECs had started to regress, we observed pockets (“vascular casts”) of ECM that were not associated with intact ECs (**Fig. 17b**). We hypothesize that release of growth factors from this remaining ECM helped promote  $\beta$ -cell proliferation, which is supported by the elevated expression of ECM-modulating enzymes and adhesion molecules in ECs isolated from  $\beta$ VEGF-A mice (**Fig. 10**).

To study the role of ECs in the human islet microenvironment, we employed an immunohistochemical approach to visualize and quantify vasculature in developing human islets. Our group and others have observed dramatic changes in islet cell composition during early postnatal development, and we have shown that  $\beta$ -cell proliferation rates peak postnatally and then rapidly decline in the first decade of life. Here, we observed that intra-islet EC area is highest during early postnatal life ( $\leq 2$ mo) and slightly declines thereafter (**Fig. 18b-c**). This trend correlates to the height of  $\beta$ -cell proliferation observed in the juvenile human pancreas (**Fig. 18b**), supporting the hypothesis that ECs are important in this process. While this is only a correlative result, it is consistent with *ex vivo* experiments that have been conducted using human fetal pancreatic tissue showing that EC-secreted factors, EC-derived ECM, and EC- $\beta$ -cell contacts promote  $\beta$ -cell differentiation and proliferation<sup>290,291,293</sup>.

In both human islet development and murine  $\beta$ -cell regeneration, our results suggest that signals derived from the local EC population are crucial in promoting  $\beta$ -cell proliferation. Though the mechanisms have not yet been thoroughly investigated in human islets, our work with  $\beta$ VEGF-A;  $\beta$ VEGF-A mice indicates that ECs can contribute to  $\beta$ -cell proliferation by recruiting macrophages to the islet microenvironment and ensuring that these macrophages attain the proper phenotype to facilitate regeneration and prevent detrimental inflammation. We also provided evidence that quiescent EC signaling may impact  $\beta$ -cell proliferation more directly by modulating growth factor bioavailability.



## CHAPTER IV

### MOLECULAR MARKERS OF DEVELOPING HUMAN PANCREAS AND MATURE BETA CELLS FACILITATE UNDERSTANDING OF HUMAN ISLET BIOLOGY AND FUNCTION

Some text and data in this chapter have been adapted from Cogger, Sinha, Sarangi, McGaugh, Saunders *et al.*, 2017<sup>319</sup>; Brissova, Haliyur, Saunders, Shrestha *et al.*, 2018<sup>320</sup>; and Saunders & Phillips *et al.*, 2018 (manuscript in preparation).

#### Introduction

In the quest to understand human  $\beta$ -cell physiology and develop therapies to restore  $\beta$ -cell mass and function to patients with diabetes, islet biologists have encountered a unique set of challenges. For example, there has been great interest in generating  $\beta$ -like cells from human embryonic stem cells (hESCs) and induced pluripotent stem cells (hiPSCs). Intricate stepwise protocols have been developed to produce pancreatic progenitors expressing the canonical markers PDX1 and NKX6.1, which have the potential to further differentiate into insulin-producing  $\beta$ -like cells. However, these protocols can be highly variable and yield a low percentage of pancreatic progenitors<sup>354,355</sup>. Furthermore, the techniques largely draw on our knowledge of mouse pancreatic organogenesis, which allows *in vivo* manipulation that is impossible in the developing human. Consequently, we know relatively little about human pancreatic and islet development, and this lack of knowledge limits development of efficient differentiation protocols.

Once  $\beta$ -cells and islets are formed, the multicellular composition and anatomical location of islets pose additional challenges to studying individual islet endocrine cell subtypes. To overcome this, several groups have developed systems to isolate subpopulations of islet endocrine cells for transcriptional, metabolic, and functional analyses. These isolations are generally accomplished by dispersing and sorting cells using antibodies that target either cell surface antigens on live cells or intracellular proteins in fixed, permeabilized cells<sup>47,330,356</sup>. Other groups have alternatively sorted  $\beta$ -cells based on zinc content, using the zinc-binding fluorochrome Newport Green<sup>357</sup>. Each approach has advantages and drawbacks, but one critical limitation is the lack of a cell surface antibody that specifically recognizes human  $\beta$ -cells.

In addition to analyzing human  $\beta$ -cells *ex vivo*, there is great need to identify and visualize  $\beta$ -cells non-invasively *in vivo*. Indeed, although reduced  $\beta$ -cell mass is an established feature of diabetes progression, current knowledge has originated from post-mortem analysis because there are no effective methods to quantify  $\beta$ -cell mass non-invasively in humans<sup>358</sup>. This limitation has greatly hindered our understanding of disease risk and progression and prevents the evaluation of interventions designed to preserve or increase  $\beta$ -cell mass. Many traditional imaging modalities lack necessary sensitivity for the small size and sparse distribution of islets, and better reagents are necessary to distinguish  $\beta$ -cells from other islet endocrine cells and neighboring exocrine tissue<sup>359</sup>. Antibodies typically have greater specificity and affinity than other molecules such as peptides and small molecules, and multiple antibodies targeting islet cell surface antigens have unsuccessfully been tried for islet imaging applications *in vivo*<sup>358,360</sup>.

In this chapter we have characterized two molecular markers that have great potential to aid  $\beta$ -cell research and overcome some of the challenges mentioned above. First, to address the developing human  $\beta$ -cell niche and the need for more efficient hESC and hiPSC differentiation, we present data on a cell surface marker identified in a proteomics screen by our collaborator Dr. Cristina Nostro<sup>319</sup>. Together with Dr. Nostro, we showed that pancreatic secretory granule membrane major glycoprotein 2 (GP2) is a specific marker of human multipotent pancreatic progenitors both *in vitro* and *in vivo*, and that selecting progenitor cells expressing GP2 during the differentiation process increases the yield of insulin-producing  $\beta$ -like cells. In the second part of the chapter, in efforts to identify cell surface markers of human  $\beta$ -cells, we describe the expression pattern of an ecto-enzyme, nucleoside triphosphate diphosphohydrolase 3 (NTPDase 3), that is expressed in pancreatic islets of both human and rodents and has been linked to regulation of insulin secretion<sup>361-363</sup>. Importantly, we found that this molecular marker is highly specific to mature human  $\beta$ -cells and its expression is preserved in  $\beta$ -cells from individuals with T1D and T2D, making it a useful and powerful new reagent for  $\beta$ -cell purification *ex vivo* and imaging and targeting *in vivo*.

## Results

### ***GP2 marks putative pancreatic progenitors in human neonatal pancreas***

GP2 expression in the human adult pancreas is restricted to the acinar compartment; however, its expression pattern during pancreatic development was not known. Using histological sections from neonates (born at G33, G37, and G39 weeks), we observed GP2<sup>+</sup> NKX6.1<sup>+</sup> INS<sup>-</sup> cells on the leading edge and INS<sup>+</sup> NKX6.1<sup>+</sup> GP2<sup>-</sup> islet clusters at the center of the developing pancreatic lobes (**Fig. 19a**). To further characterize these as multipotent pancreatic progenitors (PPs), we also labeled for PTF1A, which is expressed by NKX6.1<sup>+</sup> PPs in epithelial tips of the developing mouse pancreas<sup>364,365</sup>. Cells in the epithelial tip of the human pancreas do express PTF1A along with NKX6.1 and GP2 (**Fig. 19b**). In contrast, cells in the trunk express NKX6.1 but not PTF1A, and are GP2 negative. We were curious whether this PP population persisted after birth, so we extended our histological analysis to include pancreatic sections from infant donors (3, 10, and 20 months). We identified GP2<sup>+</sup> PTF1A<sup>+</sup> NKX6.1<sup>+</sup> PP cells in these pancreata, albeit with a less pronounced lobular pattern of GP2 expression and fewer PPs than in neonatal donors (**Fig. 20**). Together, our data provide strong evidence for the existence of multipotent pancreatic progenitor cells in the postnatal human pancreas.

### ***Purified GP2<sup>+</sup> pancreatic progenitor cells give rise to $\beta$ -like cells in vitro***

To assess whether GP2 could be used as a cell surface marker for isolating pancreatic progenitor cells, the Nostro group employed fluorescence activated cell sorting (FACS) to isolate the GP2-positive and GP2-negative fractions at day 13 of differentiation from the hESC line H1 (**Fig. 21a**). These fractions were cultured identically through day 23, at which point the cultures from GP2<sup>+</sup> cells had yielded significantly more NKX6-1<sup>+</sup> C-PEPTIDE<sup>+</sup> cells compared to GP2 negative and unsorted cultures (**Fig. 21b**). These results suggest that GP2 can be used as a positive selective marker for pancreatic progenitor cells that harbor the potential to become insulin-producing  $\beta$ -like cells.

### ***NTPDase3 is expressed specifically in adult human $\beta$ -cells, including those in islets from individuals with T1D and T2D***

To characterize expression of NTPDase3 (**Fig. 22a**), we performed immunohistochemistry on pancreatic tissue sections from human donors (n=18, age range of 0-49 years) using a monoclonal antibody<sup>362,366</sup>. We observed NTPDase3 expression on the membrane of most adult  $\beta$ -cells, but importantly, not in adult  $\alpha$ -cells (**Figs. 22b, 23a**). No colocalization of NTPDase3 with pancreatic polypeptide hormone or amylase (exocrine enzyme) was observed, though a small number of  $\delta$ -cells did express NTPDase3 (**Fig. 23b-d**). Significantly,  $\beta$ -cell NTPDase3 expression was preserved in human T1D and T2D disease states (**Fig. 22c**).

### ***NTPDase3 is dynamically expressed during human pancreas development***

Interestingly, although NTPDase3 labeled adult human  $\beta$ -cells with high specificity, its expression during early pancreas development, especially the first few years of life, is quite dynamic. At the time of birth, human acinar cells, but not  $\beta$ -cells, expressed NTPDase3 (**Fig. 22d**, top panel). Between 3 months and 2 years of age, NTPDase3 expression became less in acinar cells and appeared in an increasing proportion of  $\beta$ -cells; this transition was heterogeneous among individuals and even in islets from the same pancreas. During this age range, both acinar cells and  $\beta$ -cells expressed NTPDase3 (**Fig. 23e**). By 5 years of age, acinar expression was completely absent and NTPDase3 was only expressed in  $\beta$ -cells (**Fig. 22d**, bottom panel).

### ***NTPDase3 antibody effectively and efficiently isolates $\beta$ -cells from live dispersed human islet cells***

To investigate the utility of NTPDase3 as a biomarker for mature  $\beta$ -cells, we first developed a cell sorting strategy to label live human islet cells (**Fig. 24a**). Use of the NTPDase3 antibody in combination with previously characterized cell surface markers<sup>47,367</sup> enabled effective separation of  $\alpha$ - and  $\beta$ -cell subpopulations (**Fig. 24b**). We validated the purity of our subpopulations using two complementary approaches, immunocytochemistry and RNA sequencing (RNA-seq). Based on hormone expression (insulin, glucagon, somatostatin),  $\beta$ - and  $\alpha$ - cell populations were enriched to 96% and 98% purity, respectively, from a dispersed islet preparation composed of many disparate cell types (**Fig. 24c**). Transcripts of  $\alpha$ -cell-specific genes (e.g. *ARX*, *HNF4A*) were highly expressed in  $\alpha$ -cell samples and minimally expressed in  $\beta$ -cell samples; the inverse was true of  $\beta$ -cell-specific genes (e.g. *GLP1R*, *PDX1*), which were detected at high levels only in  $\beta$ -cell samples (**Fig. 24b, d**). Genes common to both  $\alpha$ - and  $\beta$ -cells (e.g. *ISL1*, *PAX6*) showed similar abundance in both cell types. NTPDase3 transcript (*ENTPD3*) was approximately 10-fold higher in  $\beta$ -cells than  $\alpha$ -cells.

To expand the application of our sorting strategy, we demonstrated that NTPDase3 effectively isolates  $\beta$ -cells from human islet donors of various ages and disease states (**Fig. 25**). Though islets from donors with longstanding T1D contained too few  $\beta$ -cells from which to isolate RNA, we compared transcriptional profiles of T1D  $\alpha$ -cells with those of normal  $\alpha$ -cells (**Fig. 26a-b**), and found that genes associated with  $\alpha$ -cell identity and function were significantly downregulated in the T1D  $\alpha$ -cell, while stress response factors and cell-cell contact proteins were upregulated (**Fig. 26c**). Among the islet-enriched transcription factors

downregulated in T1D  $\alpha$ -cells was *Regulatory factor X6 (RFX6)*, which lies upstream of *MAFB*, *ARX*, and *NKX6.1* in endocrine cell differentiation<sup>368,369</sup> and directly controls expression of P/Q and L-type voltage-gated calcium channels (*CACNA1A*, *CACNA1C*, *CACNA1D*) and the  $K_{ATP}$  channel subunit sulfonylurea receptor 1 (*ABCC8*)<sup>368,370</sup>. T1D  $\alpha$ -cells also had altered expression of potassium and sodium ion channels, vesicle trafficking proteins, and cyclic adenosine monophosphate (cAMP) signaling molecules, which collectively point to altered T1D  $\alpha$ -cell electrical activity and impaired glucagon exocytosis (**Fig. 26d**).

We also conducted preliminary analysis on  $\alpha$ - and  $\beta$ -cells from T2D islets, revealing reduced expression of islet-enriched transcription factors and increased expression of molecules involved in low-grade chronic inflammation (**Fig. 27**). In  $\beta$ -cells, reduced transcription factor expression (*MAFA*, *NKX6.1*, *PDX1*; **Fig. 27b**) is consistent with observations of reduced protein levels in human T2D islets and concurrent with the development of hyperglycemia in *db/db* mice<sup>371-373</sup>. Changes in  $\alpha$ -cell gene expression in T2D have not been extensively studied, though recent scRNA-seq analysis showed differential gene expression in human T2D  $\alpha$ -cells in addition to  $\beta$ -cells and other islet cell types<sup>374</sup>. Macrophages are thought to be the major source of inflammatory damage to T2D islets, so our observation of elevated chemokines (e.g. *CSF1*) is consistent with gene expression changes seen in rodent models of T2D<sup>140</sup>. Several other cytokine receptors and downstream regulators that are upregulated in our data set (*IL1R1*, *IL6R*, *NKFB*, *TNFA*) are activated by free fatty acids and have been shown to amplify proinflammatory signals in mouse and human islets *in vitro*<sup>193</sup>. Furthermore, their activity can directly induce ER stress and reduce insulin expression<sup>140,375,376</sup>, likely contributing to deterioration of  $\beta$ -cell mass and function during the progression of T2D.

### ***Targeting NTPDase3 detects human $\beta$ -cells in vivo***

Since NTPDase3 antibody allowed the sorting of live human  $\beta$ -cells, we next tested whether it could detect human  $\beta$ -cells *in vivo*. To accomplish this we utilized immunodeficient mice bearing human islets engrafted either under the kidney capsule or in the anterior chamber of the eye (ACE). When mice received an intravenous injection of unlabeled NTPDase3 antibody and grafts were removed twenty-four hours later, visualization with a secondary antibody revealed that NTPDase3 bound  $\beta$ -cells *in vivo* with high specificity (**Fig. 28**). We next performed the experiment with NTPDase3 antibody conjugated to DyLight550 (**Fig. 29a**), and twenty-four hours post-injection we observed fluorescent signal from human islet grafts that was not present with an isotype control (**Fig. 29b**). Immunohistochemistry on removed islet grafts confirmed this highly specific binding of the conjugated NTPDase3 antibody to human  $\beta$ -cells (**Fig. 29c**).

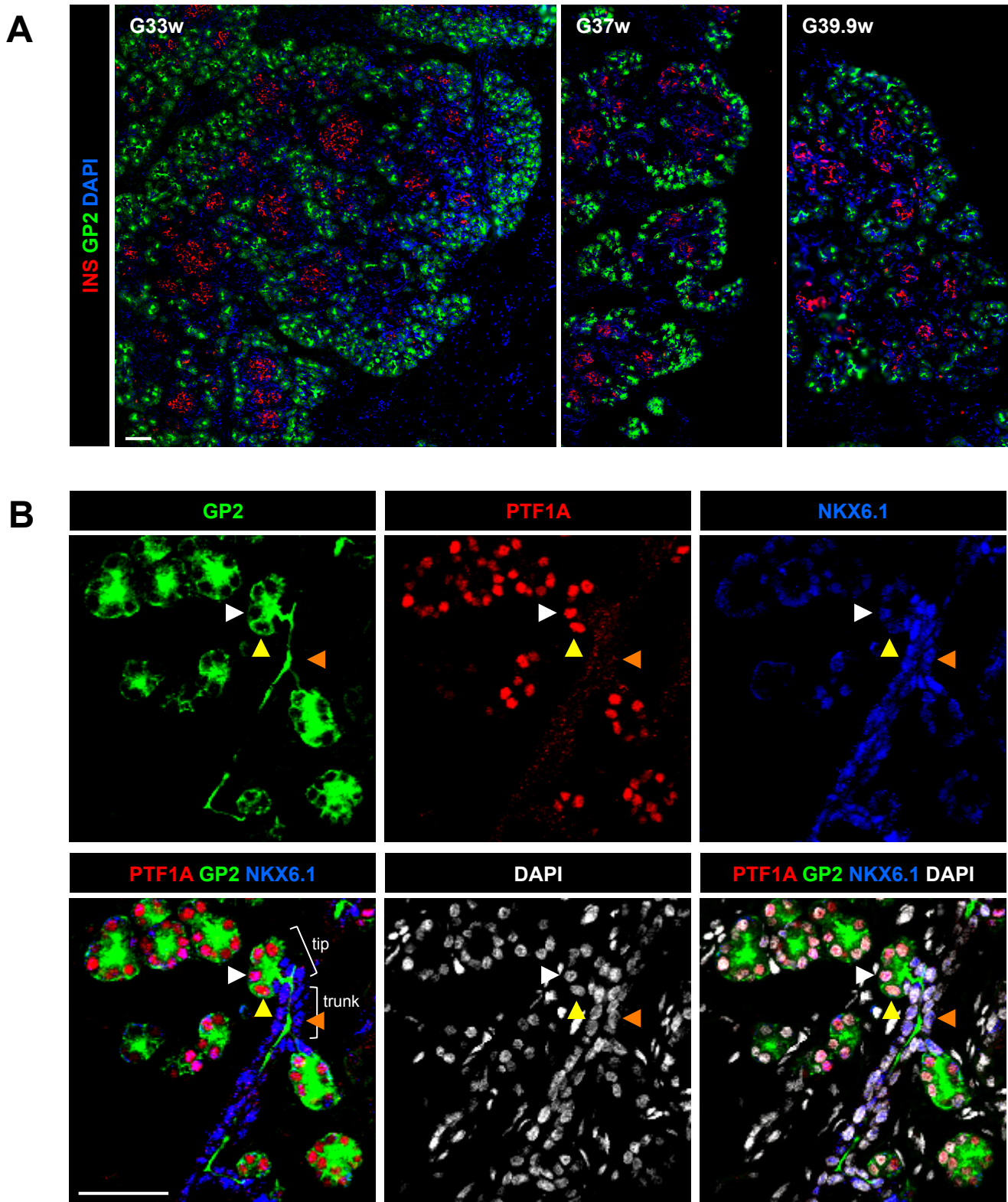


**Figure 19: Validation of the multipotent pancreatic progenitor marker GP2 in human tissue.**

**(A)** Immunohistochemical staining of pancreatic sections from human donors born at gestational (G) weeks 33, 37, and 39.9. Donor information available in **Table 4**. **(B)** Detail of developing epithelial branches at G37w. In tip region, white arrowheads point to a multipotent pancreatic progenitor cell (GP2<sup>+</sup> PTF1A<sup>+</sup> NKX6.1<sup>+</sup>) and yellow arrowheads to an acinar cell (GP2<sup>+</sup> PTF1A<sup>+</sup> NKX6.1<sup>-</sup>); in trunk region, orange arrowheads denote a ductal/endocrine progenitor (GP2<sup>-</sup> PTF1A<sup>-</sup> NKX6.1<sup>+</sup>). Scale bars are 50  $\mu$ m and apply to all images in the respective panel.

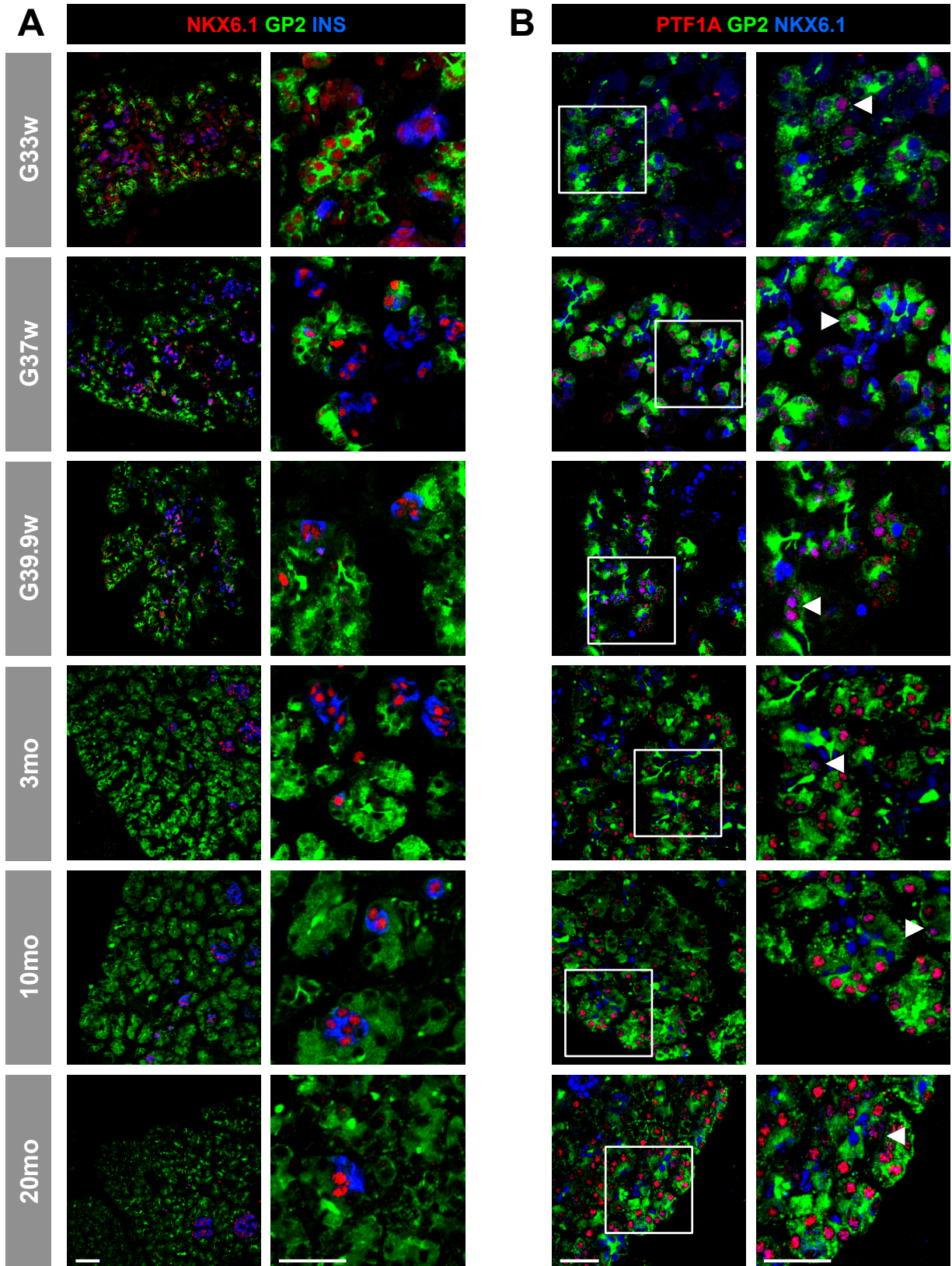


**Figure 20: Multipotent pancreatic progenitors are present in the developing human pancreas after birth.**

Immunohistochemical analysis of developing pancreatic lobes in neonates (born at G33, 37, and 39.9w) and infants (3, 10, 20mo). Scale bar represents 50  $\mu$ m and applies to all images in the respective column. **(A)** GP2 becomes broadly expressed in the epithelium but remains strong around lobe periphery; differentiated  $\beta$ -cells (NKX6.1<sup>+</sup> INS<sup>+</sup>) are GP2-negative. **(B)** GP2<sup>+</sup> multipotent progenitor (PTF1A<sup>+</sup> NKX6.1<sup>+</sup>) cells reside in epithelial branch tips towards the periphery of lobes and are marked by arrowheads. Boxes in left panel of **(B)** indicate area enlarged in right panel.

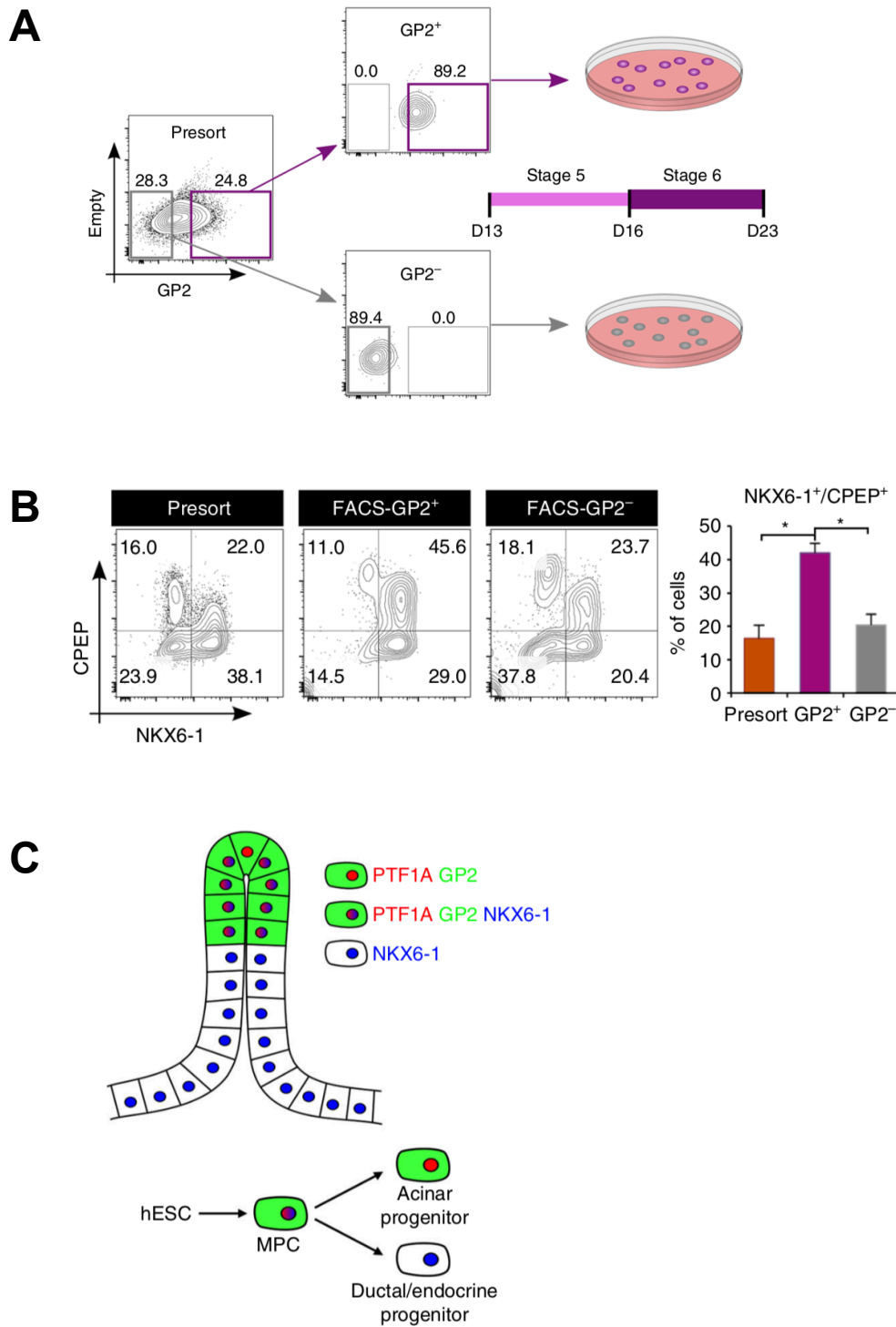


**Figure 21: Purified GP2<sup>+</sup> pancreatic progenitor cells give rise to ‘β-like’ cells *in vitro*.** (A) Flow plots showing the GP2 profile at day 13 of the unsorted (presort) and fluorescence-activated cell sorted H1 cells, which were then cultured to generate β-like cells up to day 23. (B) Representative flow cytometry plots of day 23 cultures from H1-derived unsorted (presort), GP2<sup>+</sup> or GP2<sup>-</sup> populations stained with anti- NKX6.1 and anti-C-PEPTIDE (CPEP) antibodies. The bar graph shows the average percentage of NKX6.1<sup>+</sup> C-PEP<sup>+</sup> cells. N = 5, error bars indicate s.e.m. \*p < 0.05, One-way ANOVA. (C) Model depicting the *in vivo* and *in vitro* equivalent of the human multipotent pancreatic progenitor (MPC) expressing PTF1A, GP2, and NKX6.1. The MPC residing at the tip of the developing human pancreas has the potential to develop into acinar (GP2<sup>+</sup> PTF1A<sup>+</sup>) and ductal/endocrine (GP2<sup>-</sup> NKX6.1<sup>+</sup>) progenitors. Figure panels are adapted from Cogger *et al.*, 2017<sup>319</sup>.

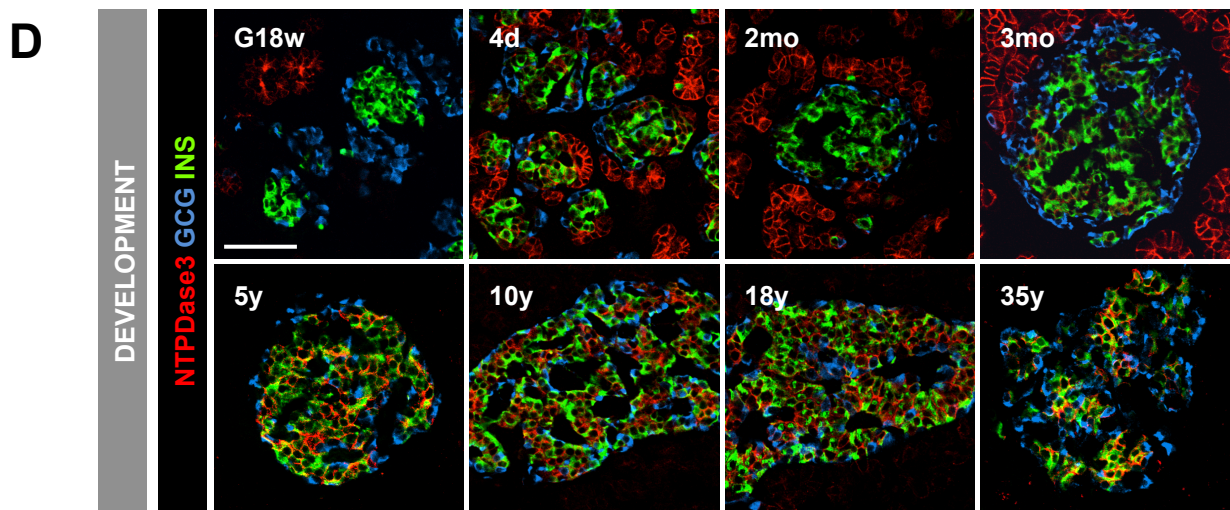
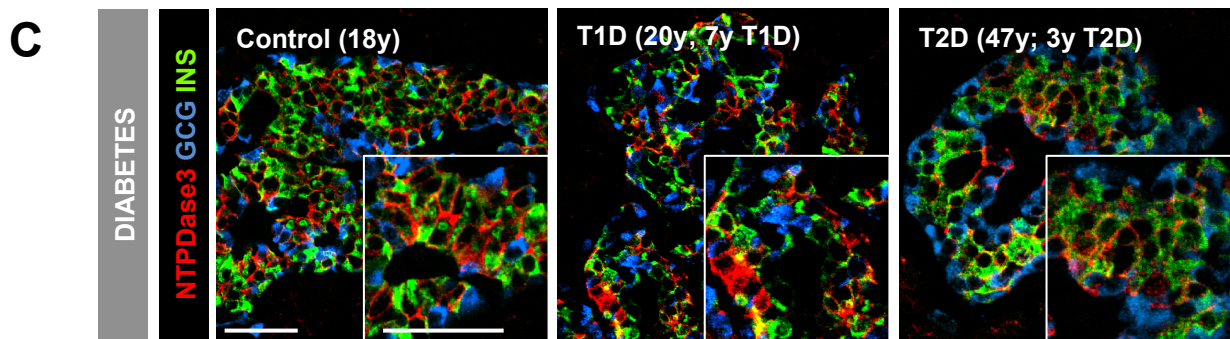
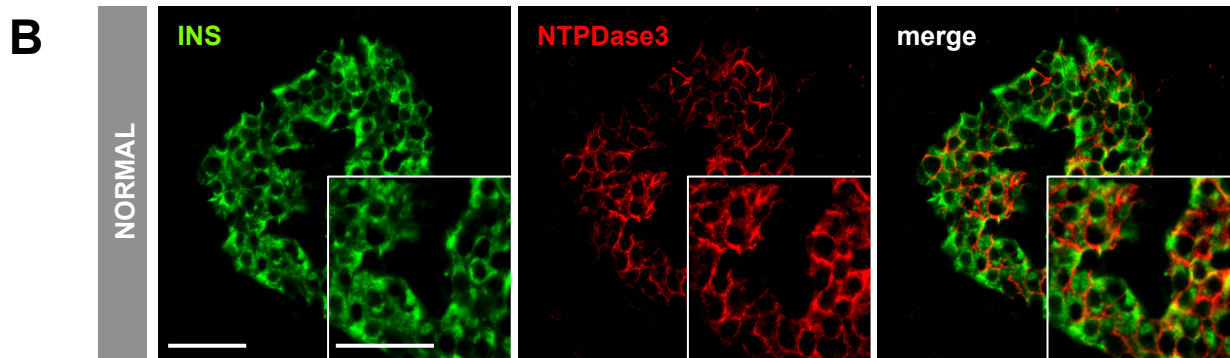
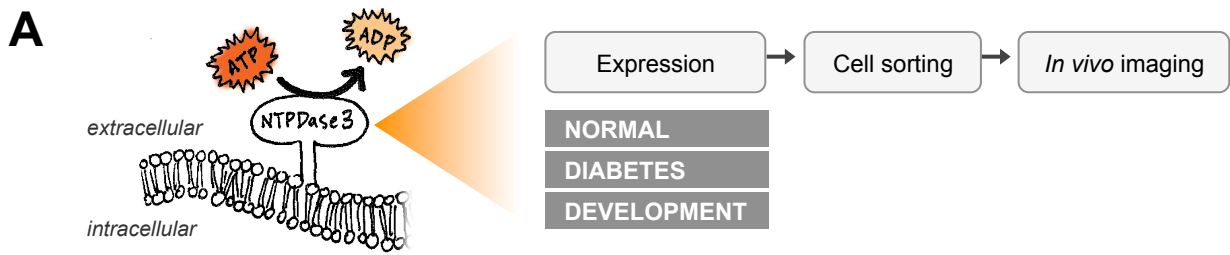


**Figure 22: NTPDase3 is expressed specifically in adult human  $\beta$ -cells.** (A) Overview of NTPDase3 analysis and experimental applications. (B) Representative image of an adult (18yM) islet showing NTPDase3 expression in INS<sup>+</sup> cells. See also Fig. 23. Monoclonal mouse antibody to human NTPDase3 generously provided by J. Sévigny. (C) NTPDase3 expression is retained in  $\beta$ -cells from individuals with type 1 (T1D) and type 2 (T2D) diabetes. (D) NTPDase3 has a different pattern of expression in the human pancreas at different stages of development; in top row, NTPDase3 is initially restricted to pancreatic epithelium and acinar cells, but by around 1 year of age, acinar cell expression dissipates and  $\beta$ -cells specifically express NTPDase3 (bottom row). Scale bars in B-D are 50  $\mu$ m. Human pancreatic donor information is available in Table 4.



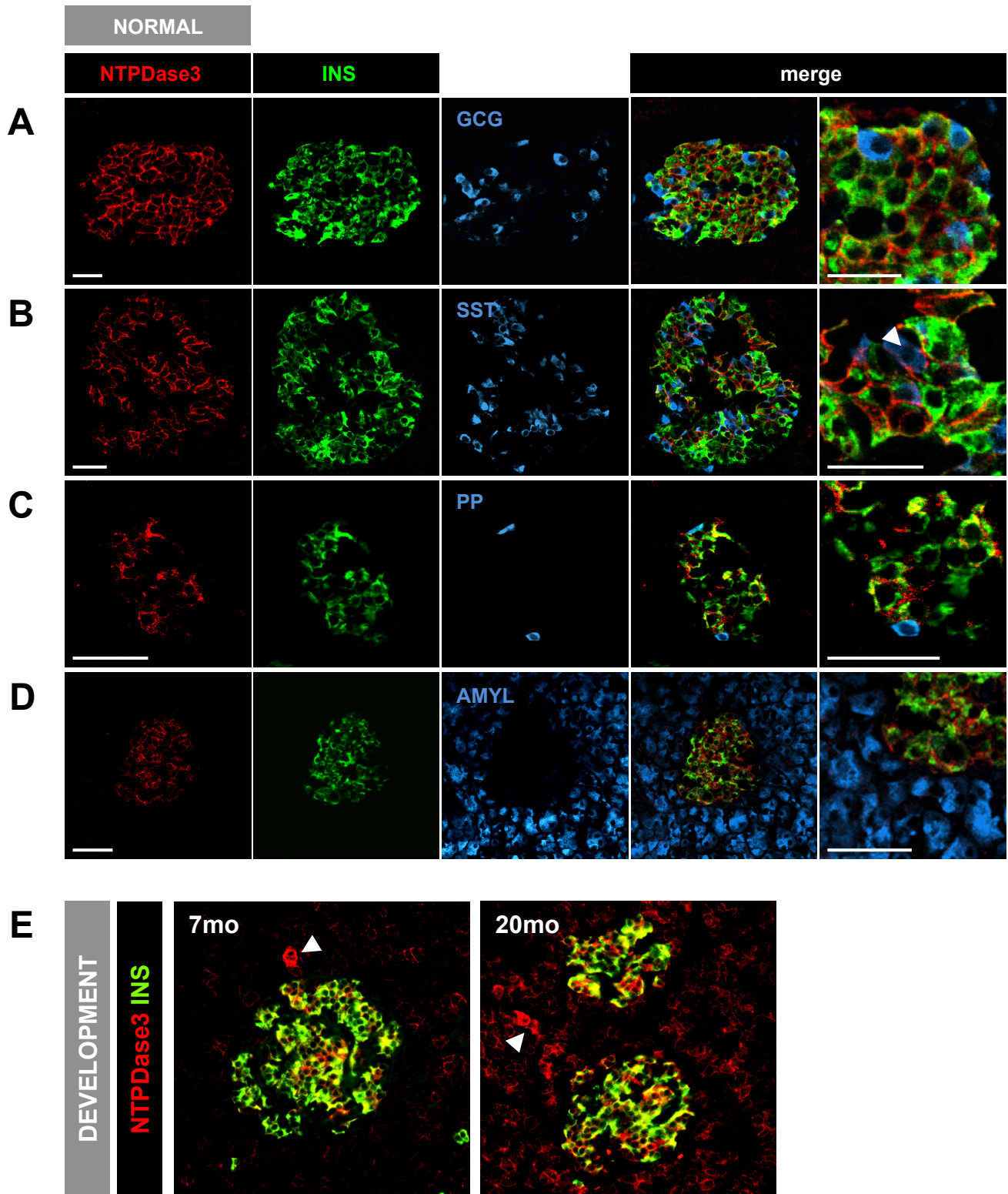


**Figure 23: Expression of NTPDase3 in adult pancreatic endocrine and exocrine cells.** (A-D) NTPDase3 is not expressed in adult  $\alpha$ -cells (labeled by GCG; **A**), PP cells (PPY; **C**), or acinar cells (AMYL; **D**). A small percentage of  $\delta$ -cells (SST; **B**) express NTPDase3, as indicated by the white arrowhead. Scale bars are 50  $\mu$ m. Sample is 18yM (see **Table 4**). (E) During infancy NTPDase3 expression can be seen both in  $\beta$ -cells and surrounding acinar tissue. Arrowheads indicate non-endocrine NTPDase3<sup>+</sup> cells.

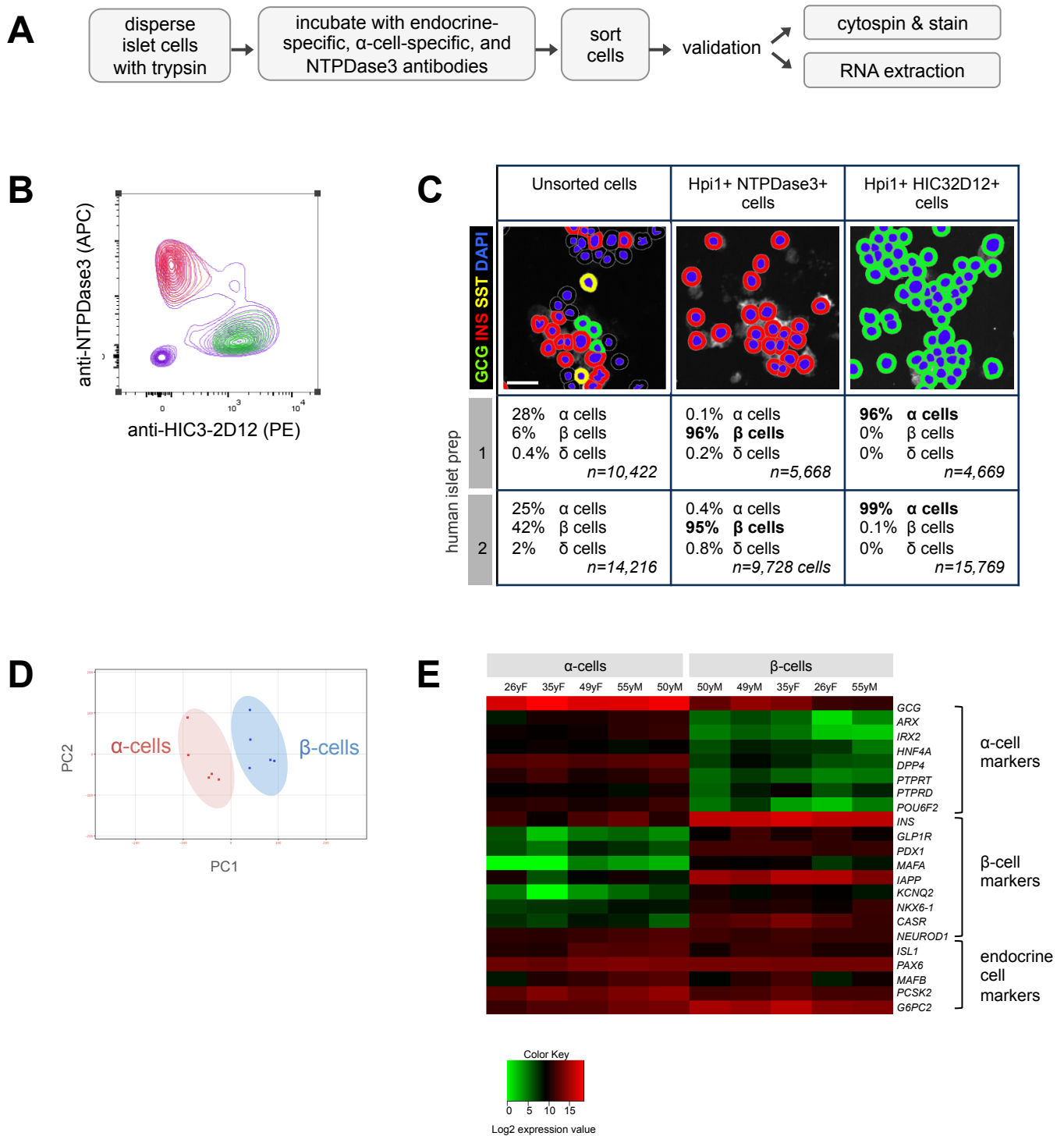


**Figure 24: NTPDase3 antibody effectively and efficiently isolates  $\beta$ -cells from live dispersed human islet cells.** (A) Experimental overview of islet dispersion and sorting. (B) Separation of  $\alpha$ - and  $\beta$ -cell subpopulations by fluorescence activated cell sorting (FACS). Indirect antibody labeling was used to preselect endocrine cells (HPI1+) and subsequently identify  $\alpha$ -cells (HPa3+) and  $\beta$ -cells (NTPDase3+). See also Fig. 25. (C) FACS-collected islet cells were dispersed and stained, and cell populations were assessed by immunocytochemistry. Two independent islet preparations are shown; donor information is available in Table 5. Scale bar is 50  $\mu$ m. (D-E) Transcriptome by RNA-sequencing analysis of purified human  $\alpha$ - and  $\beta$ -cells from normal adult donors (*n*=5; ages 26-55 years). (D) Principal component analysis (PCA) plot shows clustering of  $\alpha$ - and  $\beta$ -cell samples. (E) Heat map of a selected gene subset shows relative gene expression in individual  $\alpha$ - and  $\beta$ -cell samples.

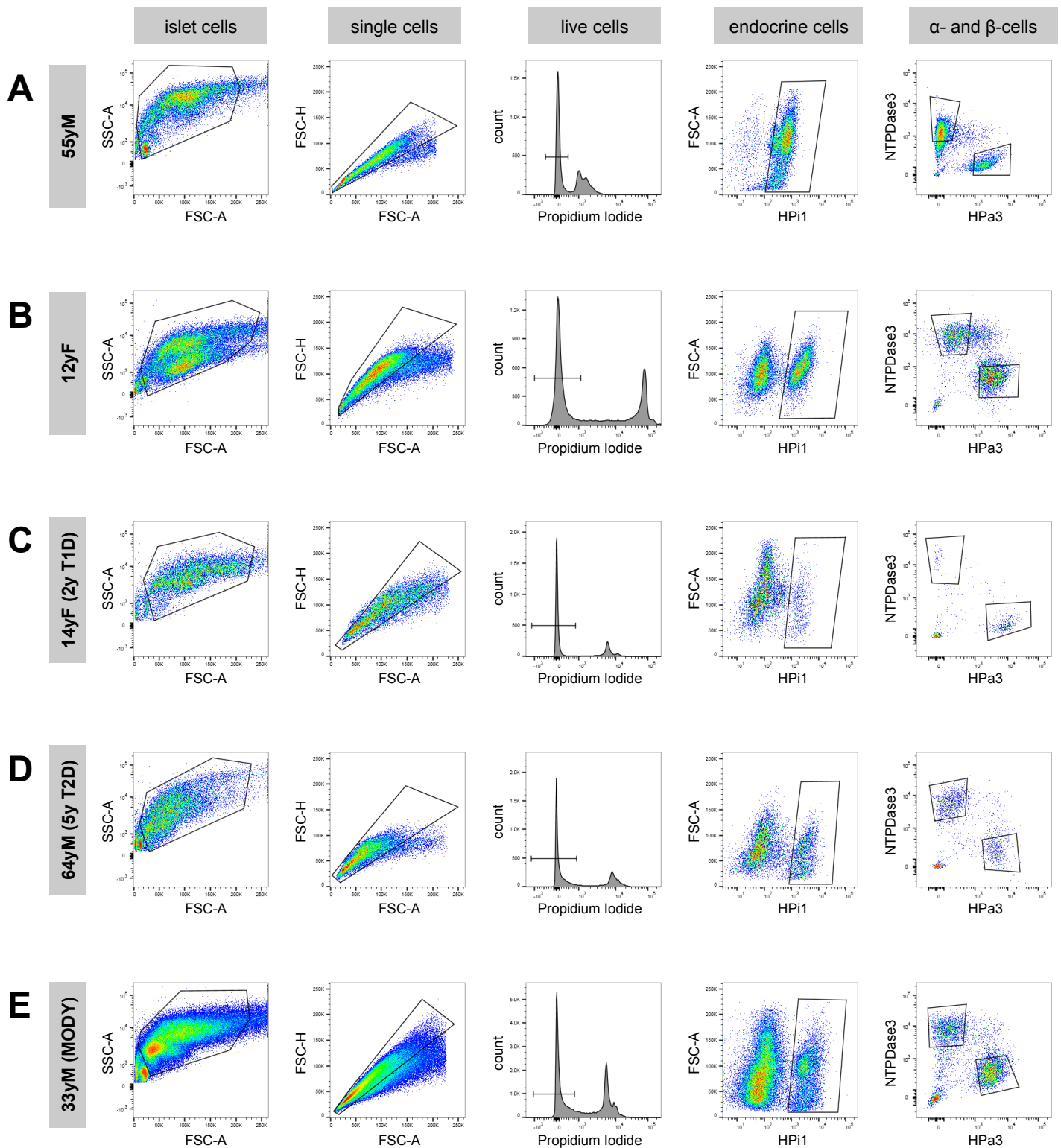


**Figure 25: NTPDase3-based cell sorting method can be applied to islets from various disease states.** The labeling strategy depicted in Fig. 23a is applicable to dispersed human islet cells from **(A)** nondiabetic adult donors, **(B)** juvenile donors, **(C)** donors with T1D, **(D)** donors with T2D, and **(E)** donors with MODY. Donor information is available in **Table 5**. Gating strategy is shown in each row, with column labels indicating the gated population. Cell debris were excluded by forward scatter (FSC) and side scatter (SSC), single cells were identified by the FSC-A v. FSC-H plot, and non-viable cells were excluded using propidium iodide (PI). Endocrine cell subpopulations were then isolated based on positivity for HPI1 and additional positivity for HPA3 ( $\alpha$ -cells) or NTPDase3 ( $\beta$ -cells).

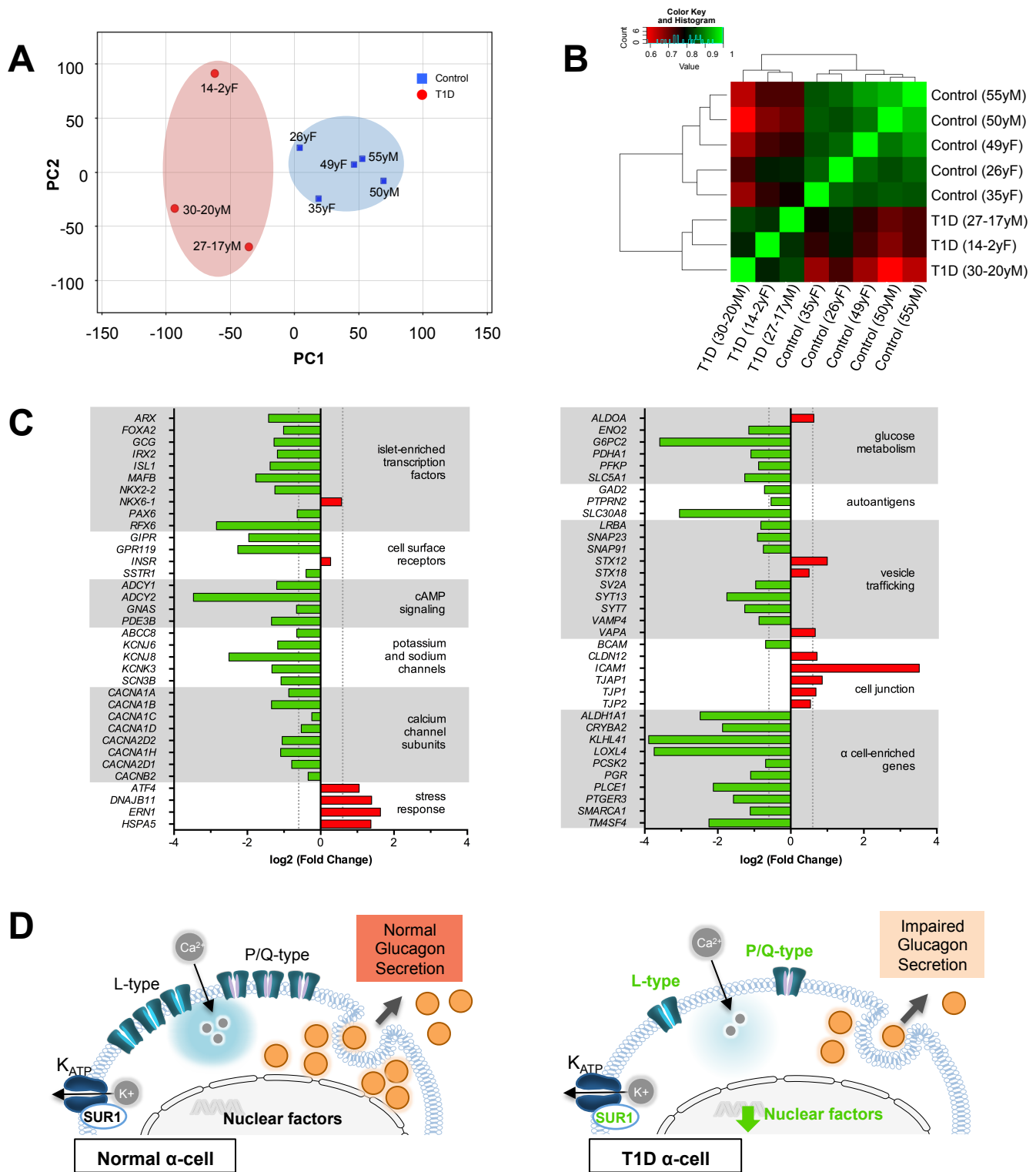


**Figure 26: Transcriptome analysis by RNA-seq reveals genes critical to  $\alpha$ -cell function are differentially expressed in T1D  $\alpha$ -cells.** (A) Principal component analysis (PCA) plot shows clustering of  $\alpha$ -cell samples from control (n=5; 26-55yrs) and T1D (n=3; 14-30yrs) donors. (B) Heat map of the pairwise correlation between all samples based on the Spearman Correlation coefficient, which ranks and quantifies the degree of similarity between each sample pair. Perfect correlation is indicated by 1. (C) Genes associated with pathways described in  $\alpha$ -cell function. Vertical dotted lines represent point of significance for FC=1.5x threshold analysis;  $p < 0.05$  for all values shown. (D) Proposed model for disrupted glucagon secretion in T1D  $\alpha$ -cells. Normal  $\alpha$ -cell function is maintained by  $\alpha$ -cell-specific transcription factors which regulate gene expression of machinery necessary for glucagon synthesis and secretion (left panel). Altered expression of transcription factors likely leads to disruption of  $\alpha$ -cell calcium homeostasis and cell signaling subsequently impairing glucagon secretion (right panel, downregulated genes labeled in green). Figure is adapted from Brissova *et al.*, 2018<sup>320</sup>.

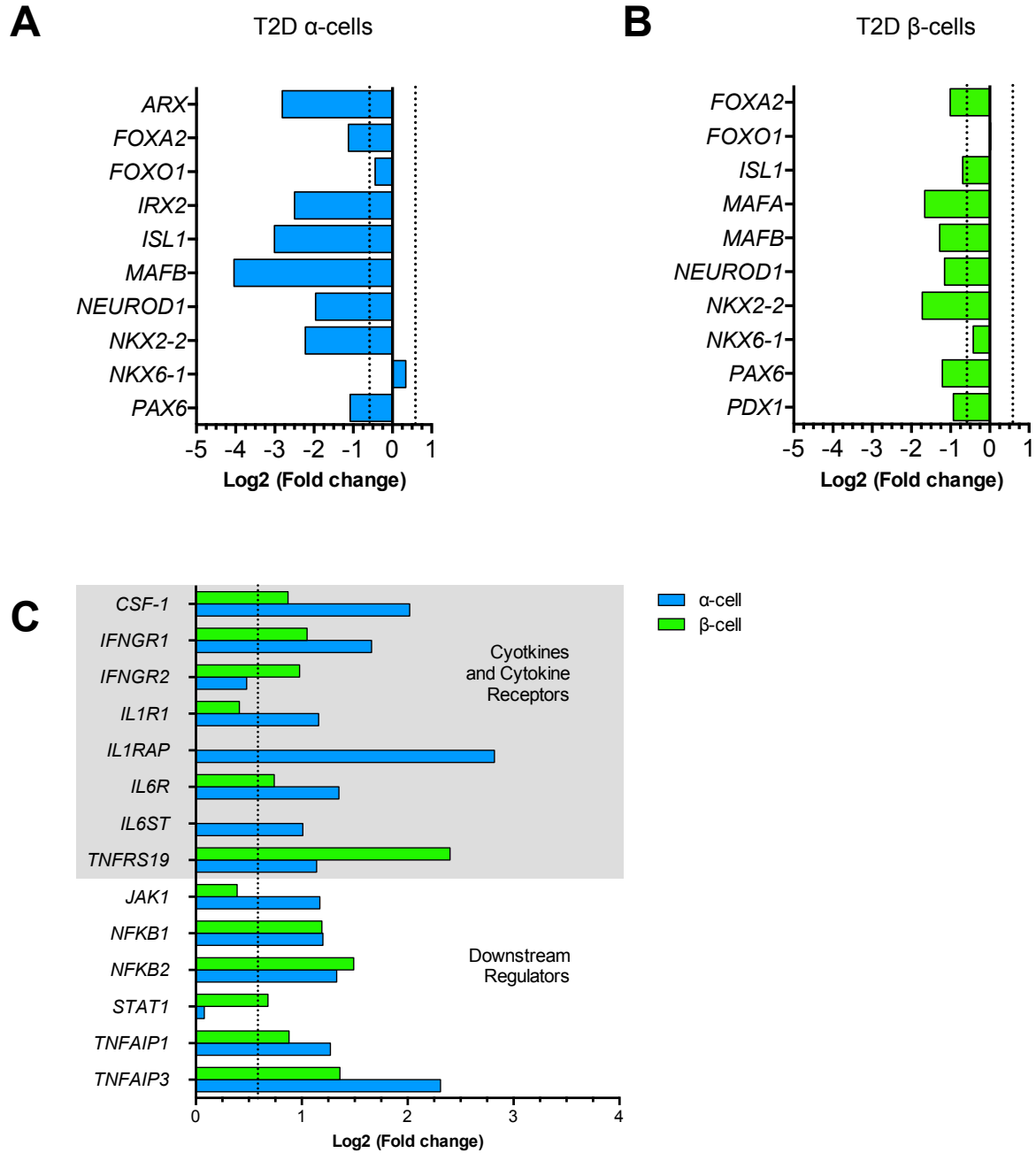


**Figure 27: T2D  $\alpha$ - and  $\beta$ -cells show reduced expression of islet-enriched transcription factors and elevated expression of inflammatory markers.** Cells from control (n=5; 26-55yrs) and T2D (n=4; 40-65yrs) donors were isolated from dispersed human islets and assayed by RNA-seq. Graphs show differential expression of endocrine cell identity genes in T2D (**A**)  $\alpha$ -cells and (**B**)  $\beta$ -cells, and genes associated with inflammatory response (**C**) in T2D  $\alpha$ -cells (blue) and  $\beta$ -cells (green). Vertical dotted lines represent point of significance for FC=1.5x threshold analysis; p<0.05 for all values shown.

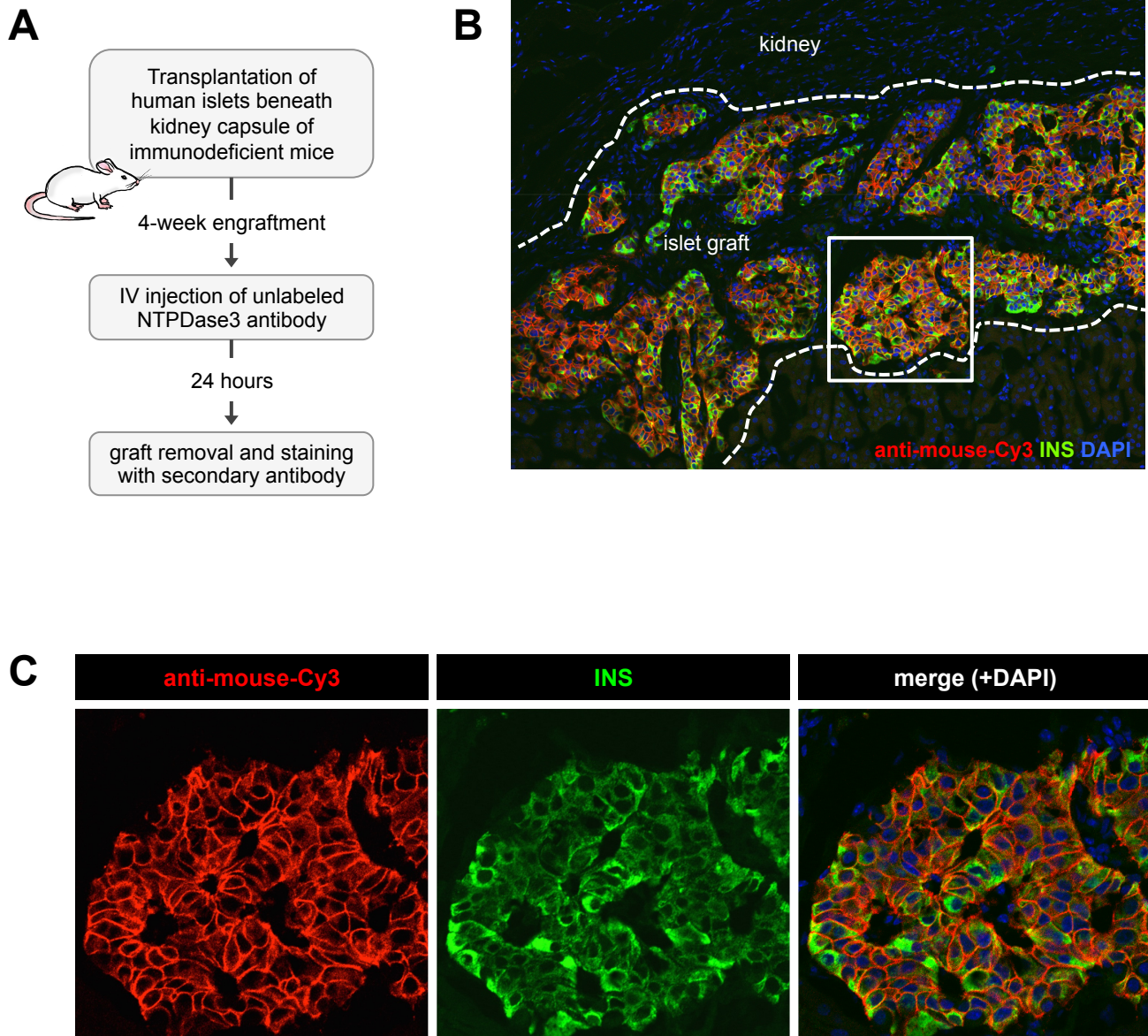


**Figure 28: Detection of IV-injected NTPDase3 antibody in human islet graft on kidney capsule of NSG mice.** **(A)** Experimental overview of human islet transplantation, antibody administration, and immunohistochemical visualization. **(B)** Macro view of islet graft (outlined in dashed white line) and surrounding kidney tissue. Anti-mouse-cy3-conjugated secondary antibody shows NTPDase3 bound to human  $\beta$ -cells. **(C)** Immunohistochemical detail of islet graft, as denoted by white box in **(B)**. Scale bars in **B-C** are 50  $\mu$ m. Transplanted islets are from 18yM (see **Table 5**).

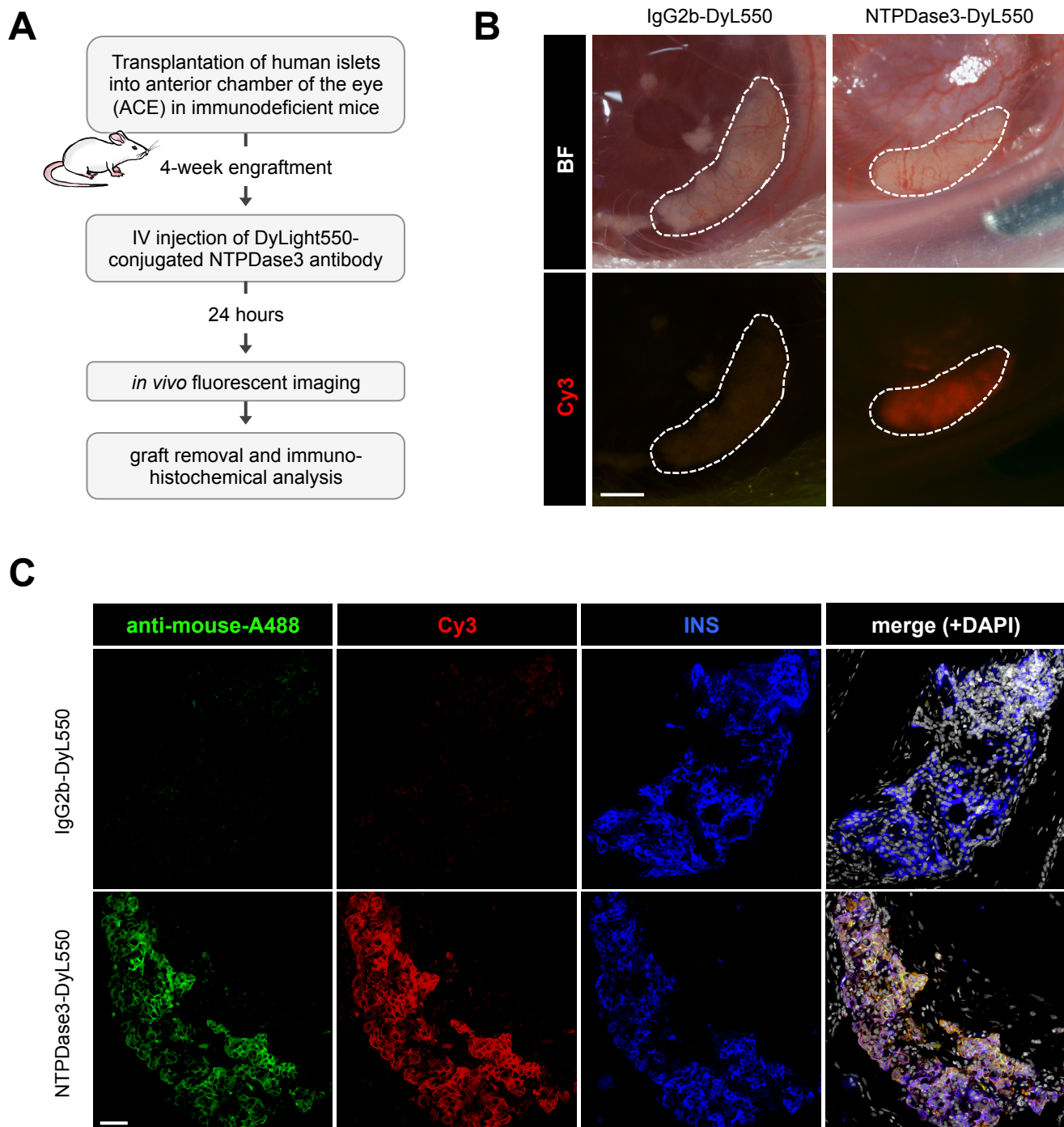


**Figure 29: Targeting NTPDase3 detects human  $\beta$ -cells *in vivo*.** (A) Experimental overview of human islet transplantation, antibody administration, and imaging. (B) Islet grafts (outlined in white dashed lines) in the anterior chamber of the eye (ACE) of NSG mice receiving injections of DyLight550-conjugated antibody (left: isotype control, IgG2b-DyL550; right: NTPDase3-DyL550). Scale bar is 200  $\mu$ m. (C) Immunohistochemistry on sections of islet grafts after removal from NSG mice. Secondary anti-mouse-Alexa488 antibody (left panel) recognized bound NTPDase3 antibody; DyLight550 signal (Cy3, second panel from left) remained intact following removal and fixation of grafts. Scale bar is 50  $\mu$ m. Grafts pictured in B and C are from 61yM human islet donor (n=2 mice each, IgG2b-DyL550 and NTPDase3-DyL550); more information is available in Table 5.

## Discussion

Our collaborators in the Nostro group identified the pancreatic secretory granule membrane GP2 as a highly enriched cell surface protein in hESC-derived PPs. We expanded on this work and showed that GP2 is expressed in the human postnatal pancreas, where it labels a subset of cells expressing PTF1A and NKX6.1 that localize to the epithelial tips (**Fig. 19, 20**). These findings suggest the existence of a multipotent PP population in the human pancreas that is characterized by co-expression of GP2, PTF1A, and NKX6.1, and which can give rise to both acinar (GP2<sup>+</sup> PTF1A<sup>+</sup> NKX6.1<sup>-</sup>) or endocrine/ductal (GP2<sup>-</sup> PTF1A<sup>-</sup> NKX6.1<sup>+</sup>) lineages (**Fig. 21c**). This model mirrors the organization of murine multipotent PPs<sup>364,365,377</sup>, with the important distinction that putative PPs in human pancreas persist beyond fetal development. Furthermore, the Nostro group showed that GP2<sup>+</sup> cells could be enriched using FACS during hESC differentiation, with GP2<sup>+</sup>-purified populations giving rise to increased numbers of insulin-expressing mono-hormonal  $\beta$ -like cells (**Fig. 21**). Though these  $\beta$ -like cells are not glucose responsive, the data nevertheless suggest that GP2<sup>+</sup> cells harbor the potential to efficiently generate  $\beta$ -cells *in vitro*.

Our data indicate that NTPDase3 is expressed on the cell surface of essentially all adult human  $\beta$ -cells, including those from individuals with T1D and T2D (**Fig. 22b-c**). In contrast to a prior report, we did not observe NTPDase3 expression in human  $\alpha$ -cells<sup>362</sup>. The level of NTPDase3 expression, which appeared more polarized than evenly distributed throughout the cell membrane, was similar across all  $\beta$ -cells, indicating that this marker of  $\beta$ -cells does not correlate with recently reported  $\beta$ -cell subtypes<sup>378</sup>. The identity and role of the few NTPDase3-negative  $\beta$ -cells will be of future interest.

Interestingly, NTPDase3 is not expressed by very young (<10 months of age) human  $\beta$ -cells, and actually is expressed broadly in the epithelium during fetal pancreas development and by young pancreatic acinar cells postnatally (**Fig. 22d**). Based on the expression pattern of NTPDase3 and current knowledge of postnatal  $\beta$ -cell development, we postulate that NTPDase3 is important for  $\beta$ -cells to attain their functional maturity. As modulators of extracellular ATP, NTPDases directly impact purinergic signaling pathways controlling processes like glucose-stimulated insulin secretion<sup>363,379-381</sup>. Furthermore, the cellular expression of specific purinergic receptor subtypes appears to change during rodent pancreatic development and also under diabetic conditions, suggesting that NTPDase expression is functionally relevant in pancreatic islets and may affect  $\beta$ -cell maturation<sup>382,383</sup>. In addition to the pancreas, isozyme NTPDase3 is also expressed in the brain (where it is proposed to regulate synaptic function, at least in rodent models), GI tract, and urinary bladder (GTEX). Future studies are necessary to establish the importance of this particular NTPDase isoform in human  $\beta$ -cell physiology and pathophysiology.

Given its specificity and membrane localization, we utilized an NTPDase3 antibody for purification of live human  $\beta$ -cells (**Fig. 24**). Prior studies have relied on isolating live  $\beta$ -cells through exclusion of other cell types<sup>47,378</sup>, which results in higher contamination (e.g. up to 13% in  $\beta$ -cells as reported by Bramswig *et al.*<sup>47</sup>) and means that existing data sets are contaminated with gene expression data from non- $\beta$ -cells. Our results using NTPDase3 as a positive selector of  $\beta$ -cells provide a more accurate transcriptional profile than other cell sorting approaches and without compromising membrane integrity, as is required for sorting using intracellular insulin staining. Furthermore, the emerging single cell RNA-seq (scRNA-



seq) technology is unable to completely define human  $\beta$ -cells. This technology lacks the sensitivity to reliably detect low-abundance transcripts that can be detected with our new sorting approach<sup>384,385</sup>. For example, recent scRNA-seq studies performed on human islet cells detected an average of only approximately 3,000-7,000 genes per cell<sup>43,386,387</sup>. In contrast, our bulk analysis identified over 20,000 genes. Currently, sequencing from “bulk” or sorted populations of cells still delivers the most comprehensive look at gene expression, and our NTPDase3-based  $\beta$ -cell sorting strategy should considerably improve the accuracy of this approach.

We next tested the use of unconjugated (**Fig. 28**) and conjugated (**Fig. 29**) NTPDase3 antibodies for *in vivo* imaging applications. The detection of transplanted human  $\beta$ -cells by NTPDase3 indicates that the antibody circulates, exits the vascular space, and reaches engrafted islet cells, where the NTPDase3 epitope is exposed on the cell surface *in vivo*. This is a major advantage since extracellular epitopes are often exposed in dispersed single cells but are hidden and not accessible in cells in the *in vivo* environment. Our results suggest that the NTPDase3 epitope would be accessible in the native pancreas, which is important for *in vivo* imaging applications. Additionally, *in vitro* analysis of T1D and T2D tissues suggests that NTPDase3 expression is not altered under pathophysiological conditions, a desirable quality of agents aimed at quantifying  $\beta$ -cell mass. These data provide evidence for critical *in vivo* imaging characteristics lacked by current imaging agents<sup>388</sup>.

## CHAPTER V

### SIGNIFICANCE AND FUTURE DIRECTIONS

The first goal of this Dissertation was to advance understanding of how microenvironmental signals, specifically ECs, regulate  $\beta$ -cell proliferation, and to translate this information into the human context. To accomplish this, we first generated a novel mouse model that allowed us to modulate VEGF-A-VEGFR2 signaling in ECs and analyze both the direct interaction between ECs and  $\beta$ -cells, as well as the interaction between ECs and macrophages. We found that loss of VEGFR2 signaling in proliferative ECs reduced macrophage recruitment and polarization, the implications of which are discussed in the first subsection (**Role of islet endothelial cells in the recruitment and polarization of macrophages**). When we inactivated VEGFR2 in quiescent ECs, we observed rapid vessel regression that led to a slight increase in  $\beta$ -cell proliferation; these studies are considered in the subsection dedicated to ECs alone (**Direct contribution of islet endothelial cells to  $\beta$ -cell proliferation**). We also performed for the first time a systematic analysis of vascular changes in human islets at different stages of postnatal development. This has provided a new understanding and insight into how these changes are related to human  $\beta$ -cell proliferation, which is discussed in the third subsection (**Endothelial cells and macrophages in the human islet microenvironment**). To integrate our findings from these human and mouse studies of the islet microenvironment, general areas that warrant future exploration are discussed (**Concluding commentary: microenvironment in  $\beta$ -cell proliferation**). Our proposed model of EC and macrophage contribution to  $\beta$ -cell proliferation is shown in **Fig. 11c** (reproduced here).

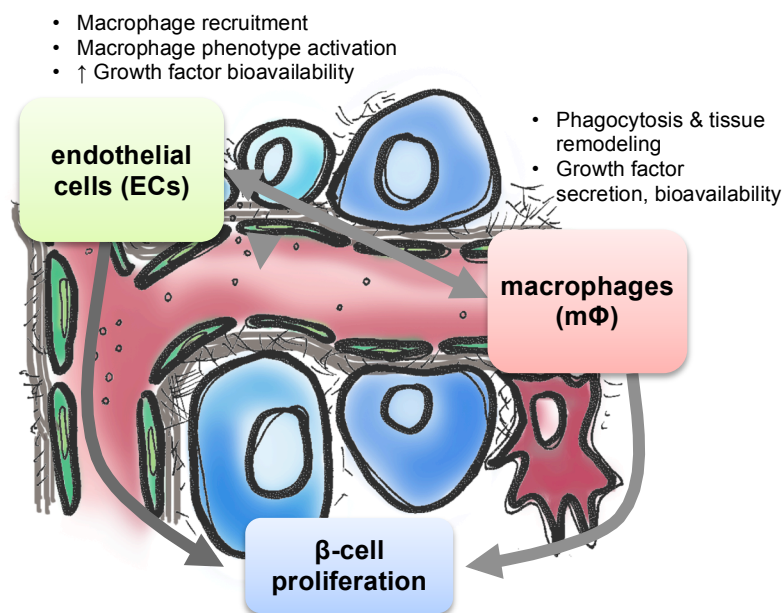


**Figure 11c:** Model depicting the interaction between ECs and macrophages to promote  $\beta$ -cell proliferation (adapted from Brissova *et al.*, 2014<sup>201</sup>).

The second overall goal of this Dissertation was to develop and apply new approaches to study changes in human  $\beta$ -cell gene expression during development and disease. We pioneered the use of two new molecular markers that identify crucial cell subpopulations in the human islet, and used these tools to advance our understanding of  $\beta$ -cell biology. The first marker, GP2, labels multipotent pancreatic progenitors in the neonatal pancreas and is discussed in the context of hESC differentiation and human postnatal development (**Molecular characterization of pancreatic progenitors: GP2**). NTPDase3, which is highly specific to mature  $\beta$ -cells, is then discussed for its application to numerous technologies, including cell sorting and *in vivo* imaging (**Molecular characterization of mature  $\beta$ -cells: NTPDase3**). Identification and study of these markers generated new knowledge about developing and mature  $\beta$ -cells

specifically from human islets, and paves the way for future experiments addressing the mechanisms of  $\beta$ -cell dysfunction in disease states.

### **Role of islet endothelial cells in the recruitment and polarization of macrophages**

Previous work in our lab established the critical role of macrophages in  $\beta$ -cell regeneration<sup>201</sup>, and we have built on this model by investigating the interaction between macrophages and intra-islet ECs. We showed that VEGFR2 inactivation prior to VEGF-A induction reduced, but did not completely prevent, macrophage infiltration to islets. We predict that the remainder of this effect is mediated by VEGFR1, which is expressed by circulating monocytes, and future experiments should focus on defining whether this is, in fact, the case. Although VEGFR1 is also abundantly expressed in islet vasculature<sup>201</sup>, it does not compensate for VEGFR2 loss; if anything, VEGF-A-VEGFR1 signaling in the absence of VEGFR2 enhances vessel stabilization.

In addition to monocyte recruitment, polarization to an M2-like phenotype was also reduced when VEGFR2 was inactivated in proliferating ECs of  $\beta$ VEGF-A; VEGFR2<sup>iAEC</sup> mice, suggesting a role for ECs in macrophage polarization. A very interesting line of investigation would be to test whether restoration of VEGFR2 signaling corrects this deficit— i.e. how long after initial knockdown before VEGFR2 expression is restored, and whether macrophage phenotype is altered when this occurs. This could be accomplished by performing a time-course analysis of islets from  $\beta$ VEGF-A; VEGFR2<sup>iAEC</sup> mice, noting the relationship between VEGFR2 expression and macrophage phenotype. It is possible that VEGFR2 inactivation has a transient effect on polarization, but also possible that the absence of VEGFR2 signaling in ECs at the onset of monocyte infiltration is sufficient to permanently affect a distinct macrophage phenotype. Using the existing paradigm of VEGFR2 inactivation followed by VEGF-A induction, we could then determine whether macrophage polarization was required for  $\beta$ -cell regeneration by assessing pancreata at 1 or 2 week WD time points. If we found that M2 polarization was reversible, we could maintain VEGF-A knockdown during the duration of VEGF-A induction to answer this question. Several groups have shown the importance of macrophages in other models of  $\beta$ -cell proliferation, and have documented M2-like properties of the macrophages involved, but there is no direct evidence showing this polarization is necessary.

Though the reduction in M2 macrophages of  $\beta$ VEGF-A; VEGFR2<sup>iAEC</sup> mice suggested that ECs contribute to macrophage polarization, it is also possible that  $\beta$ -cell death is the major driver for polarizing the recruited macrophages we observe in  $\beta$ VEGF-A mice. Since knocking out VEGFR2 also prevented VEGF-A-induced hypervascularization and  $\beta$ -cell death, an interesting line of research is to use alternative methods of  $\beta$ -cell destruction to examine the effects of EC signaling on macrophage polarization. For example, M2 macrophage recruitment has been documented in PDL<sup>139,145</sup> and treatment with DT<sup>202</sup> and STZ<sup>353</sup>. Using one of these models, cell death might be sufficient to polarize macrophages (in which case we would expect no change by then knocking down VEGFR2), or it is possible that signals derived from ECs are also required for that process. Data from STZ-mediated  $\beta$ -cell injury, in which grafted MSCs were shown to recruit M2 macrophages, suggests the latter<sup>353</sup>. Nonetheless, resolving the major source(s) of macrophage polarization signals has important

implications for improving therapies to “reprogram” macrophages, which may involve administering small molecules or other drugs to promote anti-inflammatory processes<sup>142,162,180,389,390</sup>.

In considering the signals that may polarize macrophages, in our  $\beta$ VEGF-A model as well as in the larger context of therapeutic tools, it is important to recognize that macrophage phenotype is often very fluid and highly regulated. An initial “bias” toward pro-inflammatory or pro-angiogenic signaling, for example, may resolve endogenously. M1 macrophages express high levels of iNOS that produces NO and leads to oxidative stress; however, NO also interacts with IRF5 to limit M1 gene expression, suggesting nuanced self-regulation<sup>391</sup>. Furthermore, the field of macrophage biology is rapidly evolving, with the M2 paradigm being further stratified to describe macrophages that may have very different roles in a particular tissue type or injury model<sup>392</sup>. The transcriptional profile of  $\beta$ VEGF-A macrophages seems to align with two of these subtypes: M2a, marked by increased expression of scavenger and phagocytic receptors (Retn1b, Chil3, Mrc1) and secretion of profibrotic and trophic factors (fibronectin, IGF, TGF $\beta$ ), and M2c, associated with removal of apoptotic cells<sup>393,394</sup>. There is also evidence that M2a macrophages upregulate histone demethylase JMJD3, which alters chromatin to promote expression of M2 genes and inhibit M1 genes<sup>394,395</sup>. Further analysis of  $\beta$ VEGF-A macrophages, both in the presence and absence of VEGFR2 signaling, might reveal similarities with specific macrophage subsets in other disease models. Detailed histology, flow cytometry, or scRNA-seq would all help in this process.

### **Direct contribution of islet endothelial cells to $\beta$ -cell proliferation**

Unexpectedly, VEGFR2 knockout after a week of VEGF-A normalization actually promoted  $\beta$ -cell proliferation due to accelerated vessel regression. However, this data should be carefully considered in the context of the experimental design, which is based on only 2 days of VEGFR2 knockdown. Although that amount of time was sufficient for discernible effect on proliferation in other models of tissue regeneration<sup>276,277</sup>, our model is more complex in that the islet vasculature is still greatly increased at the time of VEGFR2 knockdown. Therefore, we need to know if a prolonged period of VEGFR2 knockdown, or VEGFR2 knockdown later on in the regenerative process, might have differential effects on  $\beta$ -cells. For example, data on VEGFR2 knockout alone (in the absence of VEGF-A overexpression) showed no decrease in vasculature after 1 week, though vessel density trended downward, so it would be informative first to inactivate VEGFR2 for longer than 2 days, perhaps up to 2 weeks of the initial 6-week  $\beta$ VEGF-A recovery period. An alternative experimental paradigm could allow for more substantial vessel regression before knocking down VEGFR2 (for example, 2 weeks after VEGF-A withdrawal instead of 1 week), thereby ensuring that any effects on  $\beta$ -cell proliferation were independent of the effects of reversing hypervascularization.

Using the model we have generated, several experimental setups would provide further insight into the role of ECs in  $\beta$ -cell proliferation. As discussed in the previous section, STZ or DT administration produces similar environments ( $\beta$ -cell death and macrophage infiltration) leading to  $\beta$ -cell regeneration, and it would be very informative to block VEGFR2 in these contexts. It is possible that without the compounded effects of islet hypervascularization, loss of VEGF-A-VEGFR2 signaling in ECs would lead to reduced  $\beta$ -cell proliferation. STZ or DT would more closely mimic the environment in which Ding and colleagues inactivated VEGFR2 in ECs and observed impairment of hepatocyte and epithelial progenitor

cell proliferation in injured liver and lung tissues, respectively<sup>276,277</sup>. Alternatively, VEGFR2 signaling may simply not play as large of a role in pancreatic  $\beta$ -cell regeneration as it does in these systems. If not critical for regeneration, perhaps VEGFR2 signaling contributes to  $\beta$ -cell expansion observed during pregnancy. It is known that EC expansion precedes  $\beta$ -cell proliferation during rodent pregnancy<sup>105</sup>, so it would be interesting to analyze  $\beta$ -cell proliferation rates and  $\beta$ -cell mass in pregnant VEGFR2 <sup>$\Delta$ EC</sup> mice.

Although the increase in  $\beta$ -cell proliferation of  $\beta$ VEGF-A; VEGFR2 <sup>$\Delta$ EC</sup> mice was only slight in our current model, future work could address contributing molecular mechanisms. We began investigating structural ECM changes by staining for col-IV, which revealed that ECM “casts” were present after the rapid regression of ECs, and we hypothesized that such regression mobilized growth or other pro-proliferative factors that were normally trapped in the ECM. However, there is a great deal to be done in understanding whether ECM affects  $\beta$ -cell proliferation. One important step would be to perform tissue decellularization on islets isolated from  $\beta$ VEGF-A; VEGFR2 <sup>$\Delta$ EC</sup> mice and characterize associated growth factors by protein mass spectrometry. There are several growth factors with demonstrated effects on rodent  $\beta$ -cell proliferation that might be driving the regeneration observed in our  $\beta$ VEGF-A model, but two candidates of note are EGF and HGF. EGF, which has been shown to help restore  $\beta$ -cell mass after alloxan-induced  $\beta$ -cell loss<sup>396</sup>, appears to be highly regulated during alveolar regeneration, where matrix metalloproteinase (MMP) 14 increases its bioavailability to drive regeneration<sup>277</sup>. Liver regeneration is also modulated by release and activation of HGF through proteolysis<sup>397</sup>. HGF has been shown to suppress inflammatory signaling in macrophages<sup>398</sup>, which fits into our model of macrophage-EC crosstalk promoting  $\beta$ -cell proliferation. In addition to EGF and HGF, overexpression of CTGF has been shown to increase macrophage-mediated  $\beta$ -cell proliferation after  $\beta$ -cell loss<sup>399,400</sup>, so it would be interesting if we saw ECM-associated CTGF in  $\beta$ VEGF-A; VEGFR2 <sup>$\Delta$ EC</sup> mice. Treating mice with inhibitors or activators of ECM remodeling (i.e. MMPs) would be a next step to define whether ECM modulation had any effect on  $\beta$ -cell proliferation.

Finally, though we focused on VEGFR2 in these experiments because of its crucial role in mediating VEGF-A signaling and EC function, there are other molecules produced by ECs that could be used to directly interrogate the role of ECs in  $\beta$ -cell regeneration. For example, SDF-1 (CXCL12) produced by ECs could interact with CXCR4 to recruit macrophages<sup>353</sup>, and secretion of HGF by ECs could be critical for adaptive  $\beta$ -cell proliferation<sup>104,105</sup>. Manipulating other critical growth factor receptors could uncover signaling pathways that are crucial to macrophage recruitment and  $\beta$ -cell proliferation.

### **Endothelial cells and macrophages in the human islet microenvironment**

Our study of vasculature in developing postnatal human islets showed a correlation of EC area with  $\beta$ -cell proliferation rates. It will be essential to further analyze ECs in adult pancreatic samples, as well as to examine the composition of intra-islet macrophages during development. In mice it is known that embryonic pancreatic macrophages promote cell expansion and differentiation, having profound impacts on functional  $\beta$ -cell mass: reduced fetal  $\beta$ -cell proliferation and cell size is observed in CSF-1-deficient mice<sup>172</sup>, while culturing explants with CSF-1 causes a 3x increase in both macrophage and endocrine cell populations<sup>170</sup>. Systematically quantifying macrophages in juvenile pancreatic samples, to complement the data we generated for ECs, may give us additional insight into vascular changes

occurring during postnatal islet development. Studies by Almaça and colleagues<sup>256</sup> showed that intra-islet capillaries in “young” versus “old” mouse islets differ in abundance of immune cells, namely macrophages; still, it is not known if phenotype of these macrophages is changed by aging and whether intra-islet ECs may play a role in this process. We would like to pursue this question by (1) defining the dynamics of macrophage and EC gene expression during development, and (2) determining whether lack of intra-islet ECs alters juvenile human  $\beta$ -cell proliferation. Examining transcriptional differences in islets from donors of varying ages may capture changes not reflected in histology and structural analysis, and would generate hypotheses which we could test *in vivo* by employing siRNA knockdown in human islets. Additionally, we know that transplanted  $\beta$ -cells from juvenile donors exhibit higher proliferation rates and are more responsive to some mitogens<sup>401</sup>, so by depleting islets of ECs or macrophages, we could test whether these particular cell types played a role in this ability. Since “young” mouse ECs are able to stimulate proliferation of normally quiescent “old”  $\beta$ -cells<sup>256</sup>, it would be very interesting to test this using human ECs.

The idea of EC function declining with age, or in the context of chronic low-grade inflammation, is also an important research focus as we consider clinical strategies to enhance  $\beta$ -cell survival or function in patients with diabetes. The hyperglycemic environment in T1D and T2D can promote oxidative stress, apoptosis, and dysregulated paracrine signaling within the islet, which collectively compromise EC function<sup>217,312</sup>. Though healthy ECs may promote  $\beta$ -cell proliferation, we will need to understand the deficits in less “fit” ECs if we hope to harness EC-derived signals as a way to increase functional  $\beta$ -cell mass.

### **Concluding commentary: microenvironment in $\beta$ -cell proliferation**

The islet microenvironment provides signals that are critical to  $\beta$ -cell function, survival, and recovery from injury, so understanding the sources of these signals, and how they interact, is necessary to promote  $\beta$ -cell regeneration in a therapeutic environment. The following concepts are of particular importance and should be explored further:

- Closely regulate pro-angiogenic factors to yield beneficial effects in tissue repair and regeneration. The right balance of EC-derived signals is necessary for positive outcomes, whether during pancreatic development<sup>222,245-248,251,402</sup>, islet transplantation<sup>269,271-273</sup>, or disease<sup>263,403,404</sup>. Our experiments emphasize the importance of tightly regulated VEGF-A-VEGFR2 signaling in intra-islet ECs and deleterious effects of islet hypervascularization on  $\beta$ -cell mass and function.
- Investigate mechanisms leading to macrophage recruitment, persistence in, and withdrawal from regenerative environments. For example, a recent model of macrophage-mediated effects in  $\beta$ -cells highlighted that the presence of EGF effectively curbed the M1 inflammatory response, while injury without supplemented growth factors actually led to increased M1 infiltration<sup>396</sup>.
- Focus on cellular pathways that are commonly activated in both protective and regenerative contexts, including those involved in extracellular remodeling and ECM modulation. For example, heme oxygenase HO-1 has protective effects on  $\beta$ -cells<sup>161,394</sup> but is also associated with

amelioration of inflammation<sup>153,174</sup> and is highly upregulated (>5x) in macrophages of our  $\beta$ VEGF-A model<sup>201</sup>.

- Define changes in islet microenvironment with aging. For example, ECs tend to become less effective in defending against oxidative stress and may secrete proteins that facilitate immune cell recruitment and extravasation, leading to vascular inflammation and damage<sup>205,216</sup>. “Reprogramming” of ECs or macrophages *in vivo* is a potential mechanism for promoting  $\beta$ -cell proliferation after injury or disease. Particular attention should be paid to the differences in gene expression between mouse and human ECs and macrophages, the latter of which are incompletely defined<sup>405,406</sup>.

### **Molecular characterization of pancreatic progenitors: GP2**

Our work with GP2 highlights two ways this marker could be further explored: in native neonatal human pancreas, and in the differentiation of hESCs. First, immunohistochemical labeling of GP2 helped reveal the exciting discovery that multipotent pancreatic progenitor cells persist in the developing human pancreas even after birth. From an experimental standpoint, the GP2 marker could be further used for the isolation of multipotent pancreatic progenitor cells from neonatal human pancreas and aid their analysis by approaches such as scRNA-seq. Describing these cells would broaden our understanding of how human  $\beta$ -cell mass is established postnatally, since there is considerable heterogeneity in  $\beta$ -cell mass among adult humans<sup>35,316</sup>. A more detailed understanding of  $\beta$ -cell neogenesis during postnatal pancreatic development might help shed light on these differences and whether they influence future disease susceptibility<sup>407</sup>. Additionally, the functional role of GP2 in cell multipotency could be considered, since the only known function of GP2 is as a secreted, immunomodulatory membrane protein found in zymogen granules of acinar cells<sup>408,409</sup>. Although GP2<sup>-/-</sup> mice display normal pancreatic development<sup>410</sup>, perhaps more detailed, tissue-specific studies could be conducted to elucidate the role of GP2 in the pancreatic progenitor population. These experiments would help determine whether GP2 is involved in actively driving cell differentiation or whether it is purely a marker of multipotency.

Our collaborators in the Nostro group at the University of Toronto demonstrated that the GP2 marker is expressed in pancreatic progenitor cells derived from hESCs, and that these progenitors can be differentiated into insulin-producing  $\beta$ -like cells. This finding has the potential to greatly improve efficiency of generating insulin-producing cells from hESCs, since current approaches are plagued by inconsistent yields of  $\beta$ -like cells<sup>354,355</sup>. Large-scale purification of hESC progenitors by GP2, coupled with improvements to the functional responsiveness of  $\beta$ -like cells, would greatly advance hESC differentiation as a viable therapeutic  $\beta$ -cell replacement therapy.

### **Molecular characterization of mature $\beta$ -cells: NTPDase3**

The identification of NTPDase3 as a marker of mature human  $\beta$ -cells opens several new avenues for investigation and discovery. First, the function of this ecto-enzyme should be explored in the context of  $\beta$ -cell physiology and maturation. This could be initially investigated by creating a  $\beta$ -cell-specific NTPDase3 knockout in the mouse, which could then be assessed for normal islet formation and postnatal  $\beta$ -cell proliferation. We could also use siRNA constructs to knock down NTPDase3 in dispersed human islet cells, assessing subsequent changes in gene expression or insulin secretion.

Since we have shown that an NTPDase3 antibody can be used to sort live human  $\beta$ -cells from dispersed islet cells, it would be extremely interesting to compare transcriptional profiles of NTPDase3<sup>+</sup> and NTPDase3<sup>-</sup>  $\beta$ -cell subsets. Performing this experiment using neonatal human islets, around the age of 1-2 years when NTPDase3 is only expressed in a small subset of  $\beta$ -cells, would help determine whether NTPDase3 truly marks more physiologically “mature”  $\beta$ -cells. Additionally, the analysis of NTPDase3<sup>-</sup> adult  $\beta$ -cells might reveal a  $\beta$ -cell subset with a distinct phenotypic role.

With regard to maturation, NTPDase3 expression should also be co-registered with other  $\beta$ -cell maturation markers, such as Nkx6.1 and Pdx1. We showed that NTPDase3 expression is retained in  $\beta$ -cells from T2D donors, whose  $\beta$ -cells sometimes display evidence of de-differentiation through reduced transcription factor expression<sup>371-373</sup>, so these samples are of particular interest. If de-differentiated cells do indeed express NTPDase3, we may need to revise the idea that NTPDase3 is a specific marker of “mature”  $\beta$ -cells. Our initial results indicate that this is not likely.

The unique expression of NTPDase3 during human pancreatic development is certainly significant in that it is unprecedented in studies of mouse pancreatic development and highlights the importance of studies with human samples. Though some endocrine markers become increasingly specific in their expression (for example, Nkx6.1 is broadly expressed by ductal and endocrine progenitors before becoming restricted to  $\beta$ -cells<sup>10,11,244</sup>), NTPDase3 is unique in that it appears first in the acinar compartment and then completely inverts to expression in the endocrine compartment ( $\beta$ -cells). Further study of purinergic signaling in the islet during development, and perhaps defining transcriptional regulation of NTPDase3, might reveal additional distinctions in the way human islets develop compared to those in mice.

As mentioned, the use of NTPDase3 to improve the purity of isolated  $\beta$ -cell populations should enable physiological experiments requiring live  $\beta$ -cells, including electrophysiology, high-resolution imaging, and formation of pseudoislets. Our sorting strategy will also be valuable to pursue chromatin immunoprecipitation (CHIP)-seq and assay for transposase-accessible chromatin sequencing (ATAC-seq) experiments on human  $\beta$ -cells. Furthermore, the NTPDase3 antibody may be applicable to improving efforts aimed at generating  $\beta$ -like cells from hESCs or hiPSCs. It is possible that NTPDase3 could be used to enrich for  $\beta$ -like cells at late stages of differentiation (similar to the way GP2 might be used as a positive selector at earlier stages), or even the possibility that inducing NTPDase3 in  $\beta$ -like cells would aid in acquisition of mature  $\beta$ -cell characteristics such as GSIS.

Finally, our results suggest that NTPDase3 could be targeted as an imaging probe that might enhance the understanding of  $\beta$ -cell mass dynamics in healthy individuals and those with diabetes, which has not been possible in humans. This process might involve the creation of a “humanized” monoclonal antibody that could be tested for *in vivo* imaging in humans, perhaps a single chain antibody that would allow for maximal conjugation, efficient transport, and low background due to its small size<sup>358,411,412</sup>. Such a construct could be first labeled for PET imaging and tested in mouse models to evaluate efficacy in visualizing  $\beta$ -cells<sup>358,359,413</sup>. Another important future objective is to define the NTPDase3 epitope that our current antibody targets, as it may reveal biological characteristics that are unique to this isozyme and distinguish it from related NTPDases. Describing the epitope would also allow for use of small molecule high-throughput screening to identify molecules that could be used for *in vivo* imaging or sorting as an



alternative to the antibody itself, as antibodies sometimes have prolonged clearance and a high background when used for *in vivo* imaging<sup>388,411</sup>. In either case, the development of a  $\beta$ -cell-specific imaging tool and ability to quantify  $\beta$ -cell mass would also improve evaluation of clinical outcomes, ranging from assessment of islet transplantation to endogenous recovery of  $\beta$ -cell mass through pharmaceutical manipulation. Thus, these findings with NTPDase3 in human  $\beta$ -cells offer the opportunity to advance current knowledge of  $\beta$ -cell physiology, and provide a promising tool for basic researchers and clinical investigators.

## REFERENCES

1. Hegyi, P. & Petersen, O. H. in *Reviews of Physiology, Biochemistry and Pharmacology, Vol. 165* (eds. Nilius, B. et al.) 1–30 (Springer International Publishing, 2013).
2. Pandiri, A. R. Overview of exocrine pancreatic pathobiology. *Toxicol Pathol* **42**, 207–216 (2014).
3. Saladin, K. *Anatomy & Physiology: The Unity of Form and Function*. (McGraw-Hill, 2001).
4. Cabrera, O. et al. The unique cytoarchitecture of human pancreatic islets has implications for islet cell function. *PNAS* **103**, 2334–2339 (2006).
5. Brissova, M. et al. Assessment of human pancreatic islet architecture and composition by laser scanning confocal microscopy. *J. Histochem. Cytochem.* **53**, 1087–1097 (2005).
6. Rutter, G. A. Nutrient-secretion coupling in the pancreatic islet beta-cell: recent advances. *Mol. Aspects Med.* **22**, 247–284 (2001).
7. Newgard, C. B. et al. Stimulus/secretion coupling factors in glucose-stimulated insulin secretion: insights gained from a multidisciplinary approach. *Diabetes* **51 Suppl 3**, S389–93 (2002).
8. Lang, V. & Light, P. E. The molecular mechanisms and pharmacotherapy of ATP-sensitive potassium channel gene mutations underlying neonatal diabetes. *Pharmacogenomics Pers Med* **3**, 145–161 (2010).
9. De Vos, A. et al. Human and rat beta cells differ in glucose transporter but not in glucokinase gene expression. *J. Clin. Invest.* **96**, 2489–2495 (1995).
10. Pan, F. C. & Wright, C. Pancreas organogenesis: from bud to plexus to gland. *Developmental Dynamics* **240**, 530–565 (2011).
11. Benitez, C. M., Goodyer, W. R. & Kim, S. K. Deconstructing pancreas developmental biology. *Cold Spring Harb Perspect Biol* **4**, a012401–a012401 (2012).
12. Jørgensen, M. C. et al. An illustrated review of early pancreas development in the mouse. *Endocr. Rev.* **28**, 685–705 (2007).
13. Zaret, K. S. & Grompe, M. Generation and regeneration of cells of the liver and pancreas. *Science* **322**, 1490–1494 (2008).
14. Villasenor, A., Chong, D. C., Henkemeyer, M. & Cleaver, O. Epithelial dynamics of pancreatic branching morphogenesis. *Development* **137**, 4295–4305 (2010).
15. Cano, D. A., Soria, B., Martín, F. & Rojas, A. Transcriptional control of mammalian pancreas organogenesis. *Cell. Mol. Life Sci.* **71**, 2383–2402 (2013).
16. Cleaver, O. & Dor, Y. Vascular instruction of pancreas development. *Development* **139**, 2833–2843 (2012).
17. Puri, S. & Hebrok, M. Cellular plasticity within the pancreas—lessons learned from development. *Dev. Cell* **18**, 342–356 (2010).
18. Magenheim, J. et al. Blood vessels restrain pancreas branching, differentiation and growth. *Development* **138**, 4743–4752 (2011).
19. Gu, C. et al. Pancreatic beta cells require NeuroD to achieve and maintain functional maturity. *Cell Metabolism* **11**, 298–310 (2010).
20. Desgraz, R. & Herrera, P. L. Pancreatic neurogenin 3-expressing cells are unipotent islet precursors. *Development* **136**, 3567–3574 (2009).
21. Miyatsuka, T., Kosaka, Y., Kim, H. & German, M. S. Neurogenin3 inhibits proliferation in endocrine progenitors by inducing Cdkn1a. *PNAS* **108**, 185–190 (2011).

22. Zhang, C. *et al.* MafA is a key regulator of glucose-stimulated insulin secretion. *Mol. Cell. Biol.* **25**, 4969–4976 (2005).
23. Wang, H., Brun, T., Kataoka, K., Sharma, A. J. & Wollheim, C. B. MAFA controls genes implicated in insulin biosynthesis and secretion. *Diabetologia* **50**, 348–358 (2007).
24. Artner, I. *et al.* MafA and MafB regulate genes critical to beta-cells in a unique temporal manner. *Diabetes* **59**, 2530–2539 (2010).
25. Zehetner, J. *et al.* PVHL is a regulator of glucose metabolism and insulin secretion in pancreatic beta cells. *Genes Dev.* **22**, 3135–3146 (2008).
26. Cheng, K. *et al.* Hypoxia-inducible factor-1 $\alpha$  regulates  $\beta$  cell function in mouse and human islets. *J. Clin. Invest.* **120**, 2171–2183 (2010).
27. Zhang, H. *et al.* The FoxM1 Transcription Factor Is Required to Maintain Pancreatic  $\beta$ -Cell Mass. *Molecular Endocrinology* **20**, 1853–1866 (2006).
28. Du, A. *et al.* Islet-1 is required for the maturation, proliferation, and survival of the endocrine pancreas. *Diabetes* **58**, 2059–2069 (2009).
29. Wu, X. *et al.* Perinatal survivin is essential for the establishment of pancreatic beta cell mass in mice. *Diabetologia* **52**, 2130–2141 (2009).
30. Chen, H. *et al.* Polycomb protein Ezh2 regulates pancreatic beta-cell Ink4a/Arf expression and regeneration in diabetes mellitus. *Genes Dev.* **23**, 975–985 (2009).
31. Jennings, R. E. *et al.* Development of the human pancreas from foregut to endocrine commitment. *Diabetes* **62**, 3514–3522 (2013).
32. Pan, F. C. & Brissova, M. Pancreas development in humans. *Current Opinion in Endocrinology & Diabetes and Obesity* **21**, 77–82 (2014).
33. Lyttle, B. M. *et al.* Transcription factor expression in the developing human fetal endocrine pancreas. *Diabetologia* **51**, 1169–1180 (2008).
34. Riedel, M. J. *et al.* Immunohistochemical characterisation of cells co-producing insulin and glucagon in the developing human pancreas. *Diabetologia* **55**, 372–381 (2012).
35. Gregg, B. E. *et al.* Formation of a human  $\beta$ -cell population within pancreatic islets is set early in life. *The Journal of Clinical Endocrinology & Metabolism* **97**, 3197–3206 (2012).
36. Jeon, J., Correa-Medina, M., Ricordi, C., Edlund, H. & Diez, J. A. Endocrine cell clustering during human pancreas development. *Journal of Histochemistry & Cytochemistry* **57**, 811–824 (2009).
37. Piper, K. *et al.* Beta cell differentiation during early human pancreas development. *J Endocrinol* **181**, 11–23 (2004).
38. Bosco, D. *et al.* Unique Arrangement of  $\alpha$ - and  $\beta$ -Cells in Human Islets of Langerhans. *Diabetes* **59**, 1202–1210 (2010).
39. Brissova, M. *et al.* Human Islets Have Fewer Blood Vessels than Mouse Islets and the Density of Islet Vascular Structures Is Increased in Type 2 Diabetes. *Journal of Histochemistry & Cytochemistry* **63**, 637–645 (2015).
40. Ferrer, J., Benito, C. & Gomis, R. Pancreatic islet GLUT2 glucose transporter mRNA and protein expression in humans with and without NIDDM. *Diabetes* **44**, 1369–1374 (1995).
41. Shiao, M.-S., Liao, B.-Y., Long, M. & Yu, H.-T. Adaptive evolution of the insulin two-gene system in mouse. *Genetics* **178**, 1683–1691 (2008).
42. Rorsman, P. & Braun, M. Regulation of Insulin Secretion in Human Pancreatic Islets. *Annu. Rev. Physiol.* **75**, 155–179 (2013).

43. Xin, Y. *et al.* RNA Sequencing of Single Human Islet Cells Reveals Type 2 Diabetes Genes. *Cell Metabolism* **24**, 608–615 (2016).
44. Dai, C. *et al.* Islet-enriched gene expression and glucose-induced insulin secretion in human and mouse islets. *Diabetologia* **55**, 707–718 (2012).
45. Kondegowda, N. G. *et al.* Lactogens protect rodent and human beta cells against glucolipotoxicity-induced cell death through Janus kinase-2 (JAK2)/signal transducer and activator of transcription-5 (STAT5) signalling. *Diabetologia* **55**, 1721–1732 (2012).
46. Avrahami, D. *et al.* Targeting the cell cycle inhibitor p57Kip2 promotes adult human  $\beta$  cell replication. *J. Clin. Invest.* **124**, 670–674 (2014).
47. Bramswig, N. C. *et al.* Epigenomic plasticity enables human pancreatic  $\alpha$  to  $\beta$  cell reprogramming. *J. Clin. Invest.* **123**, 1275–1284 (2013).
48. Centers for Disease Control and Prevention (CDC). National Diabetes Statistics Report, 2017. 1–20 (2017).
49. DeSisto, C. L., Kim, S. Y. & Sharma, A. J. Prevalence Estimates of Gestational Diabetes Mellitus in the United States, Pregnancy Risk Assessment Monitoring System (PRAMS), 2007–2010. *Prev Chronic Dis* **11**, 130415 (2014).
50. Ashrafi, M. *et al.* Risk of gestational diabetes mellitus in patients undergoing assisted reproductive techniques. *European Journal of Obstetrics & Gynecology and Reproductive Biology* **176**, 149–152 (2014).
51. Angueira, A. R. *et al.* New insights into gestational glucose metabolism: lessons learned from 21st century approaches. *Diabetes* **64**, 327–334 (2015).
52. Egerman, R., Ramsey, R., Istwan, N., Rhea, D. & Stanziano, G. Maternal Characteristics Influencing the Development of Gestational Diabetes in Obese Women Receiving 17-alpha-Hydroxyprogesterone Caproate. *Journal of Obesity* **2014**, 1–4 (2014).
53. Retnakaran, R. & Shah, B. R. Fetal Sex and the Natural History of Maternal Risk of Diabetes During and After Pregnancy. *The Journal of Clinical Endocrinology & Metabolism* **100**, 1763–2580 (2015).
54. Ernst, S., Demirci, C., Valle, S., Velazquez-Garcia, S. & Garcia-Ocaña, A. Mechanisms in the adaptation of maternal  $\beta$ -cells during pregnancy. *Diabetes Management* **1**, 239–248 (2011).
55. Wang, P. *et al.* Diabetes mellitus--advances and challenges in human  $\beta$ -cell proliferation. *Nature Reviews Endocrinology* **11**, 201–212 (2015).
56. Pihoker, C. *et al.* Prevalence, characteristics and clinical diagnosis of maturity onset diabetes of the young due to mutations in HNF1A, HNF4A, and glucokinase: results from the SEARCH for Diabetes in Youth. *The Journal of Clinical Endocrinology & Metabolism* **98**, 4055–4062 (2013).
57. Tritschler, S., Theis, F. J., Lickert, H. & Böttcher, A. Systematic single-cell analysis provides new insights into heterogeneity and plasticity of the pancreas. *Mol Metab* **6**, 974–990 (2017).
58. Chang, C. A., Lawrence, M. C. & Naziruddin, B. Current issues in allogeneic islet transplantation. *Curr Opin Organ Transplant* **22**, 437–443 (2017).
59. Gamble, A., Pepper, A. R., Bruni, A. & Shapiro, A. M. J. The journey of islet cell transplantation and future development. *Islets* **12**, e1428511 (2018).
60. Vegas, A. J. *et al.* Long-term glycemic control using polymer-encapsulated human stem cell-derived beta cells in immune-competent mice. *Nature Medicine* **22**, 306–311 (2016).
61. Agulnick, A. D. *et al.* Insulin-Producing Endocrine Cells Differentiated In Vitro From Human

- Embryonic Stem Cells Function in Macroencapsulation Devices In Vivo. *Stem Cells Translational Medicine* **4**, 1214–1222 (2015).
62. Szot, G. L. *et al.* Tolerance induction and reversal of diabetes in mice transplanted with human embryonic stem cell-derived pancreatic endoderm. *Cell Stem Cell* **16**, 148–157 (2015).
  63. Bernal-Mizrachi, E. *et al.* Human  $\beta$ -Cell Proliferation and Intracellular Signaling Part 2: Still Driving in the Dark Without a Road Map. *Diabetes* **63**, 819–831 (2014).
  64. Stewart, A. F. *et al.* Human  $\beta$ -Cell Proliferation and Intracellular Signaling: Part 3. *Diabetes* **64**, 1872–1885 (2015).
  65. Porat, S. *et al.* Control of Pancreatic  $\beta$ -Cell Regeneration by Glucose Metabolism. *Cell Metabolism* **13**, 440–449 (2011).
  66. Collombat, P. *et al.* The ectopic expression of Pax4 in the mouse pancreas converts progenitor cells into alpha and subsequently beta cells. *Cell* **138**, 449–462 (2009).
  67. Courtney, M. *et al.* The Inactivation of Arx in Pancreatic  $\alpha$ -Cells Triggers Their Neogenesis and Conversion into Functional  $\beta$ -Like Cells. *PLoS Genetics* **9**, e1003934 (2013).
  68. Baeyens, L. *et al.* Transient cytokine treatment induces acinar cell reprogramming and regenerates functional beta cell mass in diabetic mice. *Nat. Biotechnol.* **32**, 76–83 (2013).
  69. Rooman, I. & Bouwens, L. Combined gastrin and epidermal growth factor treatment induces islet regeneration and restores normoglycaemia in C57Bl6/J mice treated with alloxan. *Diabetologia* **47**, 259–265 (2004).
  70. Aguayo-Mazzucato, C. & Bonner-Weir, S. Pancreatic  $\beta$  Cell Regeneration as a Possible Therapy for Diabetes. *Cell Metabolism* **27**, 57–67 (2018).
  71. Johannesson, B., Sui, L., Freytes, D. O., Creusot, R. J. & Egli, D. Toward beta cell replacement for diabetes. *EMBO J.* **34**, 841–855 (2015).
  72. Benthuyzen, J. R., Carrano, A. C. & Sander, M. Advances in  $\beta$  cell replacement and regeneration strategies for treating diabetes. *J. Clin. Invest.* **126**, 3651–3660 (2016).
  73. Pagliuca, F. W. *et al.* Generation of functional human pancreatic  $\beta$  cells in vitro. *Cell* **159**, 428–439 (2014).
  74. Reznia, A. *et al.* Reversal of diabetes with insulin-producing cells derived in vitro from human pluripotent stem cells. *Nat. Biotechnol.* **32**, 1121–1133 (2014).
  75. Millman, J. R. *et al.* Generation of stem cell-derived  $\beta$ -cells from patients with type 1 diabetes. *Nat Commun* **7**, 11463 (2016).
  76. Chera, S. *et al.* Diabetes recovery by age-dependent conversion of pancreatic  $\delta$ -cells into insulin producers. *Nature* **514**, 503–507 (2014).
  77. Chung, C.-H., Hao, E., Piran, R., Keinan, E. & Levine, F. Pancreatic  $\beta$ -cell neogenesis by direct conversion from mature  $\alpha$ -cells. *Stem Cells* **28**, 1630–1638 (2010).
  78. Thorel, F. *et al.* Conversion of adult pancreatic alpha-cells to beta-cells after extreme beta-cell loss. *Nature* **464**, 1149–1154 (2010).
  79. Zhang, Y. *et al.* PAX4 Gene Transfer Induces  $\alpha$ -to- $\beta$  Cell Phenotypic Conversion and Confers Therapeutic Benefits for Diabetes Treatment. *Mol. Ther.* **24**, 251–260 (2016).
  80. Valdez, I. A. *et al.* Proinflammatory Cytokines Induce Endocrine Differentiation in Pancreatic Ductal Cells via STAT3-Dependent NGN3 Activation. *Cell Reports* **15**, 460–470 (2016).
  81. Talchai, C., Xuan, S., Kitamura, T., DePinho, R. A. & Accili, D. Generation of functional insulin-producing cells in the gut by Foxo1 ablation. *Nat. Genet.* **44**, 406–12– S1 (2012).

82. Bouchi, R. *et al.* FOXO1 inhibition yields functional insulin-producing cells in human gut organoid cultures. *Nat Commun* **5**, 4242 (2014).
83. Kulkarni, R. N., Mizrahi, E.-B., Ocana, A. G. & Stewart, A. F. Human  $\beta$ -cell proliferation and intracellular signaling: driving in the dark without a road map. *Diabetes* **61**, 2205–2213 (2012).
84. Chen, H. *et al.* Augmented Stat5 Signaling Bypasses Multiple Impediments to Lactogen-Mediated Proliferation in Human  $\beta$ -Cells. *Diabetes* **64**, 3784–3797 (2015).
85. Amaral, M. E. C. *et al.* Participation of prolactin receptors and phosphatidylinositol 3-kinase and MAP kinase pathways in the increase in pancreatic islet mass and sensitivity to glucose during pregnancy. *J Endocrinol* **183**, 469–476 (2004).
86. Dietrich, M. G. *et al.* Specific and redundant roles of PKB $\alpha$ /AKT1 and PKB $\beta$ /AKT2 in human pancreatic islets. *Experimental Cell Research* **338**, 82–88 (2015).
87. Lakshmipathi, J. *et al.* PKC- $\zeta$  is essential for pancreatic beta cell replication during insulin resistance by regulating mTOR and cyclin-D2. *Diabetes* db151398 (2016). doi:10.2337/db15-1398
88. Xiao, X. *et al.* Transient Suppression of TGF $\beta$  Receptor Signaling Facilitates Human Islet Transplantation. *Endocrinology* **157**, 1348–1356 (2016).
89. Leibiger, B. *et al.* PI3K-C2 $\alpha$  Knockdown Results in Rerouting of Insulin Signaling and Pancreatic Beta Cell Proliferation. *Cell Reports* **13**, 15–22 (2015).
90. Fiaschi-Taesch, N. M. *et al.* Induction of Human  $\beta$ -Cell Proliferation and Engraftment Using a Single G1/S Regulatory Molecule, cdk6. *Diabetes* **59**, 1926–1936 (2010).
91. Fiaschi-Taesch, N. M. *et al.* Human pancreatic  $\beta$ -cell G1/S molecule cell cycle atlas. *Diabetes* **62**, 2450–2459 (2013).
92. Draney, C., Hobson, A. E., Grover, S. G., Jack, B. O. & Tessem, J. S. Cdk5r1 Overexpression Induces Primary  $\beta$ -Cell Proliferation. *J Diabetes Res* **2016**, 6375804–15 (2016).
93. Fiaschi-Taesch, N. M. *et al.* Cytoplasmic-nuclear trafficking of G1/S cell cycle molecules and adult human  $\beta$ -cell replication: a revised model of human  $\beta$ -cell G1/S control. *Diabetes* **62**, 2460–2470 (2013).
94. Tiwari, S. *et al.* Early and Late G1/S Cyclins and Cdks Act Complementarily to Enhance Authentic Human  $\beta$ -Cell Proliferation and Expansion. *Diabetes* **64**, 3485–3498 (2015).
95. Karnik, S. K. *et al.* Menin regulates pancreatic islet growth by promoting histone methylation and expression of genes encoding p27Kip1 and p18INK4c. *PNAS* **102**, 14659–14664 (2005).
96. Pal, A. *et al.* Loss-of-Function Mutations in the Cell-Cycle Control Gene CDKN2A Impact on Glucose Homeostasis in Humans. *Diabetes* **65**, 527–533 (2016).
97. Vasavada, R. C. *et al.* Protein kinase C-zeta activation markedly enhances beta-cell proliferation: an essential role in growth factor mediated beta-cell mitogenesis. *Diabetes* **56**, 2732–2743 (2007).
98. Guthalu Kondegowda, N. *et al.* Parathyroid hormone-related protein enhances human  $\beta$ -cell proliferation and function with associated induction of cyclin-dependent kinase 2 and cyclin E expression. *Diabetes* **59**, 3131–3138 (2010).
99. Arumugam, R., Fleenor, D. & Freemark, M. Knockdown of prolactin receptors in a pancreatic beta cell line: effects on DNA synthesis, apoptosis, and gene expression. *Endocrine* **46**, 568–576 (2013).
100. Sorenson, R. L., Brelje, T. C. & Roth, C. Effects of steroid and lactogenic hormones on islets of Langerhans: a new hypothesis for the role of pregnancy steroids in the adaptation of islets to pregnancy. *Endocrinology* **133**, 2227–2234 (1993).

101. Hyslop, C. M., Tsai, S., Shrivastava, V., Santamaria, P. & Huang, C. Prolactin as an Adjunct for Type 1 Diabetes Immunotherapy. *Endocrinology* **157**, 150–165 (2016).
102. Legorreta-Haquet, M. V. *et al.* Prolactin down-regulates CD4<sup>+</sup>CD25<sup>hi</sup>CD127<sup>low/-</sup> regulatory T cell function in humans. *Journal of Molecular Endocrinology* **48**, 77–85 (2012).
103. Kim, H. *et al.* Serotonin Regulates Pancreatic  $\beta$ -Cell Mass during Pregnancy. *Nature Medicine* **16**, 804–808 (2010).
104. Demirci, C. *et al.* Loss of HGF/c-Met signaling in pancreatic  $\beta$ -cells leads to incomplete maternal  $\beta$ -cell adaptation and gestational diabetes mellitus. *Diabetes* **61**, 1143–1152 (2012).
105. Johansson, M., Mattsson, G., Andersson, A., Jansson, L. & Carlsson, P.-O. Islet endothelial cells and pancreatic beta-cell proliferation: studies in vitro and during pregnancy in adult rats. *Endocrinology* **147**, 2315–2324 (2006).
106. Liu, Y. *et al.* Conditional ablation of Gsk-3 $\beta$  in islet beta cells results in expanded mass and resistance to fat feeding-induced diabetes in mice. *Diabetologia* **53**, 2600–2610 (2010).
107. Ouaamari, El, A. *et al.* SerpinB1 Promotes Pancreatic  $\beta$  Cell Proliferation. *Cell Metabolism* **23**, 194–205 (2016).
108. Dai, C. *et al.* Stress-impaired transcription factor expression and insulin secretion in transplanted human islets. *J. Clin. Invest.* **126**, 1857–1870 (2016).
109. Robitaille, K. *et al.* High-throughput Functional Genomics Identifies Regulators of Primary Human Beta Cell Proliferation. *Journal of Biological Chemistry* **291**, 4614–4625 (2016).
110. Wang, G. *et al.* First quantitative high-throughput screen in zebrafish identifies novel pathways for increasing pancreatic  $\beta$ -cell mass. *Elife* **4**, 3 (2015).
111. Dirice, E. *et al.* Inhibition of DYRK1A Stimulates Human  $\beta$ -Cell Proliferation. *Diabetes* **65**, 1660–1671 (2016).
112. Walpita, D. *et al.* A human islet cell culture system for high-throughput screening. *Journal of Biomolecular Screening* **17**, 509–518 (2012).
113. Shen, W. *et al.* Inhibition of DYRK1A and GSK3B induces human  $\beta$ -cell proliferation. *Nat Commun* **6**, 8372 (2015).
114. Cheng, S. T. W., Chen, L., Li, S. Y. T., Mayoux, E. & Leung, P. S. The Effects of Empagliflozin, an SGLT2 Inhibitor, on Pancreatic  $\beta$ -Cell Mass and Glucose Homeostasis in Type 1 Diabetes. *PLoS ONE* **11**, e0147391 (2016).
115. Lorenzo, P. I. *et al.* PAX4 Defines an Expandable  $\beta$ -Cell Subpopulation in the Adult Pancreatic Islet. *Sci Rep* **5**, 15672 (2015).
116. Brun, T. *et al.* The diabetes-linked transcription factor PAX4 promotes  $\beta$ -cell proliferation and survival in rat and human islets. *J. Cell Biol.* **167**, 1123–1135 (2004).
117. Liu, J. *et al.* Functionalized self-assembling peptide improves INS-1  $\beta$ -cell function and proliferation via the integrin/FAK/ERK/cyclin pathway. *International Journal of Nanomedicine* **10**, 3519–3531 (2015).
118. Brelje, T. C., Bhagroo, N. V., Stout, L. E. & Sorenson, R. L. Beneficial effects of lipids and prolactin on insulin secretion and beta-cell proliferation: a role for lipids in the adaptation of islets to pregnancy. *J Endocrinol* **197**, 265–276 (2008).
119. Maedler, K., Oberholzer, J., Bucher, P., Spinas, G. A. & Donath, M. Y. Monounsaturated fatty acids prevent the deleterious effects of palmitate and high glucose on human pancreatic beta-cell turnover and function. *Diabetes* **52**, 726–733 (2003).

120. Lifson, N., Lassa, C. V. & Dixit, P. K. Relation between blood flow and morphology in islet organ of rat pancreas. *Am. J. Physiol.* **249**, E43–8 (1985).
121. Bonner-Weir, S. in *The Pancreas Biology, Pathobiology, and Disease* (ed. Go, V. L. W.) 1–10 (1993).
122. Murakami, T. *et al.* Blood flow patterns in the rat pancreas: a simulative demonstration by injection replication and scanning electron microscopy. *Microsc. Res. Tech.* **37**, 497–508 (1997).
123. Vetterlein, F., Pethö, A. & Schmidt, G. Morphometric investigation of the microvascular system of pancreatic exocrine and endocrine tissue in the rat. *Microvasc. Res.* **34**, 231–238 (1987).
124. Richards, O. C., Raines, S. M. & Attie, A. D. The role of blood vessels, endothelial cells, and vascular pericytes in insulin secretion and peripheral insulin action. *Endocr. Rev.* **31**, 343–363 (2010).
125. Stratman, A. N., Malotte, K. M., Mahan, R. D., Davis, M. J. & Davis, G. E. Pericyte recruitment during vasculogenic tube assembly stimulates endothelial basement membrane matrix formation. *Blood* **114**, 5091–5101 (2009).
126. Sakhneny, L. *et al.* Pancreatic Pericytes Support  $\beta$ -Cell Function in a Tcf7l2-Dependent Manner. *Diabetes* **67**, 437–447 (2018).
127. Sasson, A. *et al.* Islet Pericytes Are Required for  $\beta$ -Cell Maturity. *Diabetes* **65**, 3008–3014 (2016).
128. Epshtein, A. *et al.* Neonatal pancreatic pericytes support  $\beta$ -cell proliferation. *Mol Metab* **6**, 1330–1338 (2017).
129. Ahrén, B. Autonomic regulation of islet hormone secretion - Implications for health and disease. *Diabetologia* **43**, 393–410 (2000).
130. Reinert, R. B. *et al.* Vascular endothelial growth factor coordinates islet innervation via vascular scaffolding. *Development* **141**, 1480–1491 (2014).
131. Rodriguez-Diaz, R. *et al.* Innervation patterns of autonomic axons in the human endocrine pancreas. *Cell Metabolism* **14**, 45–54 (2011).
132. Rodriguez-Diaz, R. & Caicedo, A. Neural control of the endocrine pancreas. *Best Pract. Res. Clin. Endocrinol. Metab.* **28**, 745–756 (2014).
133. Jiang, F.-X., Naselli, G. & Harrison, L. C. Distinct distribution of laminin and its integrin receptors in the pancreas. *Journal of Histochemistry & Cytochemistry* **50**, 1625–1632 (2002).
134. Otonkoski, T., Banerjee, M., Korsgren, O., Thornell, L. E. & Virtanen, I. Unique basement membrane structure of human pancreatic islets: implications for  $\beta$ -cell growth and differentiation. *Diabetes Obes Metab* **10**, 119–127 (2008).
135. Nackiewicz, D. *et al.* TLR2/6 and TLR4-activated macrophages contribute to islet inflammation and impair beta cell insulin gene expression via IL-1 and IL-6. *Diabetologia* **57**, 1645–1654 (2014).
136. Kigerl, K. A. *et al.* Identification of two distinct macrophage subsets with divergent effects causing either neurotoxicity or regeneration in the injured mouse spinal cord. *J. Neurosci.* **29**, 13435–13444 (2009).
137. Salcedo, R. *et al.* Vascular endothelial growth factor and basic fibroblast growth factor induce expression of CXCR4 on human endothelial cells: In vivo neovascularization induced by stromal-derived factor-1alpha. *Am. J. Pathol.* **154**, 1125–1135 (1999).
138. Strieter, R. M. *et al.* The functional role of the ELR motif in CXC chemokine-mediated angiogenesis. *Journal of Biological Chemistry* **270**, 27348–27357 (1995).
139. Xiao, X. *et al.* M2 macrophages promote beta-cell proliferation by up-regulation of SMAD7. *PNAS*



- 111**, E1211–20 (2014).
140. Cucak, H., Grunnet, L. G. & Rosendahl, A. Accumulation of M1-like macrophages in type 2 diabetic islets is followed by a systemic shift in macrophage polarization. *J. Leukoc. Biol.* **95**, 149–160 (2014).
  141. Edwards, J. P., Zhang, X., Frauwirth, K. A. & Mosser, D. M. Biochemical and functional characterization of three activated macrophage populations. *J. Leukoc. Biol.* **80**, 1298–1307 (2006).
  142. Stout, R. D. *et al.* Macrophages sequentially change their functional phenotype in response to changes in microenvironmental influences. *J Immunol* **175**, 342–349 (2005).
  143. Duffield, J. S. *et al.* Selective depletion of macrophages reveals distinct, opposing roles during liver injury and repair. *J. Clin. Invest.* **115**, 56–65 (2005).
  144. Goren, I. *et al.* A transgenic mouse model of inducible macrophage depletion: effects of diphtheria toxin-driven lysozyme M-specific cell lineage ablation on wound inflammatory, angiogenic, and contractive processes. *Am. J. Pathol.* **175**, 132–147 (2009).
  145. Van Gassen, N. *et al.* Macrophage dynamics are regulated by local macrophage proliferation and monocyte recruitment in injured pancreas. *Eur. J. Immunol.* **45**, 1482–1493 (2015).
  146. Van Gassen, N. *et al.* Concise Review: Macrophages: Versatile Gatekeepers During Pancreatic  $\beta$ -Cell Development, Injury, and Regeneration. *Stem Cells Translational Medicine* **4**, 555–563 (2015).
  147. Ino, K. *et al.* Monocytes infiltrate the pancreas via the MCP-1/CCR2 pathway and differentiate into stellate cells. *PLoS ONE* **9**, e84889 (2014).
  148. Shirey, K. A. *et al.* Role of the lipoxygenase pathway in RSV-induced alternatively activated macrophages leading to resolution of lung pathology. *Mucosal Immunol* **7**, 549–557 (2014).
  149. Folias, A. E., Penaranda, C., Su, A. L., Bluestone, J. A. & Hebrok, M. Aberrant innate immune activation following tissue injury impairs pancreatic regeneration. *PLoS ONE* **9**, e102125 (2014).
  150. Patrick, C. *et al.* Promotion of autoimmune diabetes by cereal diet in the presence or absence of microbes associated with gut immune activation, regulatory imbalance, and altered cathelicidin antimicrobial peptide. *Diabetes* **62**, 2036–2047 (2013).
  151. Calderon, B. *et al.* The pancreas anatomy conditions the origin and properties of resident macrophages. *J Exp Med* **212**, 1497–1512 (2015).
  152. Mathew, E. *et al.* The transcription factor GLI1 modulates the inflammatory response during pancreatic tissue remodeling. *J. Biol. Chem.* **289**, 27727–27743 (2014).
  153. Ndisang, J. F. & Mishra, M. The heme oxygenase system selectively suppresses the proinflammatory macrophage m1 phenotype and potentiates insulin signaling in spontaneously hypertensive rats. *Am. J. Hypertens.* **26**, 1123–1131 (2013).
  154. Van den Bossche, J. *et al.* Pivotal Advance: Arginase-1-independent polyamine production stimulates the expression of IL-4-induced alternatively activated macrophage markers while inhibiting LPS-induced expression of inflammatory genes. *J. Leukoc. Biol.* **91**, 685–699 (2012).
  155. Arnold, L. *et al.* Inflammatory monocytes recruited after skeletal muscle injury switch into antiinflammatory macrophages to support myogenesis. *J Exp Med* **204**, 1057–1069 (2007).
  156. Mokarram, N., Merchant, A., Mukhatyar, V., Patel, G. & Bellamkonda, R. V. Effect of modulating macrophage phenotype on peripheral nerve repair. *Biomaterials* **33**, 8793–8801 (2012).
  157. Hermano, E. *et al.* Macrophage polarization in pancreatic carcinoma: role of heparanase enzyme.

- J. Natl. Cancer Inst.* **106**, 699 (2014).
158. Chen, P. *et al.* Collagen VI regulates peripheral nerve regeneration by modulating macrophage recruitment and polarization. *Acta Neuropathol.* **129**, 97–113 (2015).
  159. Lavin, Y. *et al.* Tissue-Resident Macrophage Enhancer Landscapes Are Shaped by the Local Microenvironment. *Cell* **159**, 1312–1326 (2014).
  160. Xue, J. *et al.* Transcriptome-Based Network Analysis Reveals a Spectrum Model of Human Macrophage Activation. *Immunity* **40**, 274–288 (2014).
  161. Husseini, M. *et al.* Heme Oxygenase-1 Induction Prevents Autoimmune Diabetes in Association With Pancreatic Recruitment of M2-Like Macrophages, Mesenchymal Cells, and Fibrocytes. *Endocrinology* **156**, 3937–3949 (2015).
  162. He, H. *et al.* Endothelial cells provide an instructive niche for the differentiation and functional polarization of M2-like macrophages. *Blood* **120**, 3152–3162 (2012).
  163. Date, D. *et al.* Kruppel-like transcription factor 6 regulates inflammatory macrophage polarization. *J. Biol. Chem.* **289**, 10318–10329 (2014).
  164. Hashimoto, D. *et al.* Tissue-Resident Macrophages Self-Maintain Locally throughout Adult Life with Minimal Contribution from Circulating Monocytes. *Immunity* **38**, 792–804 (2013).
  165. Westwell-Roper, C. Y., Ehses, J. A. & Verchere, C. B. Resident macrophages mediate islet amyloid polypeptide-induced islet IL-1 $\beta$  production and  $\beta$ -cell dysfunction. *Diabetes* **63**, 1698–1711 (2014).
  166. Gautier, E. L. *et al.* Gene-expression profiles and transcriptional regulatory pathways that underlie the identity and diversity of mouse tissue macrophages. *Nature Immunology* **13**, 1118–1128 (2012).
  167. Kuziel, W. A. *et al.* Severe reduction in leukocyte adhesion and monocyte extravasation in mice deficient in CC chemokine receptor 2. *PNAS* **94**, 12053–12058 (1997).
  168. Goldszmid, R. S. *et al.* NK Cell-Derived Interferon- $\gamma$  Orchestrates Cellular Dynamics and the Differentiation of Monocytes into Dendritic Cells at the Site of Infection. *Immunity* **36**, 1047–1059 (2012).
  169. Gundra, U. M. *et al.* Alternatively activated macrophages derived from monocytes and tissue macrophages are phenotypically and functionally distinct. *Blood* **123**, e110–e122 (2014).
  170. Geutskens, S. B., Otonkoski, T., Pulkkinen, M.-A., Drexhage, H. A. & Leenen, P. J. M. Macrophages in the murine pancreas and their involvement in fetal endocrine development in vitro. *J. Leukoc. Biol.* **78**, 845–852 (2005).
  171. Wiktor-Jedrzejczak, W. *et al.* Total absence of colony-stimulating factor 1 in the macrophage-deficient osteopetrotic (op/op) mouse. *PNAS* **87**, 4828–4832 (1990).
  172. Banaei-Bouchareb, L. *et al.* Insulin cell mass is altered in Csf1op/Csf1op macrophage-deficient mice. *J. Leukoc. Biol.* **76**, 359–367 (2004).
  173. Chamson-Reig, A., Arany, E. J. & Hill, D. J. Lineage tracing and resulting phenotype of haemopoietic-derived cells in the pancreas during beta cell regeneration. *Diabetologia* **53**, 2188–2197 (2010).
  174. Nakamichi, I. *et al.* Hemin-activated macrophages home to the pancreas and protect from acute pancreatitis via heme oxygenase-1 induction. *J. Clin. Invest.* **115**, 3007–3014 (2005).
  175. Tessem, J. S. *et al.* Critical roles for macrophages in islet angiogenesis and maintenance during pancreatic degeneration. *Diabetes* **57**, 1605–1617 (2008).

176. Meng, J. *et al.* Accelerated regeneration of the skeletal muscle in RNF13-knockout mice is mediated by macrophage-secreted IL-4/IL-6. *Protein Cell* **5**, 235–247 (2014).
177. Sindrilaru, A. *et al.* An unrestrained proinflammatory M1 macrophage population induced by iron impairs wound healing in humans and mice. *The Journal of Clinical Investigation* **121**, 985–997 (2011).
178. Ruffell, D. *et al.* A CREB-C/EBPbeta cascade induces M2 macrophage-specific gene expression and promotes muscle injury repair. *PNAS* **106**, 17475–17480 (2009).
179. Robertson, T. A., Maley, M. A., Grounds, M. D. & Papadimitriou, J. M. The role of macrophages in skeletal muscle regeneration with particular reference to chemotaxis. *Experimental Cell Research* **207**, 321–331 (1993).
180. Zhang, L. *et al.* Chemokine CXCL16 Regulates Neutrophil and Macrophage Infiltration into Injured Muscle, Promoting Muscle Regeneration. *Am. J. Pathol.* **175**, 2518–2527 (2009).
181. Fallowfield, J. A. *et al.* Scar-associated macrophages are a major source of hepatic matrix metalloproteinase-13 and facilitate the resolution of murine hepatic fibrosis. *J Immunol* **178**, 5288–5295 (2007).
182. Thomas, J. A. *et al.* Macrophage therapy for murine liver fibrosis recruits host effector cells improving fibrosis, regeneration, and function. *Hepatology* **53**, 2003–2015 (2011).
183. Wang, Y. *et al.* Ex vivo programmed macrophages ameliorate experimental chronic inflammatory renal disease. *Kidney International* **72**, 290–299 (2007).
184. Salegio, E. A. A., Pollard, A. N., Smith, M. & Zhou, X.-F. Macrophage presence is essential for the regeneration of ascending afferent fibres following a conditioning sciatic nerve lesion in adult rats. *BMC Neuroscience* **12**, 11 (2011).
185. London, A. *et al.* Neuroprotection and progenitor cell renewal in the injured adult murine retina requires healing monocyte-derived macrophages. *J Exp Med* **208**, 23–39 (2011).
186. Cattin, A.-L. *et al.* Macrophage-Induced Blood Vessels Guide Schwann Cell-Mediated Regeneration of Peripheral Nerves. *Cell* **162**, 1127–1139 (2015).
187. Nicol, L. E. *et al.* Pancreatic inflammation and increased islet macrophages in insulin-resistant juvenile primates. *J Endocrinol* **217**, 207–213 (2013).
188. Ehses, J. A. *et al.* Increased number of islet-associated macrophages in type 2 diabetes. *Diabetes* **56**, 2356–2370 (2007).
189. Schulthess, F. T. *et al.* CXCL10 impairs beta cell function and viability in diabetes through TLR4 signaling. *Cell Metabolism* **9**, 125–139 (2009).
190. Eguchi, K. *et al.* Saturated Fatty Acid and TLR Signaling Link  $\beta$  Cell Dysfunction and Islet Inflammation. *Cell Metabolism* **15**, 518–533 (2012).
191. Kamata, K. *et al.* Islet amyloid with macrophage migration correlates with augmented  $\beta$ -cell deficits in type 2 diabetic patients. *Amyloid* **21**, 191–201 (2014).
192. Huang, S. *et al.* Saturated fatty acids activate TLR-mediated proinflammatory signaling pathways. *J. Lipid Res.* **53**, 2002–2013 (2012).
193. Böni-Schnetzler, M. *et al.* Free fatty acids induce a proinflammatory response in islets via the abundantly expressed interleukin-1 receptor I. *Endocrinology* **150**, 5218–5229 (2009).
194. Vives-Pi, M. *et al.* Evidence of expression of endotoxin receptors CD14, toll-like receptors TLR4 and TLR2 and associated molecule MD-2 and of sensitivity to endotoxin (LPS) in islet beta cells. *Clin. Exp. Immunol.* **133**, 208–218 (2003).

195. Dasu, M. R., Devaraj, S., Park, S. & Jialal, I. Increased toll-like receptor (TLR) activation and TLR ligands in recently diagnosed type 2 diabetic subjects. *Dia Care* **33**, 861–868 (2010).
196. Garay-Malpartida, H. M. *et al.* Toll-like receptor 4 (TLR4) expression in human and murine pancreatic beta-cells affects cell viability and insulin homeostasis. *BMC Immunol.* **12**, 18 (2011).
197. Pound, L. D. *et al.* Cathelicidin Antimicrobial Peptide: A Novel Regulator of Islet Function, Islet Regeneration, and Selected Gut Bacteria. *Diabetes* **64**, 4135–4147 (2015).
198. Lee, T.-S. & Chau, L.-Y. Heme oxygenase-1 mediates the anti-inflammatory effect of interleukin-10 in mice. *Nature Medicine* **8**, 240–246 (2002).
199. Higashimura, Y. *et al.* Preventive effect of agaro-oligosaccharides on non-steroidal anti-inflammatory drug-induced small intestinal injury in mice. *Journal of Gastroenterology and Hepatology* **29**, 310–317 (2014).
200. Sun, J. *et al.* Hemoprotein Bach1 regulates enhancer availability of heme oxygenase-1 gene. *EMBO J.* **21**, 5216–5224 (2002).
201. Brissova, M. *et al.* Islet microenvironment, modulated by vascular endothelial growth factor-A signaling, promotes  $\beta$  cell regeneration. *Cell Metabolism* **19**, 498–511 (2014).
202. Criscimanna, A., Coudriet, G. M., Gittes, G. K., Piganelli, J. D. & Esni, F. Activated macrophages create lineage-specific microenvironments for pancreatic acinar- and  $\beta$ -cell regeneration in mice. *Gastroenterology* **147**, 1106–18.e11 (2014).
203. Hogan, M. F. & Hull, R. L. The islet endothelial cell: a novel contributor to beta cell secretory dysfunction in diabetes. *Diabetologia* **60**, 952–959 (2017).
204. Olsson, R. & Carlsson, P. The pancreatic islet endothelial cell: Emerging roles in islet function and disease. *The International Journal of Biochemistry & Cell Biology* **38**, 492–497 (2006).
205. Peiris, H., Bonder, C. S., Coates, P. T. H., Keating, D. J. & Jessup, C. F. The  $\beta$ -cell/EC axis: how do islet cells talk to each other? *Diabetes* **63**, 3–11 (2014).
206. Kragl, M. & Lammert, E. in *The Islets of Langerhans* **654**, 217–234 (Springer Netherlands, 2010).
207. Huang, G. & Greenspan, D. S. ECM roles in the function of metabolic tissues. *Trends in Endocrinology & Metabolism* **23**, 16–22 (2012).
208. Nikolova, G. *et al.* The vascular basement membrane: a niche for insulin gene expression and Beta cell proliferation. *Dev. Cell* **10**, 397–405 (2006).
209. Hall-Glenn, F. *et al.* CCN2/connective tissue growth factor is essential for pericyte adhesion and endothelial basement membrane formation during angiogenesis. *PLoS ONE* **7**, e30562 (2012).
210. Crawford, L. A. *et al.* Connective tissue growth factor (CTGF) inactivation leads to defects in islet cell lineage allocation and beta-cell proliferation during embryogenesis. *Molecular Endocrinology* **23**, 324–336 (2009).
211. Crawford, S. E. *et al.* Thrombospondin-1 is a major activator of TGF-beta1 in vivo. *Cell* **93**, 1159–1170 (1998).
212. Olerud, J. *et al.* Thrombospondin-1: an islet endothelial cell signal of importance for  $\beta$ -cell function. *Diabetes* **60**, 1946–1954 (2011).
213. Gregersen, S., Thomsen, J. L., Brock, B. & Hermansen, K. Endothelin-1 stimulates insulin secretion by direct action on the islets of Langerhans in mice. *Diabetologia* **39**, 1030–1035 (1996).
214. De Carlo, E. *et al.* Endothelin-1 and endothelin-3 stimulate insulin release by isolated rat pancreatic islets. *J. Endocrinol. Invest.* **23**, 240–245 (2000).

215. Cifarelli, V. *et al.* FOXO1 mediates the autocrine effect of endothelin-1 on endothelial cell survival. *Mol. Endocrinol.* **26**, 1213–1224 (2012).
216. Szmitko, P. E. *et al.* New markers of inflammation and endothelial cell activation: Part I. *Circulation* **108**, 1917–1923 (2003).
217. van den Oever, I. A. M., Raterman, H. G., Nurmohamed, M. T. & Simsek, S. Endothelial dysfunction, inflammation, and apoptosis in diabetes mellitus. *Mediators of Inflammation* **2010**, 792393–15 (2010).
218. McKee, C. M. *et al.* Hyaluronan (HA) fragments induce chemokine gene expression in alveolar macrophages. The role of HA size and CD44. *J. Clin. Invest.* **98**, 2403–2413 (1996).
219. Arous, C., Ferreira, P. G., Dermitzakis, E. T. & Halban, P. A. Short term exposure of beta cells to low concentrations of interleukin-1 $\beta$  improves insulin secretion through focal adhesion and actin remodeling and regulation of gene expression. *J. Biol. Chem.* **290**, 6653–6669 (2015).
220. Butler, J. M. *et al.* Endothelial Cells Are Essential for the Self-Renewal and Repopulation of Notch-Dependent Hematopoietic Stem Cells. *Cell Stem Cell* **6**, 251–264 (2010).
221. Coussens, L. M. & Werb, Z. Inflammation and cancer. *Nature* **420**, 860–867 (2002).
222. Brissova, M. *et al.* Pancreatic islet production of vascular endothelial growth factor--a is essential for islet vascularization, revascularization, and function. *Diabetes* **55**, 2974–2985 (2006).
223. Lammert, E. *et al.* Role of VEGF-A in vascularization of pancreatic islets. *Curr. Biol.* **13**, 1070–1074 (2003).
224. Fulton, D. *et al.* Regulation of endothelium-derived nitric oxide production by the protein kinase Akt. *Nature* **399**, 597–601 (1999).
225. Gerber, H. P. *et al.* Vascular endothelial growth factor regulates endothelial cell survival through the phosphatidylinositol 3'-kinase/Akt signal transduction pathway. Requirement for Flk-1/KDR activation. *Journal of Biological Chemistry* **273**, 30336–30343 (1998).
226. Mazure, N. M., Chen, E. Y., Laderoute, K. R. & Giaccia, A. J. Induction of vascular endothelial growth factor by hypoxia is modulated by a phosphatidylinositol 3-kinase/Akt signaling pathway in Ha-ras-transformed cells through a hypoxia inducible factor-1 transcriptional element. *Blood* **90**, 3322–3331 (1997).
227. Rousseau, S., Houle, F., Landry, J. & Huot, J. p38 MAP kinase activation by vascular endothelial growth factor mediates actin reorganization and cell migration in human endothelial cells. *Oncogene* **15**, 2169–2177 (1997).
228. Holmes, K., Roberts, O. L., Thomas, A. M. & Cross, M. J. Vascular endothelial growth factor receptor-2: Structure, function, intracellular signalling and therapeutic inhibition. *Cellular Signalling* **19**, 2003–2012 (2007).
229. Ferrara, N., Gerber, H.-P. & LeCouter, J. The biology of VEGF and its receptors. *Nature Medicine* **9**, 669–676 (2003).
230. Matsumoto, K. & Ema, M. Roles of VEGF-A signalling in development, regeneration, and tumours. *J. Biochem.* **156**, 1–10 (2014).
231. Joško, J. & Mazurek, M. Transcription factors having impact on vascular endothelial growth factor (VEGF) gene expression in angiogenesis. *Med Sci Monit* **10**, RA89–98 (2004).
232. Vasir, B. *et al.* Hypoxia induces vascular endothelial growth factor gene and protein expression in cultured rat islet cells. *Diabetes* **47**, 1894–1903 (1998).
233. Narayanan, S. *et al.* Intra-islet endothelial cell and  $\beta$ -cell crosstalk: Implication for islet cell

- transplantation. *WJT* **7**, 117–12 (2017).
234. Olsson, A.-K., Dimberg, A., Kreuger, J. & Claesson-Welsh, L. VEGF receptor signalling - in control of vascular function. *Nat. Rev. Mol. Cell Biol.* **7**, 359–371 (2006).
  235. Simons, M., Gordon, E. & Claesson-Welsh, L. Mechanisms and regulation of endothelial VEGF receptor signalling. *Nat. Rev. Mol. Cell Biol.* **17**, 611–625 (2016).
  236. Ivarez-Aznar, A., Muhl, L. & Gaengel, K. in *Current Topics in Developmental Biology* **123**, 433–482 (Elsevier Inc., 2017).
  237. Koch, S. & Claesson-Welsh, L. Signal Transduction by Vascular Endothelial Growth Factor Receptors. *Cold Spring Harbor Perspectives in Medicine* **2**, a006502–a006502 (2012).
  238. Christofori, G., Naik, P. & Hanahan, D. Vascular endothelial growth factor and its receptors, flt-1 and flk-1, are expressed in normal pancreatic islets and throughout islet cell tumorigenesis. *Molecular Endocrinology* **9**, 1760–1770 (1995).
  239. Roberts, D. M. *et al.* The vascular endothelial growth factor (VEGF) receptor Flt-1 (VEGFR-1) modulates Flk-1 (VEGFR-2) signaling during blood vessel formation. *Am. J. Pathol.* **164**, 1531–1535 (2004).
  240. Ferrara, N. *et al.* Heterozygous embryonic lethality induced by targeted inactivation of the VEGF gene. *Nature* **380**, 439–442 (1996).
  241. Carmeliet, P. *et al.* Abnormal blood vessel development and lethality in embryos lacking a single VEGF allele. *Nature* **380**, 435–439 (1996).
  242. Fukuhara, S. *et al.* Differential function of Tie2 at cell-cell contacts and cell-substratum contacts regulated by angiopoietin-1. *Nat. Cell Biol.* **10**, 513–526 (2008).
  243. Su, D. *et al.* Angiopoietin-1 production in islets improves islet engraftment and protects islets from cytokine-induced apoptosis. *Diabetes* **56**, 2274–2283 (2007).
  244. Pierreux, C. E. *et al.* Epithelial: Endothelial cross-talk regulates exocrine differentiation in developing pancreas. *Developmental Biology* **347**, 216–227 (2010).
  245. Guney, M. A. & Gannon, M. Pancreas Cell Fate. *Birth Defects Res. C Embryo Today* **87**, 232–248 (2009).
  246. Reinert, R. B. *et al.* Vascular endothelial growth factor-a and islet vascularization are necessary in developing, but not adult, pancreatic islets. *Diabetes* **62**, 4154–4164 (2013).
  247. Yoshitomi, H. & Zaret, K. S. Endothelial cell interactions initiate dorsal pancreas development by selectively inducing the transcription factor Ptf1a. *Development* **131**, 807–817 (2004).
  248. Lammert, E., Cleaver, O. & Melton, D. Induction of pancreatic differentiation by signals from blood vessels. *Science* **294**, 564–567 (2001).
  249. Guney, M. A. *et al.* Connective tissue growth factor acts within both endothelial cells and beta cells to promote proliferation of developing beta cells. *PNAS* **108**, 15242–15247 (2011).
  250. Jabs, N. *et al.* Reduced insulin secretion and content in VEGF-a deficient mouse pancreatic islets. *Exp. Clin. Endocrinol. Diabetes* **116 Suppl 1**, S46–9 (2008).
  251. Cai, Q. *et al.* Enhanced expression of VEGF-A in  $\beta$  cells increases endothelial cell number but impairs islet morphogenesis and  $\beta$  cell proliferation. *Developmental Biology* **367**, 40–54 (2012).
  252. D'Hoker, J. *et al.* Conditional hypovascularization and hypoxia in islets do not overtly influence adult  $\beta$ -cell mass or function. *Diabetes* **62**, 4165–4173 (2013).
  253. Iwashita, N. *et al.* Impaired insulin secretion in vivo but enhanced insulin secretion from isolated islets in pancreatic beta cell-specific vascular endothelial growth factor-A knock-out mice.

- Diabetologia* **50**, 380–389 (2007).
254. Feng, Z.-C. *et al.* c-Kit Receptor Signaling Regulates Islet Vasculature,  $\beta$ -Cell Survival, and Function In Vivo. *Diabetes* **64**, 3852–3866 (2015).
  255. De Leu, N. *et al.* Short-term overexpression of VEGF-A in mouse beta cells indirectly stimulates their proliferation and protects against diabetes. *Diabetologia* **57**, 140–147 (2014).
  256. Almaça, J. *et al.* Young capillary vessels rejuvenate aged pancreatic islets. *PNAS* **111**, 17612–17617 (2014).
  257. Wan, X. *et al.* Recovery from overt type 1 diabetes ensues when immune tolerance and  $\beta$ -cell formation are coupled with regeneration of endothelial cells in the pancreatic islets. *Diabetes* **62**, 2879–2889 (2013).
  258. Villalta, S. A. *et al.* Inhibition of VEGFR-2 reverses type 1 diabetes in NOD mice by abrogating insulinitis and restoring islet function. *Diabetes* **62**, 2870–2878 (2013).
  259. Tang, S.-C., Chiu, Y.-C., Hsu, C.-T., Peng, S.-J. & Fu, Y.-Y. Plasticity of Schwann cells and pericytes in response to islet injury in mice. *Diabetologia* **56**, 2424–2434 (2013).
  260. Shah, P. *et al.* Angiopoietin-2 Signals Do Not Mediate the Hypervascularization of Islets in Type 2 Diabetes. *PLoS ONE* **11**, e0161834 (2016).
  261. Hogan, M. F. *et al.* Markers of Islet Endothelial Dysfunction Occur in Male B6.BKS(D)-Leprdb/J Mice and May Contribute to Reduced Insulin Release. *Endocrinology* **158**, 293–303 (2017).
  262. Nakamura, M. *et al.* The endocrine pancreas of spontaneously diabetic mice: microangiopathy as revealed by transmission electron microscopy. *Diabetes Research and Clinical Practice* **30**, 89–100 (1995).
  263. Agudo, J. *et al.* Vascular endothelial growth factor-mediated islet hypervascularization and inflammation contribute to progressive reduction of  $\beta$ -cell mass. *Diabetes* **61**, 2851–2861 (2012).
  264. Dai, C., Brissova, M., Reinert, R. B., Nyman, L. & Liu, E. H. Pancreatic islet vasculature adapts to insulin resistance through dilation and not angiogenesis. *Diabetes* (2013). doi:10.2337/db12-1657/-/DC1
  265. Brissova, M. *et al.* Intra-islet endothelial cells contribute to revascularization of transplanted pancreatic islets. *Diabetes* **53**, 1318–1325 (2004).
  266. Carlsson, P. O., Palm, F., Andersson, A. & Liss, P. Markedly decreased oxygen tension in transplanted rat pancreatic islets irrespective of the implantation site. *Diabetes* **50**, 489–495 (2001).
  267. Mattsson, G., Jansson, L. & Carlsson, P.-O. Decreased vascular density in mouse pancreatic islets after transplantation. *Diabetes* **51**, 1362–1366 (2002).
  268. Kaufman-Francis, K., Koffler, J., Weinberg, N., Dor, Y. & Levenberg, S. Engineered vascular beds provide key signals to pancreatic hormone-producing cells. *PLoS ONE* **7**, e40741 (2012).
  269. Phelps, E. A., Templeman, K. L., Thulé, P. M. & García, A. J. Engineered VEGF-releasing PEG-MAL hydrogel for pancreatic islet vascularization. *Drug Deliv Transl Res* **5**, 125–136 (2015).
  270. Davis, N. E. *et al.* Enhanced function of pancreatic islets co-encapsulated with ECM proteins and mesenchymal stromal cells in a silk hydrogel. *Biomaterials* **33**, 6691–6697 (2012).
  271. Zhang, N. *et al.* Elevated vascular endothelial growth factor production in islets improves islet graft vascularization. *Diabetes* **53**, 963–970 (2004).
  272. Narang, A. S. *et al.* Vascular endothelial growth factor gene delivery for revascularization in transplanted human islets. *Pharm. Res.* **21**, 15–25 (2004).

273. Lai, Y. *et al.* Vascular endothelial growth factor increases functional beta-cell mass by improvement of angiogenesis of isolated human and murine pancreatic islets. *Transplantation* **79**, 1530–1536 (2005).
274. Olerud, J., Johansson, M., Lawler, J., Welsh, N. & Carlsson, P.-O. Improved vascular engraftment and graft function after inhibition of the angiostatic factor thrombospondin-1 in mouse pancreatic islets. *Diabetes* **57**, 1870–1877 (2008).
275. Johansson, U. *et al.* Formation of composite endothelial cell-mesenchymal stem cell islets: a novel approach to promote islet revascularization. *Diabetes* **57**, 2393–2401 (2008).
276. Ding, B.-S. *et al.* Inductive angiocrine signals from sinusoidal endothelium are required for liver regeneration. *Nature* **468**, 310–315 (2010).
277. Ding, B.-S. *et al.* Endothelial-derived angiocrine signals induce and sustain regenerative lung alveolarization. *Cell* **147**, 539–553 (2011).
278. Barleon, B. *et al.* Migration of human monocytes in response to vascular endothelial growth factor (VEGF) is mediated via the VEGF receptor flt-1. *Blood* **87**, 3336–3343 (1996).
279. Sawano, A. *et al.* Flt-1, vascular endothelial growth factor receptor 1, is a novel cell surface marker for the lineage of monocyte-macrophages in humans. *Blood* **97**, 785–791 (2001).
280. Butler, J. M., Kobayashi, H. & Rafii, S. Instructive role of the vascular niche in promoting tumour growth and tissue repair by angiocrine factors. *Nat. Rev. Cancer* **10**, 138–146 (2010).
281. Bogdani, M. Thinking Outside the Cell: A Key Role for Hyaluronan in the Pathogenesis of Human Type 1 Diabetes. *Diabetes* **65**, 2105–2114 (2016).
282. Hynes, R. O. The extracellular matrix: not just pretty fibrils. *Science* **326**, 1216–1219 (2009).
283. Sorokin, L. The impact of the extracellular matrix on inflammation. *Nat. Rev. Immunol.* **10**, 712–723 (2010).
284. Virtanen, I. *et al.* Blood vessels of human islets of Langerhans are surrounded by a double basement membrane. *Diabetologia* **51**, 1181–1191 (2008).
285. Takahashi, I. *et al.* Important role of heparan sulfate in postnatal islet growth and insulin secretion. *Biochemical and Biophysical Research Communications* **383**, 113–118 (2009).
286. Ziolkowski, A. F., Popp, S. K., Freeman, C., Parish, C. R. & Simeonovic, C. J. Heparan sulfate and heparanase play key roles in mouse  $\beta$  cell survival and autoimmune diabetes. *J. Clin. Invest.* **122**, 132–141 (2012).
287. Potter, K. J. *et al.* Amyloid Formation in Human Islets Is Enhanced by Heparin and Inhibited by Heparinase. *American Journal of Transplantation* **15**, 1519–1530 (2015).
288. Bogdani, M. *et al.* Hyaluronan and hyaluronan-binding proteins accumulate in both human type 1 diabetic islets and lymphoid tissues and associate with inflammatory cells in insulinitis. *Diabetes* **63**, 2727–2743 (2014).
289. Arous, C. & Wehrle-Haller, B. Role and impact of the extracellular matrix on integrin-mediated pancreatic  $\beta$ -cell functions. *Biol. Cell* **109**, 223–237 (2017).
290. Kaido, T., Yebra, M., Cirulli, V. & Montgomery, A. M. Regulation of human beta-cell adhesion, motility, and insulin secretion by collagen IV and its receptor  $\alpha 1\beta 1$ . *Journal of Biological Chemistry* **279**, 53762–53769 (2004).
291. Yebra, M. *et al.* Endothelium-derived Netrin-4 supports pancreatic epithelial cell adhesion and differentiation through integrins  $\alpha 2\beta 1$  and  $\alpha 3\beta 1$ . *PLoS ONE* **6**, e22750 (2011).
292. Weathington, N. M. *et al.* A novel peptide CXCR ligand derived from extracellular matrix



- degradation during airway inflammation. *Nature Medicine* **12**, 317–323 (2006).
293. Beattie, G. M., Rubin, J. S., Mally, M. I., Otonkoski, T. & Hayek, A. Regulation of proliferation and differentiation of human fetal pancreatic islet cells by extracellular matrix, hepatocyte growth factor, and cell-cell contact. *Diabetes* **45**, 1223–1228 (1996).
  294. Han, B., Qi, S., Hu, B., Luo, H. & Wu, J. TGF- $\beta$ 1 promotes islet beta-cell function and regeneration. *J Immunol* **186**, 5833–5844 (2011).
  295. Gan, W. J. *et al.* Cell polarity defines three distinct domains in pancreatic  $\beta$ -cells. *J Cell Sci* **130**, 143–151 (2017).
  296. Jiang, F. X., Cram, D. S., DeAizpurua, H. J. & Harrison, L. C. Laminin-1 promotes differentiation of fetal mouse pancreatic beta-cells. *Diabetes* **48**, 722–730 (1999).
  297. Ghazalli, N. *et al.* Postnatal Pancreas of Mice Contains Tripotent Progenitors Capable of Giving Rise to Duct, Acinar, and Endocrine Cells In Vitro. *Stem Cells Dev.* **24**, 1995–2008 (2015).
  298. Banerjee, M., Virtanen, I., Palgi, J., Korsgren, O. & Otonkoski, T. Proliferation and plasticity of human beta cells on physiologically occurring laminin isoforms. *Molecular and Cellular Endocrinology* **355**, 78–86 (2012).
  299. Lin, H.-Y. *et al.* Fibronectin and laminin promote differentiation of human mesenchymal stem cells into insulin producing cells through activating Akt and ERK. *J. Biomed. Sci.* **17**, 56 (2010).
  300. Cirulli, V. *et al.* Expression and function of  $\alpha$ (v) $\beta$ (3) and  $\alpha$ (v) $\beta$ (5) integrins in the developing pancreas: roles in the adhesion and migration of putative endocrine progenitor cells. *J. Cell Biol.* **150**, 1445–1460 (2000).
  301. Diaferia, G. R. *et al.*  $\beta$ 1 integrin is a crucial regulator of pancreatic  $\beta$ -cell expansion. *Development* **140**, 3360–3372 (2013).
  302. Bosco, D., Meda, P., Halban, P. A. & Rouiller, D. G. Importance of cell-matrix interactions in rat islet beta-cell secretion in vitro: role of  $\alpha$ 6 $\beta$ 1 integrin. *Diabetes* **49**, 233–243 (2000).
  303. Weber, L. M. & Anseth, K. S. Hydrogel encapsulation environments functionalized with extracellular matrix interactions increase islet insulin secretion. *Matrix Biol.* **27**, 667–673 (2008).
  304. Rondas, D., Tomas, A. & Halban, P. A. Focal adhesion remodeling is crucial for glucose-stimulated insulin secretion and involves activation of focal adhesion kinase and paxillin. *Diabetes* **60**, 1146–1157 (2011).
  305. Hammar, E. *et al.* Extracellular matrix protects pancreatic beta-cells against apoptosis: role of short- and long-term signaling pathways. *Diabetes* **53**, 2034–2041 (2004).
  306. Riopel, M., Stuart, W. & Wang, R. Fibrin improves beta (INS-1) cell function, proliferation and survival through integrin  $\alpha$ v $\beta$ 3. *Acta Biomater* **9**, 8140–8148 (2013).
  307. Llacua, L. A., Faas, M. M. & de Vos, P. Extracellular matrix molecules and their potential contribution to the function of transplanted pancreatic islets. *Diabetologia* **14**, 552–12 (2018).
  308. Parnaud, G. *et al.* Blockade of  $\beta$ 1 integrin-laminin-5 interaction affects spreading and insulin secretion of rat beta-cells attached on extracellular matrix. *Diabetes* **55**, 1413–1420 (2006).
  309. Krishnamurthy, M., Li, J., Al-Masri, M. & Wang, R. Expression and function of  $\alpha$ 6 $\beta$ 1 integrins in pancreatic beta (INS-1) cells. *J Cell Commun Signal* **2**, 67–79 (2008).
  310. Geutskens, S. B. *et al.* Extracellular matrix distribution and islet morphology in the early postnatal pancreas: anomalies in the non-obese diabetic mouse. *Cell Tissue Res* **318**, 579–589 (2004).
  311. Evanko, S. P., Potter-Perigo, S., Bollyky, P. L., Nepom, G. T. & Wight, T. N. Hyaluronan and versican in the control of human T-lymphocyte adhesion and migration. *Matrix Biol.* **31**, 90–100

(2012).

312. Hayden, M. R. *et al.* Attenuation of endocrine-exocrine pancreatic communication in type 2 diabetes: pancreatic extracellular matrix ultrastructural abnormalities. *J Cardiometab Syndr* **3**, 234–243 (2008).
313. Miller, C. G., Pozzi, A., Zent, R. & Schwarzbauer, J. E. Effects of high glucose on integrin activity and fibronectin matrix assembly by mesangial cells. *Mol. Biol. Cell* **25**, 2342–2350 (2014).
314. Tsuchiya, H. *et al.* Extracellular Matrix and Growth Factors Improve the Efficacy of Intramuscular Islet Transplantation. *PLoS ONE* **10**, e0140910 (2015).
315. Smink, A. M. *et al.* Stimulation of vascularization of a subcutaneous scaffold applicable for pancreatic islet-transplantation enhances immediate post-transplant islet graft function but not long-term normoglycemia. *J Biomed Mater Res A* **105**, 2533–2542 (2017).
316. Meier, J. J. *et al.* Beta-cell replication is the primary mechanism subserving the postnatal expansion of beta-cell mass in humans. *Diabetes* **57**, 1584–1594 (2008).
317. Köhler, C. U. *et al.* Cell cycle control of  $\beta$ -cell replication in the prenatal and postnatal human pancreas. *American Journal of Physiology - Endocrinology and Metabolism* **300**, E221–30 (2011).
318. Kassem, S. A., Ariel, I., Thornton, P. S., Scheimberg, I. & Glaser, B. Beta-cell proliferation and apoptosis in the developing normal human pancreas and in hyperinsulinism of infancy. *Diabetes* **49**, 1325–1333 (2000).
319. Cogger, K. F. *et al.* Glycoprotein 2 is a specific cell surface marker of human pancreatic progenitors. *Nat Commun* **8**, 331 (2017).
320. Brissova, M. *et al.* a Cell Function and Gene Expression Are Compromised in Type 1 Diabetes. *Cell Reports* **22**, 1–11 (2018).
321. Okabe, K. *et al.* Neurons limit angiogenesis by titrating VEGF in retina. *Cell* **159**, 584–596 (2014).
322. Shultz, L. D. *et al.* Human lymphoid and myeloid cell development in NOD/LtSz-scid IL2R gamma null mice engrafted with mobilized human hemopoietic stem cells. *J Immunol* **174**, 6477–6489 (2005).
323. Milo-Landesman, D. *et al.* Correction of hyperglycemia in diabetic mice transplanted with reversibly immortalized pancreatic beta cells controlled by the tet-on regulatory system. *Cell Transplant* **10**, 645–650 (2001).
324. Efrat, S., Fusco-DeMane, D., Lemberg, H., Emran, al, O. & Wang, X. Conditional transformation of a pancreatic beta-cell line derived from transgenic mice expressing a tetracycline-regulated oncogene. *PNAS* **92**, 3576–3580 (1995).
325. Ohno-Matsui, K. *et al.* Inducible expression of vascular endothelial growth factor in adult mice causes severe proliferative retinopathy and retinal detachment. *Am. J. Pathol.* **160**, 711–719 (2002).
326. Hooper, A. T. *et al.* Engraftment and reconstitution of hematopoiesis is dependent on VEGFR2-mediated regeneration of sinusoidal endothelial cells. *Cell Stem Cell* **4**, 263–274 (2009).
327. Balamurugan, A. N., Chang, Y., Fung, J. J., Trucco, M. & Bottino, R. Flexible management of enzymatic digestion improves human islet isolation outcome from sub-optimal donor pancreata. *Am. J. Transplant.* **3**, 1135–1142 (2003).
328. Kayton, N. S. *et al.* Human islet preparations distributed for research exhibit a variety of insulin-secretory profiles. *American Journal of Physiology - Endocrinology and Metabolism* **308**, E592–602 (2015).

329. Aamodt, K. I. *et al.* Development of a reliable automated screening system to identify small molecules and biologics that promote human  $\beta$ -cell regeneration. *American Journal of Physiology - Endocrinology and Metabolism* **311**, E859–E868 (2016).
330. Dorrell, C. *et al.* Transcriptomes of the major human pancreatic cell types. *Diabetologia* **54**, 2832–2844 (2011).
331. Malone, J. H. & Oliver, B. Microarrays, deep sequencing and the true measure of the transcriptome. *BMC Biol.* **9**, 34 (2011).
332. Trapnell, C., Pachter, L. & Salzberg, S. L. TopHat: discovering splice junctions with RNA-Seq. *Bioinformatics* **25**, 1105–1111 (2009).
333. Dillies, M.-A. *et al.* A comprehensive evaluation of normalization methods for Illumina high-throughput RNA sequencing data analysis. *Brief. Bioinformatics* **14**, 671–683 (2013).
334. Robinson, M. D. & Oshlack, A. A scaling normalization method for differential expression analysis of RNA-seq data. *Genome Biol.* **11**, R25 (2010).
335. Benjamini, Y. & Hochberg, Y. Controlling the False Discovery Rate: A Practical and Powerful Approach to Multiple Testing. *Journal of the Royal Statistical Society, Series B Methodological* **57**, 289–300 (1995).
336. Huang, D. W. *et al.* Extracting biological meaning from large gene lists with DAVID. *Curr Protoc Bioinformatics* **Chapter 13**, Unit 13.11–13.11.13 (2009).
337. Abdulreda, M. H., Caicedo, A. & Berggren, P.-O. Transplantation into the anterior chamber of the eye for longitudinal, non-invasive in vivo imaging with single-cell resolution in real-time. *J Vis Exp* e50466 (2013). doi:10.3791/50466
338. Speier, S. *et al.* Noninvasive high-resolution in vivo imaging of cell biology in the anterior chamber of the mouse eye. *Nat Protoc* **3**, 1278–1286 (2008).
339. Speier, S. *et al.* Noninvasive in vivo imaging of pancreatic islet cell biology. *Nature Medicine* **14**, 574–578 (2008).
340. Liou, G.-Y. *et al.* Macrophage-secreted cytokines drive pancreatic acinar-to-ductal metaplasia through NF- $\kappa$ B and MMPs. *J. Cell Biol.* **202**, 563–577 (2013).
341. Hart, A. W., Baeza, N., Apelqvist, A. & Edlund, H. Attenuation of FGF signalling in mouse beta-cells leads to diabetes. *Nature* **408**, 864–868 (2000).
342. George, M. *et al.* Beta cell expression of IGF-I leads to recovery from type 1 diabetes. *J. Clin. Invest.* **109**, 1153–1163 (2002).
343. Chen, H. *et al.* PDGF signalling controls age-dependent proliferation in pancreatic  $\beta$ -cells. *Nature* **478**, 349–355 (2011).
344. Wogensen, L., Huang, X. & Sarvetnick, N. Leukocyte extravasation into the pancreatic tissue in transgenic mice expressing interleukin 10 in the islets of Langerhans. *Journal of Experimental Medicine* **178**, 175–185 (1993).
345. Huo, Y., Hafezi-Moghadam, A. & Ley, K. Role of vascular cell adhesion molecule-1 and fibronectin connecting segment-1 in monocyte rolling and adhesion on early atherosclerotic lesions. *Circulation Research* **87**, 153–159 (2000).
346. Wang, N., Liang, H. & Zen, K. Molecular mechanisms that influence the macrophage m1-m2 polarization balance. *Frontiers in Immunology* **5**, 614 (2014).
347. Manesso, E. *et al.* Dynamics of beta-cell turnover: evidence for beta-cell turnover and regeneration from sources of beta-cells other than beta-cell replication in the HIP rat. *American*

*Journal of Physiology - Endocrinology and Metabolism* **297**, E323–30 (2009).

348. Rankin, M. M. & Kushner, J. A. Aging induces a distinct gene expression program in mouse islets. *Islets* **2**, 345–352 (2010).
349. Hart, N. J. *et al.* Age-related Changes in Islet Cell Composition, Proliferation, and Mass in Human Pancreas. *American Diabetes Association Scientific Sessions* (2014).
350. Carboneau, B. A., Le, T. D. V., Dunn, J. C. & Gannon, M. Unexpected effects of the MIP-CreER transgene and tamoxifen on  $\beta$ -cell growth in C57Bl6/J male mice. *Physiol Rep* **4**, e12863 (2016).
351. Weitz, J. R. *et al.* Mouse pancreatic islet macrophages use locally released ATP to monitor beta cell activity. *Diabetologia* **61**, 182–192 (2018).
352. Savill, J., Dransfield, I., Gregory, C. & Haslett, C. A blast from the past: clearance of apoptotic cells regulates immune responses. *Nat. Rev. Immunol.* **2**, 965–975 (2002).
353. Cao, X., Han, Z.-B., Zhao, H. & Liu, Q. Transplantation of mesenchymal stem cells recruits trophic macrophages to induce pancreatic beta cell regeneration in diabetic mice. *The International Journal of Biochemistry & Cell Biology* **53**, 372–379 (2014).
354. Kelly, O. G. *et al.* Cell-surface markers for the isolation of pancreatic cell types derived from human embryonic stem cells. *Nat. Biotechnol.* **29**, 750–756 (2011).
355. Nostro, M. C. *et al.* Efficient Generation of NKX6-1+ Pancreatic Progenitors from Multiple Human Pluripotent Stem Cell Lines. *Stem Cell Reports* **4**, 591–604 (2015).
356. Blodgett, D. M. *et al.* Novel Observations From Next-Generation RNA Sequencing of Highly Purified Human Adult and Fetal Islet Cell Subsets. *Diabetes* **64**, 3172–3181 (2015).
357. Parnaud, G. *et al.* Proliferation of sorted human and rat beta cells. *Diabetologia* **51**, 91–100 (2008).
358. Laurent, D. *et al.* Pancreatic  $\beta$ -cell imaging in humans: fiction or option? *Diabetes Obes Metab* **18**, 6–15 (2015).
359. Sweet, I. R. *et al.* Systematic screening of potential  $\beta$ -cell imaging agents. *Biochemical and Biophysical Research Communications* **314**, 976–983 (2004).
360. Olafsen, T. & Wu, A. M. Antibody Vectors for Imaging. *YSNUC* **40**, 167–181 (2010).
361. Syed, S. K. *et al.* Ectonucleotidase NTPDase3 is abundant in pancreatic  $\beta$ -cells and regulates glucose-induced insulin secretion. *American Journal of Physiology - Endocrinology and Metabolism* **305**, E1319–26 (2013).
362. Lavoie, E. G. *et al.* Identification of the ectonucleotidases expressed in mouse, rat, and human Langerhans islets: potential role of NTPDase3 in insulin secretion. *American Journal of Physiology - Endocrinology and Metabolism* **299**, E647–56 (2010).
363. Petit, P., Lajoix, A.-D. & Gross, R. P2 purinergic signalling in the pancreatic  $\beta$ -cell: Control of insulin secretion and pharmacology. *European Journal of Pharmaceutical Sciences* **37**, 67–75 (2009).
364. Schaffer, A. E., Freude, K. K., Nelson, S. B. & Sander, M. Nkx6 Transcription Factors and Ptf1a Function as Antagonistic Lineage Determinants in Multipotent Pancreatic Progenitors. *Dev. Cell* **18**, 1022–1029 (2010).
365. Zhou, Q. *et al.* A multipotent progenitor domain guides pancreatic organogenesis. *Dev. Cell* **13**, 103–114 (2007).
366. Munkonda, M. N. *et al.* Characterization of a monoclonal antibody as the first specific inhibitor of human NTP diphosphohydrolase-3. *FEBS Journal* **276**, 479–496 (2009).

367. Dorrell, C. *et al.* Isolation of major pancreatic cell types and long-term culture-initiating cells using novel human surface markers. *Stem Cell Research* **1**, 183–194 (2008).
368. Piccand, J. *et al.* Rfx6 maintains the functional identity of adult pancreatic  $\beta$  cells. *Cell Reports* **9**, 2219–2232 (2014).
369. Smith, S. B. *et al.* Rfx6 directs islet formation and insulin production in mice and humans. *Nature* **463**, 775–780 (2010).
370. Chandra, V. *et al.* RFX6 regulates insulin secretion by modulating  $\text{Ca}^{2+}$  homeostasis in human  $\beta$  cells. *Cell Reports* **9**, 2206–2218 (2014).
371. Guo, S. *et al.* Inactivation of specific  $\beta$  cell transcription factors in type 2 diabetes. *J. Clin. Invest.* **123**, 3305–3316 (2013).
372. Butler, A. E. *et al.* Beta cell nuclear musculoaponeurotic fibrosarcoma oncogene family A (MafA) is deficient in type 2 diabetes. *Diabetologia* **55**, 2985–2988 (2012).
373. Spijker, H. S. *et al.* Loss of  $\beta$ -cell identity occurs in type 2 diabetes and is associated with islet amyloid deposits. *Diabetes* **64**, db141752–2938 (2015).
374. Lawlor, N. *et al.* Single-cell transcriptomes identify human islet cell signatures and reveal cell-type-specific expression changes in type 2 diabetes. *Genome Res.* **27**, 208–222 (2017).
375. Hawkins, T. A., Gala, R. R. & Dunbar, J. C. The lymphocyte and macrophage profile in the pancreas and spleen of nod mice: percentage of interleukin-2 and prolactin receptors on immunocompetent cell subsets. *Journal of Reproductive Immunology* **32**, 55–71 (1996).
376. Sharma, R. B. *et al.* Insulin demand regulates  $\beta$  cell number via the unfolded protein response. *J. Clin. Invest.* **125**, 3831–3846 (2015).
377. Gu, G., Dubauskaite, J. & Melton, D. A. Direct evidence for the pancreatic lineage: NGN3+ cells are islet progenitors and are distinct from duct progenitors. *Development* **129**, 2447–2457 (2002).
378. Dorrell, C. *et al.* Human islets contain four distinct subtypes of  $\beta$  cells. *Nat Commun* **7**, 11756 (2016).
379. Khan, S. *et al.* Autocrine activation of P2Y1 receptors couples  $\text{Ca}^{2+}$  influx to  $\text{Ca}^{2+}$  release in human pancreatic beta cells. *Diabetologia* **57**, 2535–2545 (2014).
380. Wuttke, A., Idevall-Hagren, O. & Tengholm, A. P2Y<sub>1</sub> receptor-dependent diacylglycerol signaling microdomains in  $\beta$  cells promote insulin secretion. *FASEB J* **27**, 1610–1620 (2013).
381. Silva, A. M. *et al.* Electrophysiological and immunocytochemical evidence for P2X purinergic receptors in pancreatic beta cells. *Pancreas* **36**, 279–283 (2008).
382. Coutinho-Silva, R., Parsons, M., Robson, T. & Burnstock, G. Changes in expression of P2 receptors in rat and mouse pancreas during development and ageing. *Cell Tissue Res* **306**, 373–383 (2001).
383. Coutinho-Silva, R., Parsons, M., Robson, T., Lincoln, J. & Burnstock, G. P2X and P2Y purinoceptor expression in pancreas from streptozotocin-diabetic rats. *Molecular and Cellular Endocrinology* **204**, 141–154 (2003).
384. Haque, A., Engel, J., Teichmann, S. A. & Lönnberg, T. A practical guide to single-cell RNA-sequencing for biomedical research and clinical applications. *Genome Med* **9**, 1–12 (2017).
385. Liu, S. & Trapnell, C. Single-cell transcriptome sequencing: recent advances and remaining challenges. *F1000Res* **5**, 1–9 (2016).
386. Segerstolpe, Å. *et al.* Single-Cell Transcriptome Profiling of Human Pancreatic Islets in Health and Type 2 Diabetes. *Cell Metabolism* **24**, 593–607 (2016).

387. Enge, M. *et al.* Single-Cell Analysis of Human Pancreas Reveals Transcriptional Signatures of Aging and Somatic Mutation Patterns. *Cell* **171**, 321–330.e14 (2017).
388. Eriksson, O. *et al.* In vivo imaging of beta cells with radiotracers: state of the art, prospects and recommendations for development and use. *Diabetologia* **59**, 1340–1349 (2016).
389. Stout, R. D., Watkins, S. K. & Suttles, J. Functional plasticity of macrophages: in situ reprogramming of tumor-associated macrophages. *J. Leukoc. Biol.* **86**, 1105–1109 (2009).
390. Porta, C., Riboldi, E., Ippolito, A. & Sica, A. Molecular and epigenetic basis of macrophage polarized activation. *Seminars in Immunology* (2015). doi:10.1016/j.smim.2015.10.003
391. Lu, G. *et al.* Myeloid cell-derived inducible nitric oxide synthase suppresses M1 macrophage polarization. *Nat Commun* **6**, 6676 (2015).
392. Morris, D. L. Minireview: Emerging Concepts in Islet Macrophage Biology in Type 2 Diabetes. *Mol. Endocrinol.* **29**, 946–962 (2015).
393. Zizzo, G., Hilliard, B. A., Monestier, M. & Cohen, P. L. Efficient clearance of early apoptotic cells by human macrophages requires M2c polarization and MerTK induction. *J Immunol* **189**, 3508–3520 (2012).
394. Naito, Y., Takagi, T. & Higashimura, Y. Heme oxygenase-1 and anti-inflammatory M2 macrophages. *Archives of Biochemistry and Biophysics* **564**, 83–88 (2014).
395. Satoh, T. *et al.* Critical role of Trib1 in differentiation of tissue-resident M2-like macrophages. *Nature* **495**, 524–528 (2013).
396. Song, I., Patel, O., Himpe, E., Muller, C. J. F. & Bouwens, L. Beta Cell Mass Restoration in Alloxan-Diabetic Mice Treated with EGF and Gastrin. *PLoS ONE* **10**, e0140148 (2015).
397. Mohammed, F. F. *et al.* Metalloproteinase inhibitor TIMP-1 affects hepatocyte cell cycle via HGF activation in murine liver regeneration. *Hepatology* **41**, 857–867 (2005).
398. Coudriet, G. M., He, J., Trucco, M., Mars, W. M. & Piganelli, J. D. Hepatocyte growth factor modulates interleukin-6 production in bone marrow derived macrophages: implications for inflammatory mediated diseases. *PLoS ONE* **5**, e15384 (2010).
399. Riley, K. G. *et al.* Connective tissue growth factor modulates adult  $\beta$ -cell maturity and proliferation to promote  $\beta$ -cell regeneration in mice. *Diabetes* **64**, 1284–1298 (2015).
400. Riley, K. G. *et al.* Macrophages are essential for CTGF-mediated adult  $\beta$ -cell proliferation after injury. *Mol Metab* **4**, 584–591 (2015).
401. Dai, C. *et al.* Age-dependent human  $\beta$  cell proliferation induced by glucagon-like peptide 1 and calcineurin signaling. *J. Clin. Invest.* **127**, 3835–3844 (2017).
402. Lammert, E., Cleaver, O. & Melton, D. Role of endothelial cells in early pancreas and liver development. *Mechanisms of Development* **120**, 59–64 (2003).
403. Homo-Delarche, F. *et al.* Islet inflammation and fibrosis in a spontaneous model of type 2 diabetes, the GK rat. *Diabetes* **55**, 1625–1633 (2006).
404. Li, X. *et al.* Islet microvasculature in islet hyperplasia and failure in a model of type 2 diabetes. *Diabetes* **55**, 2965–2973 (2006).
405. Murray, P. J. & Wynn, T. A. Obstacles and opportunities for understanding macrophage polarization. *J. Leukoc. Biol.* **89**, 557–563 (2011).
406. Murray, P. J. & Wynn, T. A. Protective and pathogenic functions of macrophage subsets. *Nat. Rev. Immunol.* **11**, 723–737 (2011).
407. Butler, P. C., Meier, J. J., Butler, A. E. & Bhushan, A. The replication of  $\beta$  cells in normal

- physiology, in disease and for therapy. *Nature Clinical Practice Endocrinology & Metabolism* **3**, 758–768 (2007).
408. MacDonald, M. J., Ade, L., Ntambi, J. M., Ansari, I.-U. H. & Stoker, S. W. Characterization of phospholipids in insulin secretory granules and mitochondria in pancreatic beta cells and their changes with glucose stimulation. *J. Biol. Chem.* **290**, 11075–11092 (2015).
  409. Werner, L. *et al.* Identification of pancreatic glycoprotein 2 as an endogenous immunomodulator of innate and adaptive immune responses. *J Immunol* **189**, 2774–2783 (2012).
  410. Yu, S., Michie, S. A. & Lowe, A. W. Absence of the major zymogen granule membrane protein, GP2, does not affect pancreatic morphology or secretion. *Journal of Biological Chemistry* **279**, 50274–50279 (2004).
  411. Jodal, A., Schibli, R. & Béhé, M. Targets and probes for non-invasive imaging of  $\beta$ -cells. 1–16 (2017). doi:10.1007/s00259-016-3592-1
  412. Di Galleonardo, V. *et al.* Imaging of  $\beta$ -Cell Mass and Insulinitis in Insulin-Dependent (Type 1) Diabetes Mellitus. *Endocr. Rev.* **33**, 892–919 (2012).
  413. Blomberg, B. A., Codreanu, I., Cheng, G., Werner, T. J. & Alavi, A. Beta-Cell Imaging: Call for Evidence-Based and Scientific Approach. *Mol Imaging Biol* **15**, 123–130 (2013).